FUEL COMPOSITION AND QUALITY SENSING FOR DIESEL ENGINES

BY

JOHN CLINTON SCHEIDER

THESIS

Submitted in partial fulfillment of the requirements
for the degree of Master of Science in Mechanical Engineering
in the Graduate College of the
University of Illinois at Urbana-Champaign, 2011

Urbana, Illinois

Adviser:

Professor Alan Hansen

ABSTRACT

The range of fuels that a diesel engine may be expected to burn is increasing including the use of biodiesels and alcohols produced from various plant or animal sources. Moreover, fuels can become unsuitable for application in diesel engines due to a variety of contamination, degradation, and cold flow issues. In order to optimize engine performance and meet EPA emissions standards over a wide array of fuels, information about the fuel composition must be known in real time. Furthermore, protecting the engine from potential fuel contaminants such as water, sulfur, glycerol, methanol, and urea requires a method of detecting these chemicals in the fuel system. This study evaluates a commercially available fluid properties sensor for use in diesel engines. The sensor provides four bulk outputs: temperature, density, dynamic viscosity, and dielectric constant, which can be used to monitor fuel properties.

Extensive testing was carried out on the sensor to evaluate its effectiveness at detecting fuel type, blend, and quality over a temperature range of 0°-80°C. Fuel types tested include diesel #1, diesel #2, jet A, soy biodiesel, rapeseed biodiesel, false flax biodiesel, jatropha biodiesel, soy oil, rapeseed oil, false flax oil, and jatropha oil. Blends of diesel #1 and #2 with soy biodiesel were studied. Fuel properties under contamination and the sensor's sensitivity to fuel degradation and cold flow situations were examined. A predictive model of fuel properties was developed based on fuel composition, contamination, and temperature range. Finally, an algorithm was developed to predict fuel type, blend, contamination condition, and degradation condition for unknown fuel samples.

ACKNOWLEDGEMENTS

Financial support for this work was provided through the John Deere Technology and Innovation Center located in Champaign, Illinois.

Many have contributed to this project, and I would like to extend thanks to Dr. Alan Hansen who has advised me and guided me through both the technical details of this project and the process of completing my degree. He has been an invaluable part of my success as a student and an engineer.

Furthermore, I must convey gratitude to the other members of my review committee: Dr. Mary-Grace Danao of the Department of Agricultural and Biological Engineering and Dr. Dimitrios Kyritsis of the Mechanical Science and Engineering Department.

Moreover, I would like to express appreciation for the help I have received from John Deere. Especially Jim Lenz, director of JDTIC, for connecting me with this project, and Bruce Upchurch, Sensor Development Engineer for John Deere Power Systems, for his advice and technical support. Without their help this project would not have had proper direction. Also, thanks to Ken Chao of John Deere Power Systems for his help in obtaining the fuel samples used in this study.

Finally, thanks to my family and friends who have taught me the value of education.

TABLE OF CONTENTS

LIST OF ABBREVIATIONS

ASTM	American Society of Testing and Materials
B-x	Blend of biodiesel with petroleum based diesel (#2 unless otherwise stated) where x = % biodiesel by volume
DEF	Diesel Exhaust Fluid
DPF	Diesel Particulate Filter
EPA	Environmental Protection Agency
E-x	Blend of ethanol with gasoline where x = % ethanol by volume
FAME	Fatty Acid Methyl Ester
GUI	Graphical User Interface
MEAS	Measurement Specialties Company
PPM	Parts Per Million: the concentration of a substance within a solution usually on a volume basis
RME	Rapeseed Methyl Ester
SCR	Selective Catalyst Reduction
SME	Soybean Methyl Ester
ULSD	Ultra Low Sulfur Diesel Fuel

CHAPTER 1: INTRODUCTION

Diesel engines are proven, effective power producers for a number of uses across the transportation and stationary power generation industries. While primarily run on petroleum based diesel fuel, diesel engines have been successfully operated with a number of different fuels and oils. In particular, there has been great interest in running engines on biodiesel and even vegetable oils or blends of these with traditional petroleum fuels due to the positive emissions and environmental consequences of using bio-based fuel sources. Engines can often use biodiesel or vegetable oils without any modification to the engine's physical design or controls; however, much research has been dedicated to the combustion of such fuels and their blends and improving performance and emissions as a function of engine controls, injection timing and rate, exhaust gas recirculation (EGR), or exhaust after-treatment. Controls optimization requires real time information about fuel composition that can be supplied to the engine controls unit. While there are systems currently in place to determine fuel composition in spark ignition engine applications, there exists no such complete sensing system available for use specifically in diesel engines, although several available sensor types may be suitable for such a function (Tat and Van Gerpen, 2003b).

In addition to the need for engines to be flexible in their use of fuels, fuels need to be clean and of high quality in order to assure proper engine function. The refining industry takes great care to provide fuels that meet these standards for fuel quality; however, several conditions can render fuel inappropriate for engine use. First, water can mix with fuels due to leaks in tanks and seals or from condensation. Contamination from water can damage fuel pumps, filters, and injectors as well as affecting the combustion process. Secondly, sulfur is present in all petroleum based fuels and its content is highly regulated. Studies show that high sulfur fuels very quickly

destroy the efficiency and life of many after-treatment systems such as diesel particulate filters. Third, biodiesel is susceptible to contamination from both methanol, which is a reactant in the biodiesel production reaction, and its byproduct glycerol. Biodiesel quality standards require that these components be controlled to a low concentration (ASTM, 2010a). Finally, there are many other potential contaminants of diesel fuels including gasoline and urea based diesel exhaust fluid.

Another potential problem is fuel degradation; fuels occasionally sit in storage within a machine or storage tank for long periods of time and age to the point of causing unsatisfactory engine operation. Bio-fuels have higher viscosities and cloud points which often lead to starting and fuel flow problems for engine users in cold climates (Joshi and Pegg, 2007). Ultimately there are a number of problems that can arise to make fuels less than ideal for engine use, and engine manufacturers have begun to recognize the value of protecting their customers from improper or contaminated fuels.

This study focuses on the development and application of fuel composition and quality sensors for use on diesel engines. The sensor used in this study is a commercially available fluid properties sensor developed and manufactured by Measurement Specialties (MEAS), (Model no. FPS 2800). This sensor provides four bulk fluid properties as its outputs: dynamic viscosity, density, dielectric constant, and temperature. Analysis of fluid properties could be used to supply real time information about fuel composition and quality to the engine control unit or the operator station. Such information would be useful in optimizing engine performance and protecting the engine through the use of warning signals pertaining to the suitability of the fuel for the application.

In order to employ the sensor for engine controls and diagnostic warnings, information of importance such as fuel type, blend, presence of contaminant, contamination level, type of contamination, degradation condition, or cold flow problem was extracted from the outputs of the sensor and modeled over a wide range of fuels (both petroleum and bio based) over the applicable temperature range. Also, blends of diesel and biodiesel fuels were examined. Sensor response to contamination by water, sulfur, glycerol, methanol, and urea as well as degraded fuel was studied. An in-depth understanding of the effect of composition and temperature on each sensor output was necessary. Models of the MEAS sensor's response were compiled to yield an algorithm capable of predicting the fuel type, blend, presence and level of contamination, degradation, and cold flow problems in an unknown fuel sample.

In the following chapters the objectives of this study are more precisely stated (Chapter 2), and a literature review of fuel quality sensing, fuel properties, temperature effects on fluid properties, composition/blending effects on fluid properties, and engine performance related to fuel type and quality is compiled and summarized (Chapter 3). A detailed description of the experimental methods and procedures is presented (Chapter 4). Finally, the conclusions of this study (Chapter 5), in addition to recommendations for future work sum up the content of this thesis (Chapters 6 and 7).

CHAPTER 2: OBJECTIVES

The overall goal of this project was to develop a fuel quality sensing system capable of providing information that could be used for either engine controls or warning signals that would add value to engine product lines. Within the scope of that goal there were a number of specific objectives that were realized related to both implementation of sensors and the science of fuels.

1. MEAS sensor outputs (dynamic viscosity, density, dielectric constant) were calibrated for diesel #1, diesel #2, SME B-100, and JET A, fuels over a temperature range of 0°-80° C.
2. MEAS sensor outputs (dynamic viscosity, density, dielectric constant) were calibrated for blends of SME biodiesel with diesel #2 in 10% vol. increments over the temperature range of 20°to 80° C. Also, calibration of outputs for blends of diesel #1 with SME biodiesel for blends up to 20% vol. of SME was conducted.
3. The effect on dynamic viscosity, density, and dielectric constant from contamination of diesel #2 and several blended fuels by water and urea were determined as well as contamination of B-100 by glycerol and methanol. Sulfur contamination was studied in diesel #2 only.
4. The effect storage time has on the degradation of fuels with respect to changes in dynamic viscosity, density, and dielectric constant was determined.
5. The properties of biodiesel from different sources such as soybean, rapeseed, jatropha, and false flax on viscosity, density, and dielectric constant were evaluated. These differences were related to the measured fatty acid profiles of each biodiesel.

6. MEAS sensor data were compiled and used to develop an algorithm capable of using the sensor outputs to provide the base fuel type, level of blend with biodiesel, level of contamination, type of contamination, level of degradation, and indication of cold flow problems.
7. Recommendations for the implementation of the sensor in engine applications were provided.

CHAPTER 3: REVIEW OF LITERATURE

In order to serve the primary objectives of this project which were application based and focused on delivering functional engineering results, it was necessary to understand the subject of fuel sensing on a deeper level. Knowledge of the properties of fuels and previous work on fuel sensing allowed this project to be grounded in firm science. This literature review will cover some of the extensive research that has previously been attempted within the following topics:

- Properties of fuel: Variation of these properties with temperature and composition,
- Fuel contaminants,
- Stability and degradation of fuels, and
- Sensors for detection of fuel or fluid properties.

3.1 Fuel Properties

When attempting to identify or distinguish different substances or blends it is necessary to have a measurement or set of measurements that can be used as a determinant between the possible inputs. In the case of a liquid such as fuel there are two obvious routes for measurement. The first is to identify the specific chemical composition of the liquid providing the definite ratios of elements or molecules. Spectroscopic techniques provide this level of specificity and sensitivity giving a very accurate analysis of the composition and therefore identification of a material. However, in an application such as real time fuel sensing in engines this type of sensor is often either too expensive or incapable of providing fast results. Alternatively, a measure of the bulk properties of liquids and their blends could be used. In the case of fuels there were several possible bulk properties that might be chosen for measurement in

the application of fuel sensing. Some potential properties could be identified from inspection of ASTM standard D975 such as: density or specific gravity, kinematic viscosity, volatility, colour, corrosivity, and lubricity (ASTM, 2010b). In addition other properties beyond those of typical interest within fuels standards could be identified including dielectric constant, dynamic viscosity, electrical resistivity, pH, or surface tension.

In theory, any of these properties is a potential determinant for a fuel sensing system. In practice however, the property must be easily measured in a very short time period. Therefore properties such as corrosivity and lubricity are not practical. Another criterion in determining the best properties to measure is the difference between the values of the property at each end of the range of fuels of interest. For example, to measure the blend level of biodiesel with #2 diesel a property that has a very different value for each of the two neat fuels is optimal.

There is a dearth of fuel properties for different types of biofuels and their bends. In some cases there were discrepancies between measured values and their sampling conditions, making direct comparisons difficult to achieve. For the range of fuels used in this study, both kinematic viscosity and dielectric constant vary greatly across fuel type (Table 3.1)

Table 3.1 Selected fuel properties (Dubovkin and Malanicheva, 1981; Graboski and McCormick, 1998; Tat and Van Gerpen, 2003; Yuan, 2005)

Fuel	Kinematic viscosity (cSt)[a]	Density (g/ml)[b]	Dielectric Constant
Diesel #1	1.7590	0.8162	2.0800
Diesel #2	2.6000	0.8537	2.1000
Jet A	1.1300	0.7895	1.7000
Gasoline	0.7000	0.7450	2.0000
SME B-100	4.0800	0.8853	~3.2
RME B-100	4.8300	0.8820	NA

[a] Measured at 40°C
[b] Measured at 20°C

It can be seen that kinematic viscosity and dielectric constant could be potential properties for distinguishing between fuel types while density would be useful to a lesser level. While several of the other properties previously listed have potential for application to fuels sensing, the MEAS sensor employed in this study utilizes measurement of the dynamic viscosity, density, and dielectric constant. Consequently these will be the properties of focus for the remainder of this literature review.

It should be noted that the MEAS sensor provided dynamic viscosity rather than kinematic viscosity. However, dynamic viscosity is merely the kinematic viscosity divided by the density, and the density was essentially constant in comparison to viscosity in most cases. Therefore any trends that hold for kinematic viscosity also held for the dynamic viscosity in general. This was fortunate since nearly all data available are for kinematic viscosity rather than dynamic viscosity.

3.2 Variation of Properties with Temperature

Practically all bulk properties of liquids have some dependence on temperature; therefore, in order to develop a highly accurate system of fuel composition sensing it was necessary to understand this temperature dependence for each sensor output. This section focuses on each of the three properties the MEAS sensor monitors and their relationship to temperature.

3.2.1 Viscosity

It was well documented within the literature that the temperature dependence of liquid kinematic viscosities was a very strong function with a non-linear shape. However, there had been a long history of attempts to accurately describe this relationship.

The most basic model was an exponential model which works over limited temperature ranges.

$$\eta(T) = \eta_0 \exp(-bT) \tag{3.1}$$

where T is the temperature η is the kinematic viscosity, and η_0 and b are constant coefficients. (Seeton, 2006)

A more fundamental model was the Arrhenius model based on the Arrhenius equation for molecular kinetics.

$$\eta(T) = \eta_0 \exp\left(\frac{E}{RT}\right) \tag{3.2}$$

where η_0 is a constant coefficient, T is the temperature, E is the activation energy, and R is the universal gas constant (8.3415 J K^{-1} mol^{-1}). (Seeton, 2006)

Indeed many other empirical relationships had been used to accurately describe the viscosity-temperature relationship. Seeton (2006) compiled several more of these relationships.

Valeri and Meirelles (1997) applied the Andrade correlation and its modified versions to model the temperature dependence of several fatty acids and triglycerides with high success. Their model produced mean deviations of less than 2.5% over a temperature range of 20°-90°C:

$$\ln \eta = A + B/T \tag{3.3}$$

where η is the kinematic viscosity (cSt) A, and B are empirical constants and T is the temperature (°C)

Although there have been few attempts to characterize the viscosity- temperature correlation specifically for fuel Tat and Van Gerpen (1999) utilized a form of the modified Andrade Correlation as described above to model the temperature relationship for viscosities of

blends of diesel #2 and biodiesel. Their model was accurate over a temperature range of -20° to 100°C for the entire range of blends.

Modified Andrade Correlation:

$$\ln \eta = A + \frac{B}{T} + \frac{C}{T^2} \tag{3.4}$$

where η is the kinematic viscosity (cSt), T is the temperature in Celsius and, A, B, and C are empirical constant coefficients determined from data (Tat and Van Gerpen, 1999)

3.2.2 Density

Density in fuels has been a subject of research due to its importance in the control of the mass of fuel injected in high pressure diesel injection systems. However, within this work the temperature dependence of density had been established and may be applied to a fuel sensing application. The dependence of density on temperature was known to be much less dramatic than that of viscosity and to be of nearly linear shape. As such density was much easier to model over wide temperature ranges for most liquids including fuels.

Most authors suggested that density can be simply modeled with temperature using a linear model of form:

$$\rho = b - mt \tag{3.5}$$

Where ρ is the density (g/ml), t is the temperature in Celsius, and b and m are regression coefficients

Fischer (1995) attempted to summarize and organize previous attempts of modeling fatty acid temperature relations. His study yielded results for a wide range of compounds using the above linear form with the coefficients for the model displayed in Table 3.2.

Table 3.2 Linear density temperature dependence coefficient constants for fatty acids (Fischer, 1995)

Fatty Acid	Intercept b (g/ml)	Slope m (g/ml/°C)
$C_{9:0}$	0.92106	7.923E-04
$C_{10:0}$	0.91660	7.824E-04
$C_{12:0}$	0.90813	7.486E-04
$C_{14:0}$	0.90274	7.269E-04
$C_{16:0}$	0.89809	7.083E-04
$C_{18:0}$	0.89535	6.974E-04

Tat and Van Gerpen (2000) applied a similar linear model to fuels including diesel #1, diesel #2, SME B-100, B-75, B-50, and B-20. They also compared their results for biodiesel and blends to the established guidelines from ASTM standard D1250 which provides tables for temperature correction of density measurements for diesel fuels. These tables were established to allow engineers to measure fuel density at any temperature and then correct their findings to a common standard temperature for comparison. The study found that the same linear model was appropriate for biodiesel and its blends, and that ASTM D1250 tables could be used for any of these fuels. This suggested the rate of change of density with temperature was independent of fuel blending with biodiesel. In addition the accuracy of their models was apparent in the R^2 values of the regressions provided which were all above .998 (Table 3.3).

Table 3.3 Regression coefficients and errors for linear models of fuel density temperature dependence (Tat and Van Gerpen, 2000)

	Fuel Type	Intercept a	Slope b	R^2	MSD
Blends with #2 Diesel	B-100	0.8976	-6.62E-04	0.9989	4.830E-07
	B-75	0.8869	-6.80E-04	0.9997	1.200E-07
	B-50	0.8750	-6.71E-04	0.9994	3.138E-07
	B-20	0.8613	-6.60E-04	0.9989	6.211E-07
	Diesel #2	0.8527	-6.41E-04	0.9989	5.969E-07
Blends with #1 Diesel	B-75	0.8831	-6.82E-04	0.9995	2.654E-07
	B-50	0.8678	-6.70E-04	0.9995	2.368E-07
	B-20	0.8506	-6.61E-04	0.9995	3.024E-07
	Diesel #1	0.8403	-6.63E-04	0.9994	3.548E-07

3.2.3 Dielectric Constant

A general model of the dielectric constant developed from the geometry of the basic molecules or atoms of the substance is an achievement not yet fully realized. Fortunately there is a great deal known about the dielectric constant of liquids and temperature although this theory had not been widely applied to fuels. The study of dielectric constant has to be broken up into two regimes: polar liquids and non-polar liquids. The behavior of these two types of liquids is quite different. Moreover, the ability of polar molecules to align themselves with the electric field is the primary cause for the much higher dielectric constants of such materials. Also, the temperature dependence of dielectric constant is different in each of the two cases. In general within the liquid phase polar molecules have a much higher rate of change of dielectric constant with temperature compared to non-polar liquids. Non-polar liquids were of higher interest since fuels fall within this category. However, polar liquids were of some interest as well since water is highly polar and is one of the main fuel contaminants to be addressed in later sections.

Non-polar liquids such as fuel have dielectric properties that are largely insensitive to temperature change although the dielectric constant will decrease slightly as temperature increases.

Sen et al. (1992) found that the static dielectric constants of many hydrocarbons decrease linearly with temperature over a range of 100-300 K within which the alkanes were liquid. Sen et al (1992) were able to explain these results through use of an established model. Furthermore, it was found that the dielectric constant was actually dependent on the density of the liquid. The number of molecules available to store energy within the electric field will decrease as density decreases causing the subsequent decline in dielectric constant. Succinctly, dielectric constant was inversely linearly proportional to temperature since density was inversely linearly proportional to temperature and is best described by the Clausius- Mosotti Relation:

$$\frac{(e'-1)}{(e'+2)} = 4\pi\rho N_a \frac{\alpha}{3M} \tag{3.6}$$

where ε' is the dielectric constant, ρ is the density, N_a is Avogadro's number, α is the electric polarizability of the molecule, and M is the molecular weight of the liquid (Sen et al., 1992).

Comparisons of measurement to this model produced less than 0.3% error above 0°C and less than 1% error below 0°C.

3.2.4 Cold Flow

The trends of fuel properties described above are relevant for the liquid form of the fuel in temperature ranges approximately near standard conditions above 0°C. Consequently, as fuels are cooled to near the phase transition point to a solid these models would no longer be accurate. When developing algorithms based on measurements taken with a fluid properties sensor the

lower limit of application of these prediction formulae was near the cloud point of the fuel, the temperature at which the fuel begins to cloud or show evidence of crystal formation.

Fortunately, research has been conducted to quantify the cloud point for diesel fuels and blends with biodiesel. Joshi and Pegg (2007) measured the cloud points of diesel #2 and blends with biodiesel made from fish oil, and fitted a model to relate cloud point to blend level. The model was a quadratic polynomial of the form shown in equation 3.7. Also, Table 3.4 includes results from this model and experimentation.

$$T_{cp} = 256.4 + .1991\,V_B + .000223V_B^2 \tag{3.7}$$

T_{cp} refers to the cloud point temperature in Kelvin, and V_B is the blend percentage by volume.

Table 3.4 Cloud points of blends of diesel #2 and biodiesel from fish oil (Joshi and Pegg, 2007)

Blend	Cloud Point (K)	Cloud Point °C	Predicted Cloud Point (K)
B100	279	6	278.6
B80	273	0	273.8
B60	269	-4	269.2
B40	265	-8	264.7
B20	261	-12	260.5
B0	256	-17	256.4

The model and measurements agree that the cloud point of diesel #2 was much lower than that of biodiesel. Moreover, considering normal temperatures in the US, diesel #2 would almost never be cooled to its cloud point but pure biodiesel would often be colder than its cloud point in winter seasons. The model presented predicted cloud point with high accuracy; however, as can be seen by the small coefficient on the quadratic term this relationship was nearly linear suggesting a simpler model would also be successful.

Other studies indicated that cloud point could vary significantly based on the fatty acid composition of the biodiesel. Imahara et al. (2006) measured the cloud points of several biodiesel samples in order to verify a model developed to predict cloud point based on fatty acid composition (Table 3.5)

Table 3.5 Cloud points of biodiesel (Imahara et al., 2006)

Biodiesel	Cloud point (K)
Linseed	268
Safflower	267
Sunflower	274
Rapeseed	267
Soybean	272
Olive	268
Palm	283
Beef tallow	286

3.3 Variation of Properties with Fuel Composition or Blend

The versatility of diesel engines with respect to the fuel they may combust places a requirement on any reliable fuel sensing system that it be able to detect and distinguish between a wide range of fuels. Consequently, a review of research related to how the chemical composition of fuel affects its bulk properties was necessitated.

3.3.1 Comparison of Petroleum-Based Diesel and Biodiesel

The two most important sources of fuel for diesel engines are oil removed from the earth and bio based oils harvested from various plant and animal sources. Moreover, a popular strategy in North America and Europe is to use some combination of diesel fuels refined from these two types of sources. Accordingly a successful fuel sensor had to be able to distinguish between fuels from these two separate origins.

Again, the dynamic viscosity, density, and dielectric constant of these fuels and blends must be examined. Viscosity and density for each type of fuel had been measured and compared in several studies while discussion of the dielectric constant remained largely unavailable in fuel literature.

Graboski and McCormick (1998) performed a detailed study on the properties of bio-fuels in comparison with standard diesel fuels. Included within this work were some measurements of the viscosity and density of diesel #2 and several biodiesels from different sources. Also, Tat and Van Gerpen (1999, 2000, 2003) researched the density and viscosity of diesel, biodiesel, and its blends over some temperature variation (Tables 3.6 through 3.9)

Table 3.6 Viscosity of several fuels (Graboski and McCormick, 1998)

Fuel	Viscosity (cSt 40°C)
No. 2 Diesel Fuel	2.60
Soybean oil methylester	4.08
Rapeseed oil methylester	4.83
Tallow oil methylester	4.80
Soybean oil ethylester	4.41
Rapeseed oil ethylester	6.17
Palm oil methylester	4.50
Palm stearin methylester	4.60
Frying oil ethylester	5.78
Tallow ethylester	5.93
Tallow butylester	6.17

Table 3.7 Viscosity of several fuels (Tat and Van Gerpen, 2003)

Fuel	Kinematic Viscosity (cSt 40°C)
No. 2 Diesel	2.8911
Soybean oil methylester	4.5926
Yellow Grease methylester	5.9156
Soybean oil isopropyl ester	5.2649
Yellow grease isopropyl ester	6.0997

Table 3.8 Specific gravity of several fuels at 20°C (Graboski and McCormick, 1998)

Fuel	Specific Gravity
No. 2 Diesel Fuel	.8500
Soybean oil methylester	0.8853
Rapeseed oil methylester	0.8820
Tallow oil methylester	0.8756
Soybean oil ethylester	0.8810
Rapeseed oil ethylester	0.8760
Sunflower oil methylester	0.8800
Cottonseed oil methylester	0.8800
Palm oil methylester	0.8700
Palm stearin methylester	0.8713
Frying oil ethylester	0.8716
Tallow ethylester	0.8710
Tallow butylester	0.8680

Table 3.9 Specific Gravity of several fuels (Tat and Van Gerpen, 2000)

Fuel	Specific Gravity 20°C
#1 Diesel	0.8844
#2 Diesel	0.8399
Soybean oil methylester	0.8270

McCrady (2007) analyzed several types of biodiesel in his work on biodiesel property definition for combustion modeling. Tables 3.10 and 3.11 show results for viscosity and density. In general plant based biodiesels were more viscous than diesel #2 and percent increase in density of plant-based fuels over diesel #2 ranged from 4 to 6%.

Table 3.10 Percent increase of viscosity of several biodiesels over diesel #2 (McCrady, 2007)

Percent Increase of Viscosity compared to #2 diesel					
Temperature °C	Soybean	Rapeseed	Coconut	Palm	Lard
20	58.0	84.0	30.5	65.9	81.2
40	65.1	84.8	34.2	87.8	75.6
60	75.0	92.3	36.1	89.5	83.8
80	75.4	89.7	37.3	83.5	80.0
100	60.4	72.9	30.7	75.1	68.3

Table 3.11 Percent increase of density of several biodiesels over diesel #2 (McCrady, 2007)

Percent Increase of Density compared to #2 diesel					
Temperature °C	Soybean	Rapeseed	Coconut	Palm	Lard
20	6.13	5.53	5.30	4.30	4.70
40	5.96	5.36	5.11	4.75	4.50
60	6.77	6.14	5.53	4.30	4.55
80	6.84	5.97	5.59	4.97	4.60
100	6.19	5.56	5.31	4.68	4.31

Unlike viscosity and density, dielectric constant had not been of interest to researchers in the fuels and combustion area since this property seemed to have little effect on the ability of the fuel system to pump and inject the fuel or the ability of the engine to perform combustion. However for fuel sensing it was a very important and useful property to record.

One piece of research available looked at the feasibility of using the dielectric constant as a fuel composition determinant. Tat and Van Gerpen (2003b) used a commercially available dielectric flex fuel sensor similar to what Ford Motor Co. has used for on-board ethanol- gasoline blending determination, for blends of diesel #1 or #2 and soybean biodiesel (Table 3.12). This sensor measured changes in how the fluid responds to vibration and its output was a frequency which was directly correlated with the dielectric constant.

Table 3.12 Dielectric resonance sensor response to different fuels (Tat and Van Gerpen, 2003b)

Fuel	Sensor Output (frequency hz)
Diesel #1	51.84
Diesel #2	52.63
Soy methylester	58.96

3.3.2 Blends of Fuels

Standard petroleum-based diesel fuels are often blended with biodiesel in order to maintain similar combustion or injection performance while taking advantage of some of the advantages of biodiesel. A highly important variable that a diesel fuel sensing system in North America could output is the blend percentage between diesel and biodiesel. Several studies have

reported the effects on density and viscosity but few ascertained the effects on dielectric constant.

Density

Of the three properties of interest density is the easiest to model with changing fuel blend. Since density is merely a measure of the amount of mass per unit volume this property changed linearly when blending liquids.

Yang et al. (2004) studied 114 blends of diesel fuels as part of a study related to developing a prediction system for the cetane number of these blends. Furthermore, as parts of this work the density of the fuel was modeled using a mass weighting equation.

$$\rho = \sum_1^n \rho_i W_i \tag{3.8}$$

where ρ is the density, W is the mass fraction, and i denotes the ith component of the blend.

Tat and Van Gerpen (2000) applied this relationship to blends of diesel #1 or #2 with SME biodiesel. The density of blends of these fuels was predicted with less than 0.3% error from actual measurements.

McCrady (2007) confirmed the validity of this model with blends of #2 diesel and soybean biodiesel, noting that the average percent increase of density over that of #2 diesel was linear with the addition of biodiesel.

Viscosity

Compared to density the viscosity of blended fuels is more difficult to model over wide temperature ranges because each component's viscosity responds to temperature changes at different rates.

Tat and Van Gerpen (1999) had studied the viscosity properties of blends in some detail. Blends of diesel #1 or #2 with soy biodiesel were modeled with a correlation similar to the Grunberg-Nissan equation.

$$\ln \eta_B = m_1 \ln \eta_1 + m_2 \ln \eta_2 \tag{3.9}$$

where η is the viscosity, m is the mass fraction, and the subscripts refer to components or blend.

The inaccuracy of this model was less than 2% for all blends which was below the natural deviation within the viscosity of fuel reported in the market. In addition it was noted that this model was slightly more accurate for blends with #2 diesels attributable to the smaller ranges between the viscosities of these two fuels in comparison to blends with #1 diesel.

McCrady (2007) used this model for blends of #2 diesel and soy biodiesel effectively. This study observed the near exponential shape of the relationship between viscosity and blend due to the use of the logarithm of each component in the correlation.

Dielectric Constant

Compared to density and viscosity, there is a dearth of information with regards to the dielectric constant of biodiesel blends. Tat and Van Gerpen (2003b) did address the issue in their study of commercial dielectric sensors for fuel composition determination. The results of this work made clear the linear nature of dielectric constant with blending. A linear model was applied to the sensor data in this study with errors of less than 10%, although most of this error was introduced by the use of both #1 and #2 diesel as well as biodiesel from multiple sources.

$$\varepsilon_{Blend} = \varepsilon_{B0} + \frac{\epsilon_{B100} - \epsilon_{B0}}{100} * B\% \tag{3.10}$$

where ε_{Blend} is the dielectric constant of the blended fuel, ε_{B0} is the dielectric constant of B-0, ε_{B100} is the dielectric constant of B-100, and $B\%$ is the blend percentage.

3.3.3 Biodiesel from Different Sources

Biodiesel is a very broad term which encompasses the fuel products from the chemical reaction of any oil from plant or animal origins with an alcohol. Consequently, biodiesel has been refined from many different crops, waste oils, or animal fats. Additionally, in different regions of the world diverse oil sources are used based on what is available. Hence, for robust fuel sensing it was of important to examine the variation between biodiesels from different oil sources. In addition some significance could be tied to the composition of biodiesel with respect to the length of the carbon chains and number of double bonds in the general structure of the fuel molecules.

Yuan (2005) analyzed the properties of biodiesel from different sources in some detail. Table 3.13 shows both the structure of several biodiesels as well as the kinematic viscosity and specific gravity where applicable. The specific gravity data was drawn from Graboski and McCormick (1998).

Table 3.13 Carbon structure of biodiesel from multiple sources with viscosity and specific gravity (Yuan, 2005; Graboski and McCormick, 1998)

Number of Carbon atoms and degree of saturation	Yellow Grease	Coconut	Peanut	Soybean	Palm	Canola
C8:0	0.0000	0.0750	0.0000	0.0000	0.0000	0.0000
C10:0	0.0000	0.0600	0.0000	0.0000	0.0000	0.0000
C12:0	0.0000	0.5330	0.0000	0.0000	0.0040	0.0000
C14:0	0.0170	0.1710	0.0000	0.0000	0.0130	0.0000
C16:0	0.1947	0.0730	0.1050	0.0580	0.4810	0.0420
C16:1	0.0000	0.0000	0.0040	0.0080	0.0030	0.0040
C18:0	0.1438	0.0190	0.0270	0.0160	0.0400	0.0200
C18:1	0.5467	0.0550	0.4660	0.6000	0.3730	0.5740
C18:2	0.0796	0.0140	0.3010	0.1990	0.0800	0.2130
C18:3	0.0069	0.0000	0.0100	0.0960	0.0020	0.1120
C20:0	0.0025	0.0000	0.0130	0.0070	0.0030	0.0120
C20:1	0.0052	0.0000	0.0140	0.0160	0.0010	0.0210
C22:0	0.0021	0.0000	0.0240	0.0000	0.0000	0.0010
C22:1	0.0000	0.0000	0.0000	0.0000	0.0000	0.0000
C24:0	0.0000	0.0000	0.0350	0.0000	0.0000	0.0000
Viscosity (mPa-s) (40°C)	4.00	2.30	3.73	3.70	3.94	3.64
Specific Gravity (20°C)	0.8716	NA	NA	0.8853	0.8700	NA

In general the chain length and double bonds had an effect on the properties of biodiesel including viscosity (Yuan, 2005). The viscosity of biodiesel increases with both the number of carbon atoms and the degree of saturation. However, the relationship with double bonds was weak.

Several studies had measured the properties of individual fatty acid methyl esters (FAME) of varying length and saturation. Table 3.14 reviews some of the published data for fatty acid methyl ester kinematic viscosities and densities. Viscosity increased with increasing chain length and saturation. For density the trend was reversed.

Table 3.14 Kinematic viscosities and densities of fatty acid methyl esters (Bornhurst et al., 1948; Swern, 1979)

	Temperature, °C					
	20	40	60	20	37.8	60
FAME	Kinematic Viscosity (mm^2/s)			Density (g/ml)		
8:00	1.59	1.16	0.911	0.8775	0.8615	0.842
10:00	2.44	1.69	1.276	0.873	0.8581	0.8399
12:00	3.54	2.28	1.732	0.8695	0.8553	0.8376
14:00	5.2	3.23	2.323	0.8671	0.8534	0.8361
16:00	NA	4.32	2.998	NA	0.852	0.8354
18:00	NA	5.61	3.666	NA	0.8524	0.8363
18:01	7.23	4.45	NA	0.875[a]	.86[b]	NA
18:02	5.58	3.64	NA	.890[a]	.875[b]	NA
18:03	4.84	3.27	NA	NA	NA	NA
22:01	12.5	7.21	NA	NA	NA	NA

[a] Measured at 25°C
[b] Measured at 45°C

This literature review did recover one study related to the dielectric constant of different biodiesels. Gouw and Vlugter (1964, 1967) measured the dielectric constant of several triglycerides and fatty acid methyl esters (Table 3.15).

Table 3.15 Dielectric constant of fuels from bio-sources (Gouw and Vlugter, 1964, 1967)

FAME	Dielectric Constant (40°C)
Methyl laurate	3.413
Methyl palmitate	3.124
Methyl stearate	3.021
Methyl oleate	3.117
Methyl linoleate	3.245
Methyl linolenate	3.349

3.3.4 Vegetable Oil Composition

Diesel engines have been operated on pure vegetable oils for many years. While many engines will combust oils without modification a number of potential problems have been identified with this process especially related to the much higher viscosity of these fuels. This fact had prevented the practice from gaining widespread popularity. Nevertheless, there is some demand to return to the use of vegetable and animal fat oils and their blends with diesel due to the positive environmental consequences and the desire to skip the biodiesel refining process, bio-oil properties and their effect on fuel injection and combustion systems need further investigation.

Hossain and Davies (2010) published a comprehensive study of the effects of operating diesel engines on straight vegetable oils of various sources including the viscosities and densities of many plant oils. Table 3.16 summarizes the density and kinematic viscosity of some plant oils.

Table 3.16 Density, viscosity, and iodine number of plant oils (Hossain and Davies, 2010)

Fuel	Density (g/ml)	Kinematic Viscosity[a] (cSt)	Iodine Value[b]
Sunflower oil	0.918	58.50	125
Cottonseed oil	0.912	50.10	105
Soybean oil	0.914	65.40	130
Peanut oil	0.903	39.60 [c]	93
Corn oil	0.915	46.30	103-140
Opium poppy oil	0.921	56.10	NA
Rapeseed oil	0.914	39.20	98
Sesame seed oil	0.913	35.50	104-120
Palm oil	0.918	39.60	54
Coconut oil	0.915	31.59	10
Mahua oil	0.900	37.18 [d]	NA
Rice bran oil	0.916	44.52 [d]	NA
Jatropha oil	0.918	49.90	94
Pongamania oil	0.912	37.12 [d]	NA
Jojoba oil	0.863	25.48 [d]	NA
rubber seed oil	0.922	33.91 [d]	135
Deccan hemp oil	0.913	53.00 [e]	NA
Jatropha biodiesel	0.880	5.65	NA
Soybean biodiesel	0.885	4.50 [e]	NA
Pongamania biodiesel	0.904	106.10 [d]	NA

[a] Viscosities were measure at 27°C unless otherwise noted
[b] The iodine number is a measure of the level of unsaturated fatty acids in the substance
[c] Measured at 38°C
[d] Measured at 40°C
[e] Measured at 23°C

The viscosity and density of plant oils were higher than that of the corresponding biodiesels or petroleum based diesel fuels. The large sizes of the triglyceride molecules within the oils led to the higher viscosity property.

The dielectric constant of oils had been studied not for the purpose of fuels characterization but instead for food processing. In fact several published articles discussed the use of the dielectric constant for monitoring cooking oil quality. Lizhi et al. (2008) measured the dielectric properties of 8 different plant oils (Table 3.17). Specifically, it was noted that the dielectric constant of the oil tends to increase with increasing degree of un-saturation. One

measure of the degree of un-saturation is the iodine number so the dielectric constant would increase with increasing iodine number.

Table 3.17 Dielectric constant of plant oils (Lizhi et al., 2008)

Oil	Dielectric Constant (at 25°C)
Sesame	3.11
Soybean	3.115
Olive	3.062
Corn	3.127
Safflower	3.057
Sunflower	3.065
Canola	3.11
Modified	3.22

3.4 Effects of Contaminants on Fuel Properties

Although the process of refining and distributing fuel is highly regulated in the United States fuels occasionally become contaminated through unintended consequences of transport and storage. The presence of contaminants could have significant impacts on the fuel pumping and injection systems, combustion, or exhaust gas after-treatment within a diesel engine. Consequently, there is a critical need for a fuel sensor to detect contaminants and extend the lifetime of a diesel engine.

3.4.1 Water

Water is one of the most common fuel contaminants as it is present in the air and can easily condense within storage tanks. Water content in diesel fuel is regulated to 500 ppm by volume (ASTM D975, 2010b; ASTM D6751, 2010a). Fuel filters are designed to remove water from fuel; however, they are not 100 percent effective, and water could be corrosive to metal parts, damaging to the fuel pump and affect combustion. Detecting water within a fuel sample

could be done by observing a change in one property of the fuel relative to the other measured properties. Blends of two liquids have a linear change of density and dielectric constant over the range of mixtures while viscosity had a near exponential form. Therefore, one approach for approximating the effect a contaminant would have on fuel is to compare the properties of the pure contaminant to that of pure fuel. If any of the properties of the pure liquids differed greatly then there was a good chance this would manifest itself in a contamination situation. Water, a non-viscous, polar liquid has a higher density and dielectric constant than fuels (Table 3.18).

Table 3.18 Properties of Water (Mays, 2001; Clipper Controls, 2011)

	Dynamic Viscosity[a] (cP)	Density[b] (g/ml)	Dielectric Constant[b]
Water (distilled)	0.653	0.998	80.4

[a] Measured at 40°C
[b] Measured at 20°C

Lee (2008) examined the effects that water contamination has on blends of gasoline and alcohol such as ethanol. Water was added to samples of E-85 blended fuels and the viscosity was monitored (Table 3.19). The viscosity of E-85 fuels increased steadily with added water content. It was noted that although the viscosity of water is lower than that of E-85 the addition of water to this fuel caused the viscosity to increase rather than decrease. Also, the limit of water addition without phase separation was 15.6%. Water concentrations in the fuel above this level were not stable and would separate out.

Table 3.19 Viscosity of E-85 blended fuel with water contamination (Lee, 2008)

% Water (vol.)	Dynamic Viscosity (cP at 20°C)
0.0	1.0610
3.0	1.1330
6.0	1.2410
9.0	1.3400
11.9	1.4680
14.9	1.7730
15.6	1.7190

There had also been some research conducted related to the effect water can have on dielectric constant measurements. Lizhi et al. (2008) conducted dielectric experiments on various plant oils for food consumption. Within this work the effect of moisture content on oil dielectric constant was considered. The study found that dielectric constant increases nearly linearly as water was added to cooking oil (R^2= .9724).

$$\varepsilon' = 7.43 \times 10^3 MC^2 + 28.2MC + 3.11 \quad (3.11)$$

This result was explained through the highly polar nature of the water molecule which allows water to store much energy in electric fields thus yielding a high dielectric constant.

Tat and Van Gerpen (2003b) studied the dielectric response of biodiesel to water contamination within a study of dielectric sensors for diesel fuel sensing. Three samples of biodiesel were studied: dry, normal, and saturated. The dry sample referred to biodiesel that was boiled under a vacuum to remove any water and then tested for dielectric response. The normal sample was allowed to reach equilibrium with the room temperature and relative humidity. The saturated sample was mixed with water and then left to sit over night. Much of the water separated out in this case and the author noted that the approximate saturation limit of biodiesel was 1500 ppm by volume. The sensor took measurements though the resonant vibration

frequency of a small sensing element in the fluid. Therefore, data was recorded in units of frequency but this measurement was directly proportional to the actual value of the dielectric constant (Table 3.20)

Table 3.20 Dielectric sensor response of biodiesel to water contamination (Tat and Van Gerpen, 2003b)

Sample	Dielectric response (hz)
Dry	59.20
Normal	59.10
Saturated	59.50

Overall the effect of water on dielectric response was negligible although there was a slight increase for the saturated sample. This study illustrated the insolubility of water in many fuels as much of the water in the saturated case separated out given enough time.

Van Gerpen et al. (1996) compiled a thorough study of the effects of contaminants on fuels in which the solubility of water in fuels was reviewed. The solubility of water in diesel fuel is near 50 ppm at 0°C and increases non-linearly to 300 ppm at 80°C. The water concentration in several fuels after vigorous mixing as the fuels were allowed to settle over time was measured (Table 3.21).

Table 3.21 Water concentration in fuel with varying settling time (Van Gerpen et al., 1996)

	Water Concentration (ppm) at 25°C with varying time after mixing					
Fuel	0 hr	1 hr	3 hr	18hr	1 D	5 D
Soy Biodiesel	37	1460	1595	-	1255	1255
Diesel #2	28	-	81	30	-	-
B-20	40	37	38	-	33	45

The solubility of water in diesel #2 was below the ASTM D975 limit of 500 ppm over the entire range of temperatures applicable to a fuel system. Moreover, this was a positive result since most fuels would have adequate time to settle and allow water to separate out to an acceptable level. In pure biodiesel however, the solubility limit appeared to around 1,250 ppm which was well above the ASTM standard limit. A B-20 blend had only modestly higher water solubility that pure diesel #2. Water contamination was a much more serious issue in neat biodiesel.

3.4.2 Sulfur

Sulfur is present in all petroleum based fuels due to the sulfur compounds that are present in organic material, which oil forms from. Sulfur is a highly regulated contaminant of fuel due to its tendency to form sulfur dioxide during combustion which can contribute to acid rain formation and lower the effectiveness of exhaust after-treatment systems. ASTM D975 (2010b) limited sulfur content to 15 ppm by volume for ULSD which is the requisite fuel as of 2010. Sulfur in diesel fuels exists as part of functional groups within larger organic molecules. Within diesel #2 sulfur largely manifests itself as part of highly hindered compounds such as dibenzothiophene (Foster, 2010).

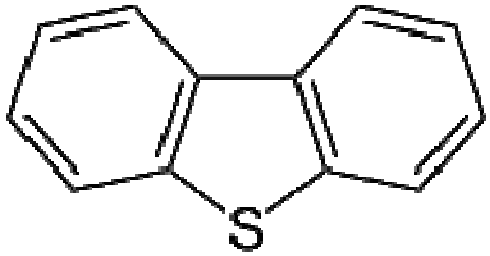

While a great deal of research has been dedicated to the effects of sulfur on engine performance and life, this literature review found no studies directly measuring the effects of sulfur content on fuel properties.

3.4.3 Glycerol

Glycerol is a byproduct of the transesterification process used to convert oils to biodiesel. Moreover, this glycerol has to be separated and cleaned from the biodiesel in order to assure the quality of the fuel. ASTM 6751 (2010a) required biodiesel to have free glycerol levels below 0.02 percent by mass and total glycerol below 0.24 percent by mass. These limits convert to 160 ppm and 1,900 ppm by volume, respectively. Glycerol contamination is an indicator of poor biodiesel quality and conversion efficiency and could have some effect on the properties of fuel.

Table 3.22 Properties of glycerol (Segur and Oberstar, 1951) (Clipper Controls, 2011)

Dynamic Viscosity[a] (cp)	Density[b] (g/ml)	Dielectric Constant[c]
284.0	1.261	42.5

[a] Measured at 40° C
[b] Measured at 20° C
[c] Measured at 25° C

All three properties are significantly higher than that of biodiesel. This suggested that glycerol contamination may have a large effect on the properties of fuel.

Van Gerpen et al. (1996) comprehensively studied biodiesel quality. The effect of monoglycerides on the viscosity of fuel was presented within their results (Table 3.23). The authors asserted that added monoglycerides mimicked increasing bound glycerin.

Table 3.23 Viscosity of fuels with added monoglycerides (Van Gerpen et al., 1996)

	Kinematic Viscosity (cSt) at 40° C		
% Monoglycerides	Methyl Soyate	B-20 (#1 diesel)	B-20 (#2 diesel)
0	4.147	1.856	2.756
0.1	4.282	1.841	2.8
0.5	4.343	1.875	2.849
1	4.513	1.872	2.854
2	4.406	1.913	2.993
3	4.405	2.013	3.009
5	4.607	2.141	Crystals

The kinematic viscosity of neat biodiesel and blends with pertrodiesel increased significantly with increasing monoglyceride content. Also, "crystals" denoted the formation of glycerin crystals within the fuel sample. This case indicated significant contamination and that the solubility limit of glycerin in the fuel had been reached. Furthermore, these crystals strongly impacted engine function and combustion. In addition it was noted that a significant amount of the material removed from plugged fuel filters was related to glycerol deposits.

Van Gerpen et al. (1996) also conducted an experiment illustrating the glycerol solubility limit in biodiesel. Pure glycerol was added to a sample of soy biodiesel and vigorously mixed. The free glycerin concentration was then measured (Table 3.24). Free glycerol solubility doubled from 0.072% after 4 h of mixing to 0.144% after 48 hr of mixing. The solubility limits were above the standard limit of 0.02% for free glycerol. Free glycerol was a contributor to deposit buildup in engines and at the bottom of fuel tanks. It was also noted that glycerol was more soluble in water than in fuel so it would tend to attract water and other sediments.

Table 3.24 Free glycerol solubility limit in biodiesel (Van Gerpen et al., 1996)

Mixing time	4 hr	24 hr	48 hr
% Free glycerol in ester	0.072	0.082	0.144

3.4.4 Alcohol

In the transesterification reaction the oil is reacted with an alcohol in excess to ensure complete conversion of the oil. Moreover, some of the alcohol could be left in the resulting biodiesel if improperly cleaned and separated. The properties of the most common alcohol used for transesterification, methanol, are listed in Table 3.25. Methanol has a higher dielectric constant than fuel while its density and viscosity are lower.

Table 3.25 Properties of methanol (Methanex, 2011)

	Dynamic Viscosity[a] (cp)	Density[b] (g/ml)	Dielectric Constant[b]
Methanol	0.544	0.7915	33.4

[a] Measured at 25°C
[b] Measured at 20°C

Methanol, even in low concentrations, significantly increased the flash point of fuels which made them less safe to handle and transport. Also, at high concentrations methanol would affect the cetane number or lubricity of the fuel. The study pointed out that even with poor washing and separation alcohol contamination should be low enough to only influence flash point. Therefore if the biodiesel met the ASTM D6751 limit for flash point of 100°C then the fuel should otherwise be suitable for engine use. Results indicated that 0.2% methanol in biodiesel was enough to increase the flash point above 100°C. Alcohol contamination was deemed a less significant problem than water, sulfur, or glycerol contamination.

Tat and Van Gerpen (2003b) briefly studied the effect of methanol contamination of biodiesel on the dielectric response of a resonant dielectric sensor. Dielectric response was monitored for methanol contamination up to 1% by volume and was found to increase. The dielectric constant increased with added methanol. A 1.0% by volume contamination yielded a 1.3% increase in dielectric constant. This indicated that at the likely contamination levels of 0.5% or less the dielectric effect of methanol contamination would not be detectable.

3.5 Effect of Time or Degradation on Fuel Properties

Fuels may be stored for long periods of time before use such as in the tank of a machine waiting to be sold. Moreover, the properties of fuel have long been known to change with time, and these changes could affect the performance of an engine. A substantial amount of research had been dedicated to the study of degradation of fuels and the chemical mechanisms that define this process. One of the disadvantages of the use of biodiesel was that it tends to be less stable and degrade more quickly.

Jain and Sharma (2010) compiled a very thorough review of many fuel stability studies. This study breaks fuel stability into three categories: oxidative stability, thermal stability, and storage stability. Storage stability was the most relevant to this study since it covers the way fuel properties change when exposed to the ambient environment for extended periods of time. This review also described the chemistry of degradation. The oxidation of fuel was described in two stages. The first was primary oxidation or peroxidation. This was a very complex process that broke fatty acids down into hydroperoxides (ROOH). Furthermore it was stated that fuel with further poly-unsaturation were more susceptible to primary oxidation. Figure 3.1 shows the chemical mechanism. The figure uses (I) to indicate initiation, not the presence of Iodine.

Initiation: $RH + I \rightarrow R\cdot + IH$

Propagation: $R\cdot + O_2 \rightarrow ROO\cdot$

$ROO\cdot + RH \rightarrow ROOH + R\cdot$

Termination: $R\cdot + R\cdot \rightarrow R\text{-}R$

$ROO\cdot + ROO\cdot \rightarrow$ Stable Products

Figure 3.1 Primary oxidation reactions for fuel degradation (Jain and Sharma, 2010)

The second stage was secondary oxidation. In this process the hydroperoxides decomposed to form aldehydes such as hexanal, heptanal, and propanal. This led to increased acidity and shorter chain fatty acids. Next, many of the short chain fatty acids underwent oxidative linking to form higher molecular weight polymers. These larger molecules directly led to an increased viscosity of the fuel.

Storage stability was also affected by interaction with contaminants, light, or sediment formation. Jain and Sharma (2010) summarized the results of several studies of the properties of fuels over time. Several studies reported a dramatic increase in viscosity and acid number. Other experiments showed some increase in density, peroxide value, and UV absorption. The effects of long term storage on the dielectric constant need to be further investigated.

Bondioli et al. (2003) studied several types of biodiesel under standard storage conditions. Rapeseed, sunflower, frying oil, and tallow biodiesel were allowed to sit in closed drums exposed to outside temperatures over the course of one year while properties of interest were measured monthly (Table 3.26). Kinematic viscosity increased by as much as 7% over a 12 month storage period.

Table 3.26 Kinematic viscosity change in biodiesels over time (Bondioli et al., 2003)

	Kinematic Viscosity (cSt) at 40°C							
Ageing Time (months)	0	1	2	3	5	7	9	12
Rapeseed	4.36	4.56	4.41	4.44	4.46	4.46	4.49	4.52
Sunflower	4.07	4.10	4.12	4.17	4.07	4.15	4.22	4.22
Used frying oils	4.67	4.72	4.80	4.87	4.92	4.87	4.96	4.94
Tallow	4.73	4.94	4.90	4.89	5.06	4.98	5.00	5.04

Bouaid et al. (2007) experimented with five samples of biodiesel over a 30 month period. Each fuel was stored under two conditions: light and dark, at room temperature. The kinematic viscosity among other properties was measured monthly and increased gradually over the initial 12 months and exponentially for the remainder of the storage period. Sunflower biodiesel showed the largest increase in kinematic viscosity doubling over the course of the experiment and the trend increased with increasing moisture content. The kinematic viscosities of brassica biodiesel and used frying oil biodiesel increase at the same rates.

3.6 Sensors for Detection of Fuel Composition

Alcohol- gasoline blend sensors have been in use since the early 1990's and have been shown to be a reliable and proven technology (Kopera et al., 1993). Furthermore, flexible fuel gasoline engines were highly popular comprising 3.3% of the 2009 US fleet (BAFF, 2009). Relatively, the application of fuel sensing to diesel fuels was a much less developed notion. However, there were several published studies in the last decade related to fuel composition sensing in diesel engines.

3.6.1 Resonant Cavity Dielectric Sensors

Tat and Van Gerpen (2003b) experimented with a commercially available, resonating cavity, dielectric sensor that was applied by Ford Motor Company to measure blends of ethanol and gasoline. They utilized this sensor to measure dielectric properties of various petroleum and bio based diesel fuels. This sensor gave an output in frequency (hz) which was the resonant vibration frequency of the sensing element in the fuel. The resonant frequency measured had been found to be proportional to the dielectric constant.

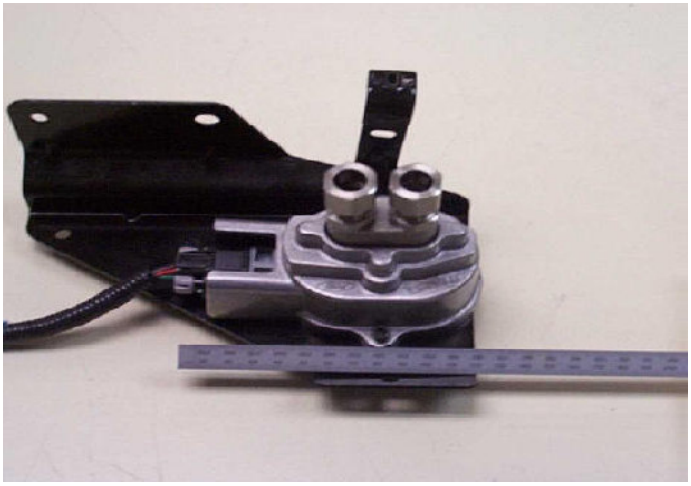

Figure 3.2 Ford Motor Company resonant cavity dielectric sensor (Tat and Van Gerpen, 2003b)

Within this study biodiesels from soybean, canola, tallow, yellow grease, brown grease, and lard as well as diesel #1, diesel #2, and blends of SME with diesel #1 and diesel #2 at levels of B-20, B-50 and B-75 were evaluated. In addition the effect of temperature, methanol contamination, and moisture content were tested. The sensor output ranged from 58.5 to 60.23 hz for biodiesel and from51.84 to52.62 hz for petroleum diesel. This range of 7.14 hz was determined adequate for diesel- biodiesel blend determination within 10% by volume as

described by Tat and Van Gerpen (2003b). The influence of temperature on sensor output was a linear decrease with increasing temperature. The effect of methanol and moisture was a slight increase in sensor output, but the outputs were not significantly different.

3.6.2 Spectroscopic Techniques

Several attempts had been made to determine if a spectroscopic approach for fuel composition determination was appropriate and if so which method is the most accurate. Chuck et al. (2010) applied three techniques in an attempt to measure blend levels of diesel- biodiesel blends: Fourier Transform Infrared (FT-IR) spectroscopy, refractive index, and UV–VIS spectroscopy. Blends were formulated by volume using ultra low sulfur diesel (ULSD) and biodiesel from four sources: sunflower, rapeseed, coconut, and palm oil. Each of the three measurement techniques was used to determine if blend level between diesel and biodiesel was feasible for real- time measurement. Also, the ability to distinguish blends from different biodiesels was investigated. Results showed that FT-IR spectroscopy was very successful at determining not only blend levels, but also at determining the biodiesel type.

The refractive index method was also found to be moderately successful at predicting blend level; however, at low blend levels some of the different biodiesels were indistinguishable. Furthermore, the added cost of implementing this sensor was likely not worth the value of supplementing the infrared approach with refractive data. Finally, the UV-VIS technique was found to be effective at yielding the amount of poly-unsaturated esters in B-100 samples, but it was found that the high aromatic content of diesel fuel inhibited the sensor's usefulness in blends of biodiesel and diesel. Also, this technique would not be easily applied to on-board fuel sensing. The study concluded that the near infrared approach was the most accurate and

promising method and might be applied as a commercial fuel sensing technology (Chuck et al., 2010).

Johnson et al. (2006) applied three spectroscopic methods to 45 fuel samples all of petroleum origin. The practices used were near infrared (NIR), Raman spectroscopy, and gas chromatography with mass selective detection (GC-MS). Each of these methods was applied to samples of jet fuel. The spectroscopic data was then placed in a partial least squares model (PLS), which then attempted to predict physical properties of the fuel. This was implemented with moderate success. Each of the three methods was reliable at predicting density, specific heat capacity, pour point, and aromatic content. However, some properties were not well modeled by any approach including sulfur content, viscosity, or conductivity. Table 3.27 shows errors for each of the fuel properties of interest.

Of particular interest was the fact the sulfur content is apparently the fuel property least able to be predicted by spectroscopic methods. Johnson et al. (2006) concluded that NIR and Raman Spectroscopy were of similar value for fuel property prediction and that GC-MS was modestly better than the other two techniques. Additionally, the authors remarked that a much larger sample size of fuels may be needed to refine their model.

Table 3.27 PLS regression model root mean errors of cross-validation for various spectroscopic methods for fuel property prediction (Johnson et at., 2006)

		ASTM Method Errors		PLS minimum RMSECV		
ASTM	Property	Reprod.[a]	Repeat.[b]	NIR	Raman	GC
D4052	density	0.0005	0.0001	0.0026	0.0018	0.0031
D93	flash point (PM)	8.5	3.5	8.8	8.9	7.1
D3828	flash point (mini)	6.2	1.6	7.8	7.5	7.4
D5972	freeze point.	1.3	0.7	3.6	4.2	3
D5949	pour point	6.8	3.4	2.7	2.2	2.1
D2622	sulfur	30	21	283	233	419
D1840	napthalenes	0.069	0.051	0.47	0.41	0.55
D1319	aromatics., FLA	2.7	1.3	0.66	0.92	1.32
D6379	aromatics., HPLC	1.897	0.938	0.64	1.09	1.48
D1319	saturates	4.4	1.4	0.75	1.2	1.37
D1159	olefins	0.4	0.2	0.21	0.34	0.22
D1319	olefins, FIA	2.1	0.6	0.34	0.48	0.31
D3701	hydrogen	0.11	0.09	0.11	0.2	0.12
D4809	heat content	77.4	22.9	27	48	40.4
D445	viscosity at 20°C			0.25	0.3	0.24
D445	viscosity at -20°C			0.47	0.47	0.39
D445	viscosity at -40°C			1.16	1	0.86
D1218	refractive index	0.0005	0.0002	0.0012	0.0019	0.0013
D2624	conductivity	17	5	77	92	87
D3242	TAN	0.003	0.001	0.0034	0.003	0.0034
D3241	thermal stability			46	58	47
D5001	lubricity	0.07	0.046	0.037	0.038	0.033
D86	initial boiling pt.	15.3	6.3	11	11.4	9.6
D86	10%	10.8	5.1	9.2	7.8	5.7
D86	20%	13.9	5.3	8.5	6.9	5.1
D86	50%	24.2	9	8.9	15.2	10.5
D86	90%	11.6	5.4	14	13.3	10.9

[a] Reproducibility
[b] Repeatability

3.6.3 Microelectromechanical Systems

Sparks et al. (2010) experimented with a microfluidics sensor with the objective of using its outputs to distinguish between several fuels and contaminants. The sensor was an example of a microelectromechanical system and utilized resonating silicon tube and resistive temperature sensor. This sensor provided density, viscosity, and temperature of a fluid and was smaller than a fingertip (Figure 3.3).

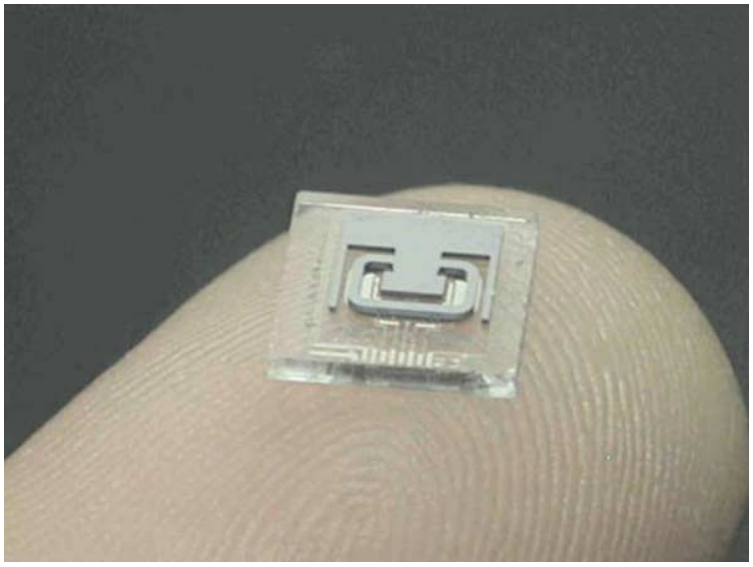

Figure 3.3 Microfluidics sensor

The study investigated the ability of the sensor to distinguish between gasoline, ethanol, butanol, diesel, biodiesel, water and air. In addition blends of these fuels were utilized. Results showed that the density measurement with linear correction for temperature was sufficient to distinguish all of the aforementioned fuel types. The viscosity measurement may be helpful in determining biodiesel blends. In addition the sensor was tested for sensitivity to vibration and flow rate and was found to be more reliable in these conditions than resonant tube density sensors.

CHAPTER 4: MATERIALS AND METHODS

A significant amount of testing using a variety of experimental tools was performed in order to evaluate and model the MEAS sensor's response to a variety of fuels and contaminants. Experiments were carefully laid out to obtain reliable, repeatable data. This section presents descriptions of the method of operation of the sensors used and the preparation of fuel samples. In addition the format of each experiment is described in some detail. Finally, the remainder of the chapter addresses the use of sensor data to formulate a system capable of identifying the composition and quality of fuel samples.

4.1 Sensor Operation

The primary sensor (Figure 4.1) used in this study was developed by Measurement Specialties (model no. FPS2800), a leader in sensor development over a number of areas including fluids. This sensor provided three outputs: dynamic viscosity, density, and dielectric constant, since it was theorized that the information from multiple outputs might allow much more information to be gleaned about the liquid. The sensor supplied a standard CAN J1939 protocol so it was ideal for use in vehicular applications (Measurement Specialties, 2009).

The MEAS sensor could be classified as a resonant dielectric cavity sensor. This type of sensor utilizes a small tuning fork which is placed in fluid and caused to vibrate. Properties of vibration could be related to properties of the fluid (Measurement Specialties, 2009). In addition this sensor was designed with threads and seals to make it ready for implementation into applications. The tuning fork and sensing elements were protected by a shield.

Figure 4.1 Measurement Specialties fluid properties sensor

Specifically, the solid state piezoelectric tuning fork resonator operated on the principle of resonance of two thin metal protrusions placed in a liquid environment. As described by Measurement Specialties (2009) sensor specifications, vibrations were induced through an electrical circuit including capacitors, inductors, and resistors in series. When a voltage was applied to such a circuit the tuning forks could be made to oscillate at a specific frequency. This oscillation displaced the fluid; moreover, the resonance of this oscillation was dependent on the fluid present. The inclusion of such a fluid in the circuit could be represented as additional impedance added to the system. The electrically equivalent circuit is shown below in Figure 4.2.

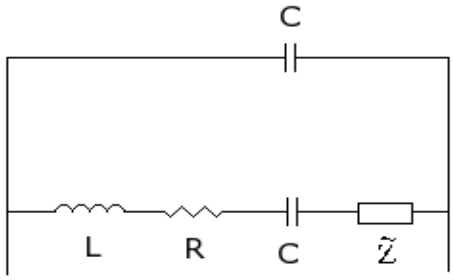

Figure 4.2 Sample electrical circuit representing liquid impedance

Figure 4.2 is a simple model that represented capacitors (C), inductors (L), resistors (R), and impedance (Z) where the impedance was from the influence of the fluid around the tuning fork. The impedance was found experimentally to be related to the sum of two terms. One that was proportional to the liquid density and the other to the square root of the liquid viscosity. This model allowed the measurement of both density and viscosity independently.

4.2 Fuel Acquisition and Preparation

Fuels of many types and blends were used for testing and had to be obtained before experimentation could begin. Base fuels were acquired from the Waterloo Oil Company; (Waterloo, IA), and these included diesels #1 and diesel #2 at 15 ppm, 500 ppm, and 5000 ppm sulfur levels, SME B-100, and Jet A fuel. Fuels were stored in a cold dark environment to minimize degradation. In addition, new fuels were ordered every two months to ensure quality.

Blends of diesel #1 or #2 with SME were prepared in the Agricultural Engineering Sciences Building Tractor Laboratory at the University of Illinois. Blend levels were determined by volume and were measured using a 250 ml graduated cylinder with 1 ml resolution. Each test required 400 ml samples of each relevant blend.

Furthermore, the properties of several different biodiesels from variant sources were of interest. Since these fuels were not commercially produced in the United States the samples had to be prepared from direct oil sources. Oils chosen for conversion were soybean, rapeseed, false flax, and jatropha. Soybean and rapeseed were used since they were the primary sources for biodiesel in the US and Europe respectively. False flax and jatropha were chosen since they were available through known sources, and they were different than any other samples previously experimented with in this laboratory. Soybean oil was purchased from a grocery store, and the other oil sources were obtained through John Deere Power Systems (Waterloo, IA).

The soybean, rapeseed, and false flax oil samples were converted to biodiesel using a transesterification reaction in which methanol and oil were reacted together at a temperature of 50°C with a sodium hydroxide catalyst. The ratio of the reactants used was 250 ml of methanol and 4.0 grams of sodium hydroxide per liter of oil. The reaction occurred over the course of 30 minutes with stirring performed every 5 minutes. This procedure was perfected in previous studies by other graduate students in the same department (McCrady, 2010). The products of this reaction were glycerol and methyl esters (Figure 4.3).

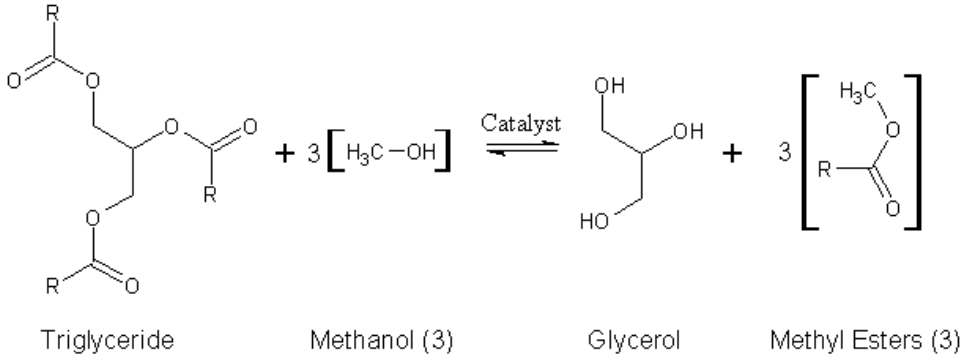

Figure 4.3 Oil transesterification reaction

The products of the reaction were placed in a separation vial and allowed to settle. Glycerol has a higher density than that of biodiesel so it could be drained from the bottom of the container. Next, water droplets were sprayed through the fuel sample numerous times to clean the excess methanol, soap, glycerin, or catalyst. Finally, air was bubbled through the sample using a fish tank air pump to remove the water from the fuel.

The conversion of jatropha oil was initially undertaken in the same manner as described for the other oils; however, the product of the reaction was very high in soap content yielding a solid mass of partially converted biodiesel and waste. Subsequent research into jatropha oil showed that this oil was extremely high in free fatty acid content compared to other plant oils. Free fatty acids refer to non-esterified fatty acids that have been separated from triglyceride molecules in the oil. Tiwari et al. (2007) approximated the free fatty acid content of jatropha oil to be 14% compared to less than 1% for most plant oils. Hence, conversion of this oil had to be performed in a two step acid pretreatment- base transesterification process. Sulfuric acid was used to convert the majority of the free fatty acids to usable compounds.

The first step in this two step process was to perform a titration with the base that was to be used for transesterification. As described by Alovert (2005) this titration could be performed by mixing 1 ml of oil with 10 ml 99% isopropyl alcohol and a small amount of pH indicator. This blend was then titrated with a 1gram per liter solution of sodium hydroxide in distilled water. The volume of base required to trigger the pH indicator while stirring allowed the volume of acid to be determined for addition. Titrations of jatropha oil with sodium hydroxide yielded an average of 9 ml required to reach neutral pH. Furthermore, the appropriate amount of acid can be approximated by the difference between the actual titration and desired titration.

Therefore, in order to reach a titration of 2 ml sodium hydroxide, sulfuric acid at a ratio of 7 ml per liter of oil was used.

The pretreatment step was performed by mixing methanol with the sulfuric acid. Then this mixture was added to the oil at a temperature of 60°C. The reaction was kept at 60°C for 3.5 hours. Titrations were performed periodically to monitor the progress of the reaction. Table 4.1 shows titration results during acid pretreatment.

Table 4.1 Sodium hydroxide titration results during acid pretreatment of Jatropha oil

	Time passed since beginning of reaction					
Time (hrs)	0	1.5	2	2.5	3	3.5
Titration volume with NaOH	9 ml	3.5 ml	3.3 ml	3.0 ml	2.2 ml	2.0 ml

Once the desired titration was reached the product was placed in a separation vial and allowed to settle overnight. A small amount of glycerol was drained from the sample.

The second step was performed similarly to the reaction that was used to convert the soybean, rapeseed, and false flax oils. Methanol and sodium hydroxide were mixed and then added to the product of the pretreatment step at a temperature of 55°C. The reaction was maintained at this temperature while vigorous stirring was performed by hand once every 5 minutes. The resulting products were placed in a separation vial and allowed to settle for 48 hrs. Glycerol was then drained off and the fuel was washed using water droplets. Finally, the water was removed by bubbling air through the sample using a fish tank air pump. Table 4.2 details each of the reactions used to convert oil to biodiesel.

Table 4.2 Oil conversion reactants and conditions

	Methanol[a]	NaOH[a]	H_2SO_4[a]	Temperature	Duration	Other conditions
1-step transesterification	250 ml	4.0 g	none	50°C	30 min	Periodic stirring
Acid pretreatment	100 ml	none	7 ml	60°C	3.5 hrs	Periodic stirring
Transesterification after pretreatment[b]	150 ml	6.0 g	none	55°C	30 min	Periodic stirring

[a] Measured per 1 liter of oil
[b] Used for Jatropha Oil conversion only

Each of the resulting biodiesels had a different chemical makeup. As discussed in Section 3.3.3 both the distribution of carbon chains making up the fuel and the degree of saturation could have a significant effect on bulk fuel properties. In addition as was discovered with jatropha oil the free fatty acid concentration in an oil source could have large impacts on the conversion process to biodiesel. Moreover, the refined fuels were analyzed for fatty acid composition (AACL, 2011). Table 4.3 gives the results of testing.

Table 4.3 Measured Fatty Acid Compositions of Biodiesels (AACL, 2011)

	Percent Fatty Acid Composition					
	16:0	16:1	18:0	18:1	18:2	18:3
Soybean	12.31	0.16	5.05	23.56	52.13	6.74
Rapeseed	5.72	0.27	2.09	59.91	21.59	10.47
False Flax	8.70	0.17	3.53	15.63	23.31	47.64
Jatropha	16.68	1.08	7.01	39.15	35.55	0.50

4.3 Fuel Type Property Measurement

Initial testing was performed using the base fuel types: diesel #1 (15, 500, 5000 ppm sulfur), diesel #2 (15, 500, 5000 ppm sulfur), SME B-100, and Jet A fuel. This experimentation gave an initial evaluation of the sensor's ability to distinguish between fuels of interest and an

opportunity to investigate the effect of temperature on fuel properties. In addition the diesel samples of varying sulfur content were added to provide base information about the ability of the MEAS sensor to detect high sulfur fuels. Samples of 400 ml volume were prepared of each fuel and tested at 20°, 40°, and 60°C. The outputs were recorded and plotted in a 3D space with each sensor output as an axis for analysis. These baseline tests showed few significant differences between the diesel samples of varying sulfur content so continued testing was performed only on the 15 ppm sulfur (ULSD) samples in addition to the SME B-100 and Jet A fuels. Next, these four fuels were tested in 10° C increments from 20°-80°C. The laboratory used did not have the ability to cool fuel samples below ambient conditions easily and 80°C was deemed to be approximately the upper limit of the temperature a fuel sample might be subjected to in a normal application environment. Temperature was controlled using an Omega water-bath and thermoregulator. Additionally, special care was taken to allow the temperature of the entire system: water bath, fuel sample, beaker, and sensors to come to equilibrium prior to taking data. Fuel samples were continually stirred using an IKA RW 20 digital overhead stirrer at 100-150 rpm. This was necessary in order to assure proper sensor function as this prevented any contaminants or air bubbles from becoming lodged on the tuning fork leading to inaccurate results. CAN data were collected using a Vector CANcaseXL and were processed with John Deere proprietary Phoenix Utility 2 software. Three sensors were used for each test and data were taken for 10 minutes at each temperature.

4.4 Fuel Blend Property Measurement

After completing testing with the base fuel types an investigation of blended fuel properties were conducted. Blends of diesel #1 or diesel #2 with SME biodiesel are the most common blended fuel types used in the US and were therefore the focus of this work. Blends

were made by volume using a 250 ml graduated cylinder with one ml resolution and samples of the two neat, unblended fuels. Once more 400 ml samples were used. Some samples were tested at 0°C to verify that models formed from 20°-80°C would be valid at lower temperatures. The same experimental setup and data processing were used.

Blends of diesel #2 with SME ranged from B-0 to B-100 in 10% (v/v) increments. A B-5 sample was also included since blend levels from B-0 to B-10 are popular with diesel engine manufacturers and operators. Special care was taken to allow each sample reach the same temperature each time which often required 30 minutes or more between changes of 10°C.

Blends of SME with diesel #1 were also tested in a very similar manner. The same equipment was used. The temperature range was 20°-80°C in 10°C increments. However, blends studied were B-0, B-2, B-5, B-10, and B-20 because higher biodiesel levels were much less common and thus deemed less important to include in the experimentation.

Several samples including B-0 and B-100 were tested at 0°C using an ice bath. This test presented some problems because the beaker used was stainless steel, and water tended to condense on the lip of the beaker at this low temperature. Moreover, this often led to water contamination which affected the measurement. A glass beaker was used to overcome the water condensation issue, and subsequent data was used to verify that the trends developed over 20-80°C were appropriate down to 0°C or below as long as the fuel had not reached its cloud point.

4.5 Fuel Contamination Experimentation

In order to test the sensor's ability to detect contaminants of varying form and concentration, its performance with fuel samples under several contamination conditions was evaluated. Several substances of interest included water, sulfur, urea, glycerol, and methanol.

Each of these potential contaminants was chosen due to the likelihood that they would occur in normal fuels.

Water is the most common fuel contaminant and can manifest itself in the transport and storage of formerly clean fuels through condensation. Sulfur is present in petroleum based fuels and is now highly regulated, although, older fuels or fuels from other countries would yet contain high sulfur content. Glycerol and methanol are possible contaminants of biodiesel due to their presence in the transesterification process. Urea is used as the active ingredient in diesel exhaust fluid which is employed in selective catalyst reduction (SCR) after-treatment systems to remove NOx from diesel systems. Additionally, it is possible that urea might be poured into the fuel tank by accident.

Contaminants for use in the experimentation were obtained through several sources. Distilled water was purchased from a Walmart (Savoy, IL). Sulfur doping agent was obtained from British Petroleum (BP) (Naperville, IL) in the form of di-tertiary-butyl-disulfide (Foster, 2010). This compound was considered suitable as a sulfur analog in diesel fuel through testing BP had previously conducted (Foster, 2010). Also, choosing the correct way to mimic sulfur in fuels was relatively difficult given the number of compounds that contain sulfur within diesel fuel. Pure glycerol and methanol were purchased through Fischer Scientific. Finally, liquid urea was purchased in the form of diesel exhaust fluid (DEF) from BlueDEF (Northbrook, IL) rather than pure urea which is typically a granular solid. DEF contained about 50-60% urea, and this was regarded as acceptable since DEF contamination was the case of interest anyway.

Water, sulfur, glycerol, and methanol are regulated by either ASTM or government standards (ASTM, 2010a; ASTM 2010b). Moreover, concentration levels for testing were based

on these standards. Table 4.4 gives the maximum accepted limits for each of these contaminants in fuel.

Table 4.4 Fuel contaminants standards (ASTM, 2010a; ASTM, 2010b)

Contaminant	Water	Sulfur	Glycerol (total)	Methanol	Urea
ASTM Standard Limit	500 ppm	15 ppm	1,900 ppm	2,000 ppm	NA

Based on these limits the concentrations to be tested were set. The sensor was tested at concentrations of contaminants at or below the set standard and at higher levels for each case except sulfur. It was not feasible to accurately measure 15 ppm contamination levels with the available lab equipment so sulfur could not be tested at its regulated level. In addition, concentration levels were chosen based on the expected ability of the sensor to detect that particular substance (Table 4.5).

Table 4.5 Fuel contaminant concentration levels

	Concentrations tested (ppm by volume)				
Water	0	250	500	1,000	10,000
Sulfur	0	1,000	2,000	5,000	10,000
Glycerol	0	250	500	1,000	10,000
Methanol	0	1,000	2,000	5,000	10,000
Urea	0	1,000	2,000	5,000	10,000

Next, the appropriate fuel samples for testing with each contaminant were selected. Water and urea were potentially applicable to any fuel as they were contaminants introduced through processes independent of fuel type. Sulfur was only present in high levels in petroleum based fuels. Glycerol and methanol were relevant only in biodiesel since they resulted from the transesterification method. Consequently, fuel samples were chosen based on these criteria.

Furthermore, several blends were tested in all cases except sulfur. Table 4.6 lists the fuel samples used to test contamination on for each selected contaminant.

Table 4.6 Fuel samples and level of contamination

	Diesel #2	B-30	B-50	B-70	B-100
Water	X	X	X	X	X
Sulfur	X				
Glycerol		X	X	X	X
Methanol		X	X	X	X
Urea	X	X	X		

"X" indicates tests were conducted on that fuel

Water was deemed the most important contaminant since it was the most likely contaminant to be incidentally introduced to fuel. Therefore, testing was conducted over the entire blend range. Sulfur was tested on the pure petroleum based fuel as a best case scenario for sulfur detection. Finally, glycerol and methanol were tested on fuels containing biodiesel.

The final testing variable to determine was temperature. In order to provide an adequate number of data points to be collected in the time available, each fuel sample at each contamination level was tested at 30°, 50°, and 70°C. This range was regarded as wide enough to illuminate any effect temperature would have on contaminant detection.

Testing was conducted on each fuel sample in the following manner. Fuels and blends were prepared in 400 ml samples. The clean, uncontaminated fuel was then tested through 30°, 50°, and 70°C using the same equipment as in the fuel type and blend studies. Then the fuel sample was removed from the water bath, and the amount of contaminant by volume necessary to meet the first contamination level recorded in table 4.2 was measured into a 1 ml or 5 ml graduated cylinder. The contaminant was then added to the fuel sample and vigorously stirred

by hand for several minutes. The sample was allowed to stand for approximately 30 minutes while the water bath was re-filled and brought to 30°C. Subsequently the sample was stirred vigorously for several more minutes. Next, the fuel was placed in the beaker within the water bath; moreover, the stirring device served to keep the samples well mixed while temperature equilibrium was reached and data collection performed. After testing at the three temperature levels the fuel was again removed and the procedure repeated for each contaminant level.

4.6 Fuel Degradation Experimentation

The chemical composition and physical properties of fuels change over time through instability and degradation. This study sought to determine whether any of the viscosity, density, or dielectric properties of fuel changed over time and were detectable by a fluid properties sensor.

Six fuel samples were prepared in 400 ml containers near the beginning of the project. The samples could be categorized into two classes: one with samples open to ambient air and the other being closed container samples. Three fuels were stored in open containers in a dark place within a laboratory environment where the temperature ranged from about 18° to 26°C throughout the year. The containers had a shield over them to prevent dust contamination, but they were allowed to evaporate and absorb water from the air. Three fuel samples in closed containers were also placed in the laboratory environment and were in a dark place, but they were closed to the air with very little head space in the container. The goal of testing these two conditions was to mimic the environment fuel would see in the storage tank of a machine. Furthermore, it was not clear which of the two situations was more appropriate in a field situation; therefore, testing both was facilitated. Each of the two cases contained a sample of

diesel #1, diesel #2, and SME B-100. Testing each of these base fuels was expected to give an indication of how blends might be susceptible to degradation as well.

Samples were tested at the beginning of the study and then approximately once per month for the duration. The closed container samples were initially tested in August 2009, but the decision to begin the degradation testing was not made until winter of that year so there was no data for the first several months in the closed container case. The open containers were tested as fresh fuel in February 2010. Each study continued until April 2011 thus providing approximately 20 months of data collection for the closed container samples and about 14 months for the open containers. Data collection for the closed containers was taken at a temperature of 40°C while the data for the open containers were measured at 30°C. This discrepancy was brought about because of the initial data being taken before the decision to use the samples for a degradation test. Nevertheless, the percent change of a property over the time period was regarded as relevant in evaluating the degradation effect. Testing was performed with a water bath, beaker, and stirring device, and temperature was closely controlled to improve accuracy of the viscosity comparisons which were highly dependent on temperature (Table 4.7).

Table 4.7 Degradation test conditions

	Fuel Sample	Light Condition	Temperature	Environment
Open container	Diesel #1	Dark	18-26° C	Open to ambient air and humidity
	Diesel #2	Dark	18-26° C	Open to ambient air and humidity
	SME B-100	Dark	18-26° C	Open to ambient air and humidity
Closed container	Diesel #1	Dark	18-26° C	Closed with little head space
	Diesel #2	Dark	18-26° C	Closed with little head space
	SME B-100	Dark	18-26° C	Closed with little head space

4.7 Development of a Classification Model

Fuel data collected with varying temperature or composition could be used to develop models and decision criteria for the design of algorithms that would identify the fuel type entering the engine and assess the quality of this fuel from a contamination and degradation standpoint. Many types of algorithms might be used for this purpose although only regression models and neural networks were investigated in this study. This section describes the methods used in processing the data and developing algorithms.

4.7.1 Algorithm Format

Development of a basic algorithm for engine applications required that the sensor outputs be first used to determine the type of fuel tested. Then this information allowed the algorithm to assess the quality of the fuel by comparing the outputs to the normal properties for that fuel. Furthermore, the sensor had to be able to perform this function over the entire applicable temperature range. For modern engine applications in the US the sensor primarily needed to be able to distinguish diesel #1 from diesel #2, and then give the blend percentage of each with biodiesel. In addition, contamination by water and degradation were deemed to be the most important of the quality issues tested so the algorithm focused on first being able to detect these two conditions.

4.7.2 Regression Models for Fuel Properties

Models were used to estimate the properties of clean fuels for a given temperature. These models can then be employed to estimate the type of fuel and blend of fuel for an unknown sample. As was seen in the literature review linear models accurately described the temperature dependence of both density and dielectric properties of fuel. Viscosity was represented by a non-

linear model. For each of these properties with changing blend density and dielectric constant were again linear while viscosity was not. The models utilized to predict properties with temperature and blend are detailed as follows (Table 4.8).

Table 4.8 Models for fuel property estimation (Tat and Van Gerpen, 1999; Tat and Van Gerpen, 2000)

		Model Applied
Dynamic Viscosity	Temperature	$\eta = Ae^{BT} + Ce^{DT}$
	Blend	$\ln \eta_B = V_1 \ln \eta_1 + V_2 \ln \eta_2$
Density	Temperature	$\rho = b + mT$
	Blend	$\rho = b + m * B\%$
Dielectric Constant	Temperature	$\varepsilon = b + mT$
	Blend	$\varepsilon = b + m * B\%$

T is the measured temperature, *B%* is the blend level by volume, V_i is the volume fraction of the ith component, η_i is the dynamic viscosity of the ith component, ε is the dielectric constant, ρ is the density, and *A, B, C, D, b, m* are constant coefficients fit to the data. These models were chosen based on the literature available and the accuracy of fit. The temperature correlation for viscosity was included in MATLAB and provided a better fit to the data than other models that were applied.

4.7.3 Sensitivity and Limits of Regression Models

Two additional issues with applying regression models were defining the limits for which the model was valid and determining the amount of sensitivity it should have. The models developed for temperature were fit from data taken from 20°-80°C. The temperature range that fuels would experience in either ambient conditions or in the fuel handling system of an engine

ranged approximately from -30° to 80°C. Fuel samples were tested in limited cases to check the accuracy of the model at 0°C, but testing below that temperature was not possible with the lab setup available. However, the models should be accurate down to the cloud point of the fuel, which is a property dependent on fuel type. Biodiesels typically have a cloud point near 0°C while diesel fuel has a much lower cloud pt approximately -17°C. Joshi and Pegg (2007) used a quadratic polynomial to predict the cloud point for blends of biodiesel and diesel given the cloud points of the neat fuels. However, the quadratic coefficient was nearly zero and the data appeared to be nearly linear. Therefore, a simple linear interpolation was used in this study to estimate the cloud point of blends of fuel. This temperature was the lower limit of validity for the sensor algorithm.

Another problem was setting the ranges for what the algorithm would consider normal variation in fuel properties and where it would interpret variation as due to contaminants or degradation. This required some knowledge of the natural variation of fuel properties. There was little to no literature related to the amount fuel properties vary; however, it was reasonable to conclude that there was more deviation in the properties of biodiesel since it is refined from various oil stocks and the refining technology was much newer. Also, the fatty acid composition of oils was known to vary significantly. Properties of diesel fuels from petroleum sources may also have variation; however, it was deemed that these deviations were likely less than those present in biodiesel.

In the case of biodiesel although no literature was found on the subject of property variation some research existed as to the variation of composition within biodiesels refined from specific oil sources. Graboski and McCormick (1998) compiled measured fatty acid compositions for soybean and rapeseed biodiesels. This range in compositions could be used to

estimate the range in properties given known trends about the effect of composition on viscosity and density. Yuan (2005) developed BDProp software (University of Illinois, Champaign, IL) to predict properties of biodiesel based on fatty acid composition. This software was used to calculate the natural range in viscosity and density for biodiesel from soybean and rapeseed sources using the fatty acid data from Graboski and McCormick (1998). These ranges were used to determine the composition that would yield the highest and lowest viscosity and density possible for each fuel type (Tables 4.9 and 4.10).

Table 4.9 Fatty acid compositions used for estimation of high and low limits for biodiesel dynamic viscosity estimation

		14:0	16:0	18:0	20:0	22:0	16:1	18:1	18:2	18:3	22:1
SME	High	0.003	0.070	0.060	0.050	0.050	0.000	0.247	0.500	0.020	0.000
	Low	0.003	0.070	0.030	0.025	0.025	0.000	0.220	0.600	0.100	0.000
RME	High	0.000	0.050	0.010	0.005	0.005	0.002	0.150	0.100	0.050	0.600
	Low	0.000	0.050	0.010	0.005	0.005	0.002	0.100	0.200	0.100	0.500

Table 4.10 Fatty acid compositions used for estimation of high and low limits for biodiesel density estimation

		14:0	16:0	18:0	>18:0	16:1	18:1	18:2	18:3	>18:1
SME	High	0.003	0.070	0.030	0.050	0.000	0.220	0.527	0.100	0.000
	Low	0.003	0.110	0.060	0.087	0.000	0.220	0.500	0.020	0.000
RME	High	0.000	0.020	0.010	0.009	0.002	0.100	0.200	0.100	0.559
	Low	0.000	0.050	0.020	0.009	0.002	0.150	0.119	0.050	0.600

The outputs from BDProp for the natural range of viscosity and density for soybean and rapeseed biodiesels provided some estimation of how sensitive the models should be. There was no existing tool for estimation of the dielectric constant from fatty acid composition.

4.7.4 Sensor Outputs to Identify Contamination or Degradation

The largest challenge in algorithm design for the MEAS sensor was accurately identifying the presence of contaminants. When contaminant was added in most cases all three properties of the fuel were affected. If none of the properties was completely unchanged by contamination then the only information left to recognize the problem was a comparison of the three outputs. Each of the viscosity, density, and dielectric constant were modified in varying degrees by the addition of contaminant and this difference could be used by the algorithm. Also, the amount of change relative to the size of the range in property values between the two neat fuels in a blended fuel was the most important characteristic for blend determination. In order to define this fact a variable (*E*) for each sensor output and contaminant was calculated to show the ratio of these differences. *E* estimated the blend prediction error introduced into each output by contamination. *E* was simply calculated for dielectric constant and density outputs by using the linearity of each property with blend. Viscosity required application of the Grunberg-Nissan equation.

$$E_{dielectric} = \frac{\varepsilon_{cont.} - \varepsilon_{clean}}{\varepsilon_{SME} - \varepsilon_{diesel\,\#2}} \quad 4.1$$

$$E_{density} = \frac{\rho_{cont.} - \rho_{clean}}{\rho_{SME} - \rho_{diesel\,\#2}} \quad 4.2$$

$$E_{viscosity} = \left[\frac{\ln \eta_{blend} - \ln \eta_{diesel\,\#2}}{\ln \eta_{SME} - \ln \eta_{diesel\,\#2}}\right] - B\%_{actual} \quad 4.3$$

Where E_i gives the blend prediction error for the ith output, ε is the dielectric constant, ρ is the density, η is the dynamic viscosity, and $B\%$ is the blend percentage by volume of SME in diesel #2. In order for contamination to be detected at least two of these values would need to be significantly different from each other. Furthermore, if contamination induced the same error in all three outputs this fuel would be indistinguishable from a clean fuel at higher blend level.

For the case of contaminated fuel the blend prediction based on direct outputs was expected to be less accurate and was at best the minimum of the errors in blend prediction. More accurate fuel identification required adjusting the values of the sensor outputs if contamination was detected. One possible way to do this was to measure the average fuel properties for a range of contamination levels, blends, and temperatures. Then the measured values could be compared to a calculated value from another measured property. For example from the literature review it was expected that the dielectric constant will be affected most by water contamination. Therefore the algorithm could compare the measured value of dielectric constant to the dielectric constant estimated from the measured viscosity output. This comparison is the difference given by $D_{dc,\,\eta}$.

$$D_{dc,\eta} = dielectric\ constant\ measured - dielectric\ constant\ calculated\ from\ viscosity \quad 4.4$$

Experimentation could lead to a plot of $D_{dc,\eta}$ over a range of temperatures and contamination levels. Therefore, for an unknown fuel sample this value could lead to an estimate of contamination level. Once the contamination level was known the correlation for contamination level and change in each property would be used to estimate the actual clean fuel properties. Finally, the recalculated properties would be used in the interpolations described in Section 5.2.2 to provide the fuel blending level.

4.7.5 Neural Networks for Fuel Classification

Another approach to the problem of data classification and algorithm development was the use of a neural network fitting tool. Neural networks provided an alternative to algorithm development for fuel data sets that was desirable due to the ease of application and the ability to generate an accurate model while utilizing the computing power of software. A neural network operates on the basis of layers of neurons containing weighted transfer functions. Each of these neurons is interconnected. Given the inputs and outputs from a set of example data, training the network can be performed which adjusts the weights and structure of the neurons to fit the data. Once the network has been trained it can be applied to any other set of data and it will predict the outputs. Neural networks provide prediction capability without requiring the user to understand the details of the system.

The neural network fitting tool in the MATLAB neural network package was used to generate a prediction network for data taken from the water contamination experimentation. MATLAB provided a graphical user interface (GUI) for development of such a method. The inputs to the network were chosen to be the four sensor outputs: dynamic viscosity, density, dielectric constant, and temperature. Furthermore, two outputs were chosen for the network to predict: blend percentage (diesel #2 and SME B-100) and contamination level. Blend percentage is a number between 0 and 100. The contamination level was first quantified as a number between 0 and 10,000 based on the ppm concentration of the water. However, this method was found to be much more successful if the contamination level was classified in the following way. If fuel is uncontaminated it had a contamination level of zero. If the fuel was contaminated at 250, 500, or 1000 ppm then it was referred to as contamination level 0.25, 0.5, and 1.0

respectively. Finally, if the fuel was at the 10,000 ppm water addition the contamination level was denoted as 2.0.

The network was trained using the default settings in MATLAB for training algorithm and division of data between training, validation, and testing. Levenburg-Marquardt back-propagation was the algorithm MATLAB applies. Seventy percent of the input data was used for training, 15% for validation, and 15% for independent testing. In total 25 neuron layers were recommended by the program. Finally, sets of input/output vectors were applied to the network tool and the software completed the model fitting. The accuracy of the model was confirmed through the testing data selected by the program.

CHAPTER 5: RESULTS AND DISCUSSION

The following sections detail the results of the experimentation undertaken. Data are presented for the MEAS sensor. Additionally, methods for the development of an algorithm based on this study's results are presented. All results are discussed and implications are examined.

5.1 Fuel Type Properties Measurement

Baseline experimentation was conducted to indicate the ability of the sensor to accurately distinguish between base fuels of interest. Diesel fuels with varying sulfur content were tested. Also, dynamic viscosity, density, and dielectric constant for oils and biodiesel from several plant sources were characterized using the MEAS sensor.

5.1.1 Sensor Output for Petroleum Based Fuels and Biodiesel

Determination of different fuels is the most valuable function of fuel composition sensors. For the application of diesel engines a large number of potential fuels exist, although the most common were fuel oils refined from petroleum and biodiesel refined from plant oils. The properties of diesel #1, diesel #2, Jet A, and SME biodiesel were measured using the MEAS sensor and results are tabulated below. Figure 5.1 gives the measured viscosities over a range of 20°-80°C.

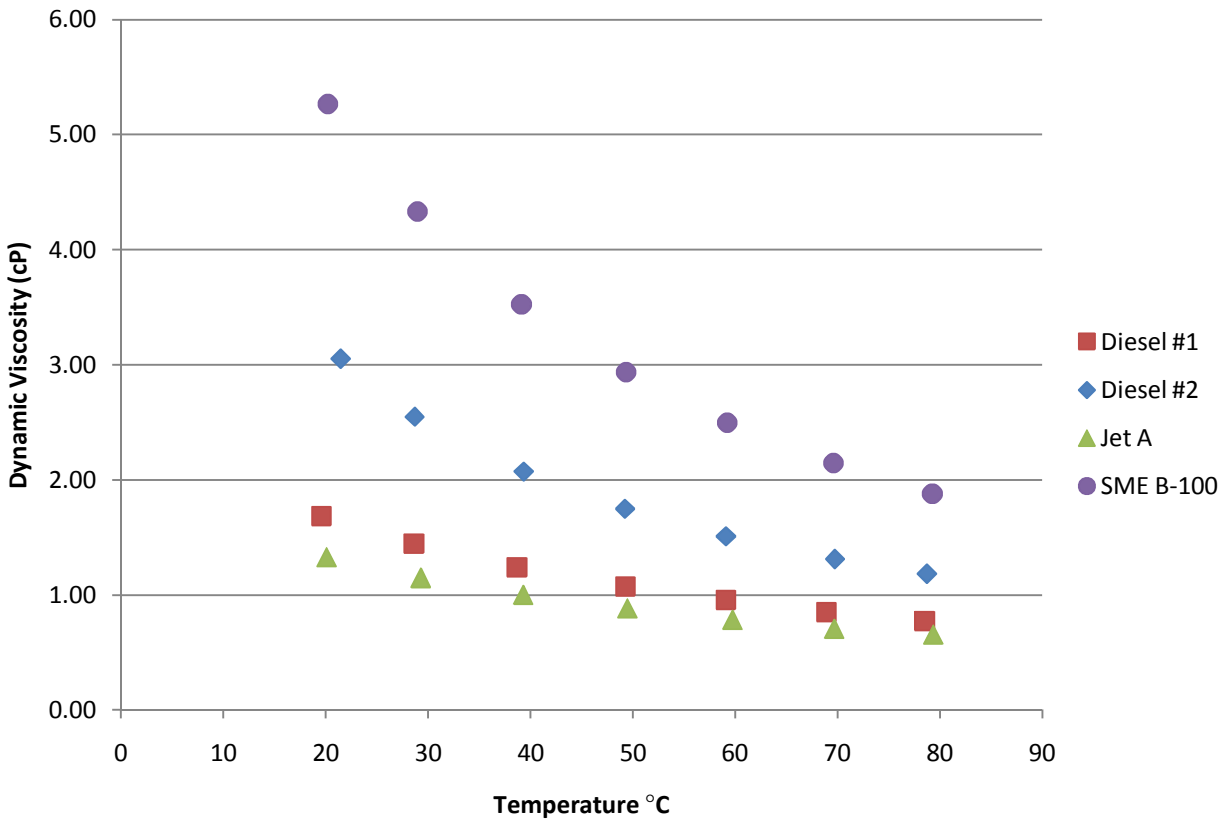

Figure 5.1 Dynamic Viscosity of several fuels under varying temperature

From Figure 5.1 it can be seen that the SME biodiesel had significantly higher viscosity than that of the other fuels. Diesel #2 had the next highest viscosity while diesel #1 and Jet A fuel had similar viscosity properties (within 5%). In addition, the rate of change of viscosity with temperature was higher for fuels with higher viscosities. These results agreed with previous studies such as reported by Tat and Van Gerpen (1999) who used the Modified Andrade Equation (Eqn. 3.4) to model viscosity- temperature relationships for fuel. The MEAS sensor's viscosity output was able to distinguish between any of the four measured fuels over the applicable temperature range.

Density measurements were also taken over the temperature range of 20°-80°C. Results of this experimentation are presented in Figure 5.2.

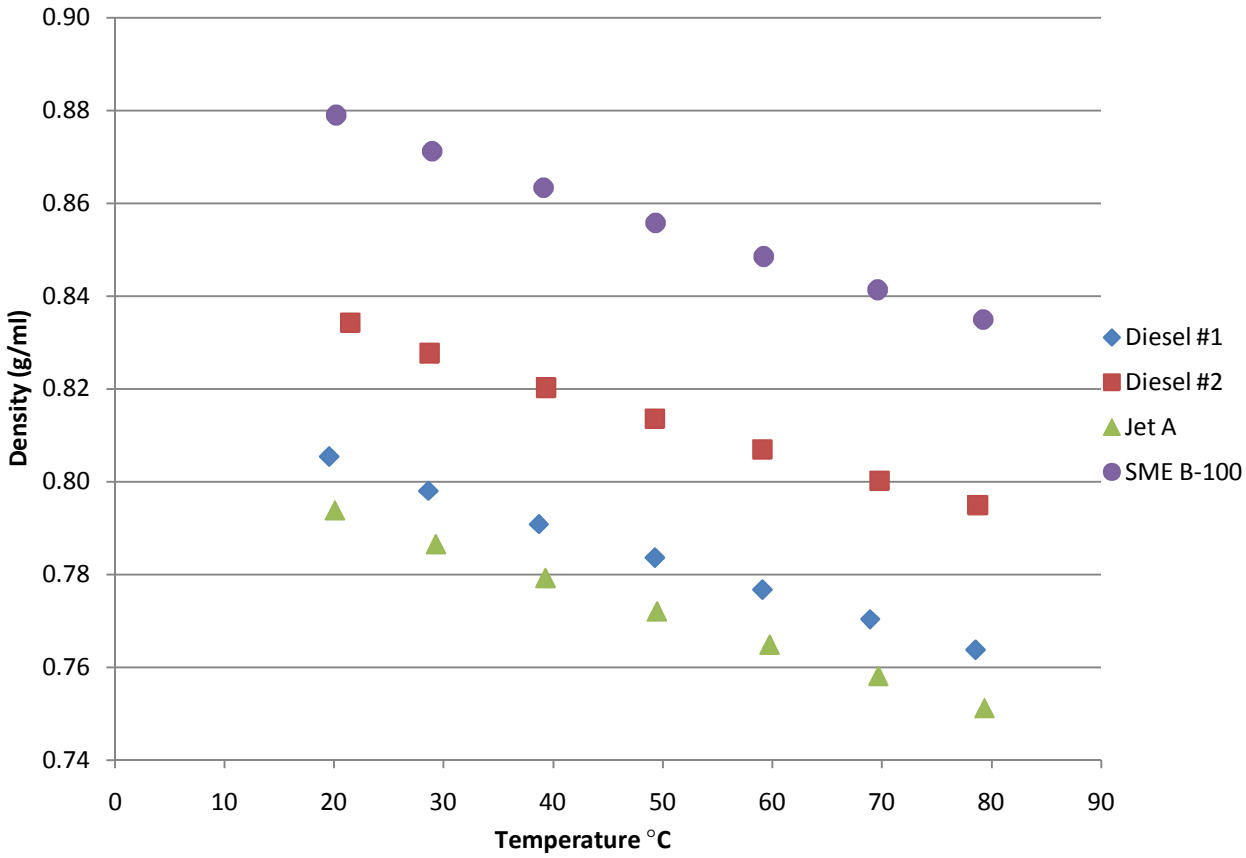

Figure 5.2 Density of several fuels under varying temperature

Again, the SME biodiesel was significantly different from the petroleum based fuels with respect to density. In addition, diesel #2 was the next most dense followed by diesel #1 and Jet A fuel. This same trend was seen with viscosity. The rate of change of density with temperature was very linear for all fuels. The figure suggested that the slope of the linear change with temperature was nearly the same between all of the measured fuels (variation of less than 0.5%). Once more, the MEAS sensor was able to distinguish between these fuels using the density output in conjunction with its temperature measurement.

The MEAS sensor utilized a dielectric measurement in addition to density and viscosity. Dielectric constant measurements for the four fuel types over a temperature range of 20°-80°C are summarized in Figure 5.3.

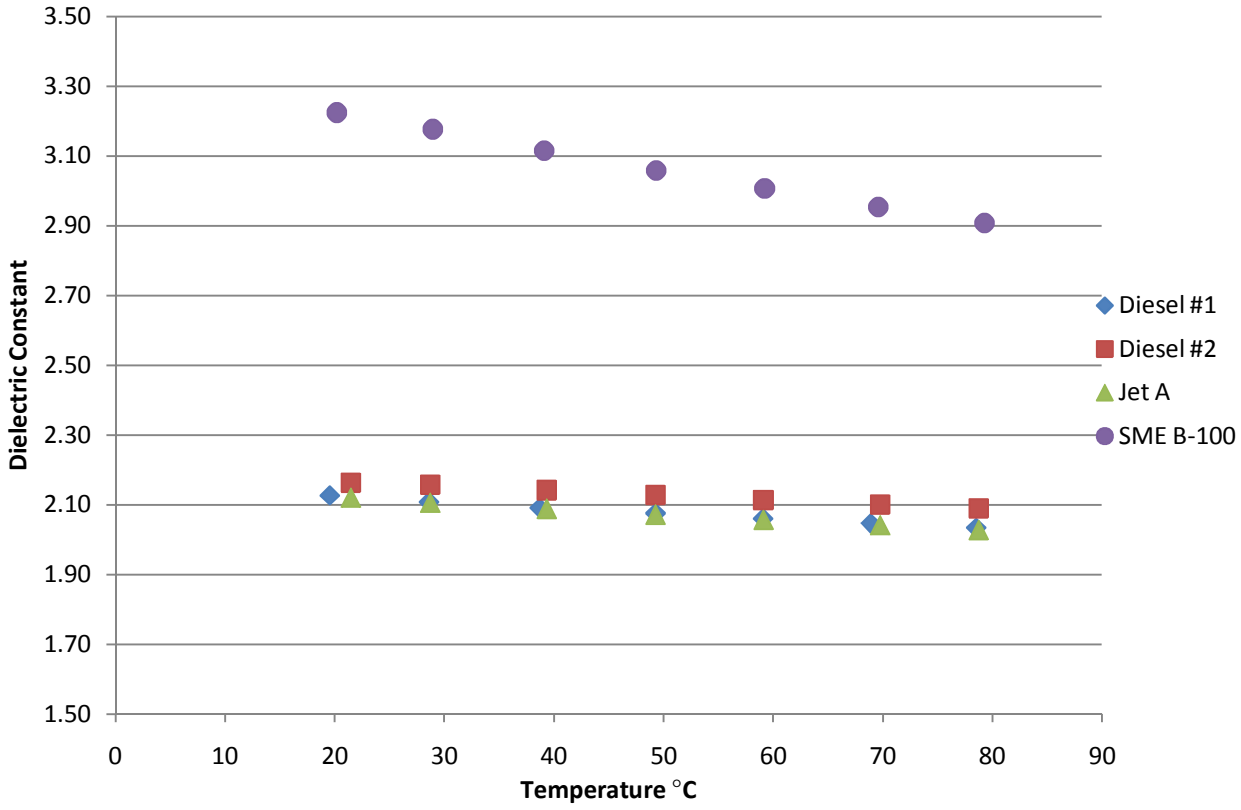

Figure 5.3 Dielectric constant of several fuels under varying temperature

Figure 5.3 indicates that SME biodiesel had a much larger dielectric constant than the petroleum based fuels. Each of diesel #1, diesel #2, and Jet A had very similar dielectric properties (within 1.0%). The rate of change of the dielectric constant of these fuels with temperature was linear in form and the slope of this linear fit was higher for biodiesel compared to the petroleum based fuels. These results showed that the dielectric constant output on the MEAS sensor would be very effective as a determinant for the identification of SME biodiesel

from petroleum based fuels; however, it would not be effective at discerning between diesel #1, diesel #2 and jet A fuels.

The behavior of the dielectric properties of these fuels agreed in general with that reported by the available literature. The higher dielectric constant of SME biodiesel indicates that its constituent molecules had a higher polarity than those in petroleum fuels. Polarity allows molecules to align with an electric field storing more energy and thus yielding a higher dielectric constant. However, all of these fuels would still be categorized as non-polar liquids. For non-polar liquid alkanes Sen et al. (1992) described the temperature dependence to be a function of the density of the liquid. Moreover, the decrease in density as temperature increases equated to a decrease in dielectric constant (Eqn. 3.6). However, the density of SME B-100 decreased with temperature at approximately the same rate as the other fuels so this model did not explain the higher dependence on temperature for the biodiesel's dielectric constant. Furthermore, this phenomenon was also related to polarity. For more polar liquids the average alignment of the molecules with the electric field decreased with temperature due to the amplified vibration and movement of the molecules as a result of larger kinetic energies at increased temperatures. Thus, as the polarity of a liquid increased both the actual value of the dielectric constant and its dependence on temperature increased.

5.1.2 Measurement of Diesel Fuels with Different Sulfur Content

Sulfur content in diesel fuel is of high interest to engine manufacturers, and as such was identified as an important variable for detection by the MEAS sensor. Initial tests on fuel type included several samples of diesel fuel with different sulfur concentrations in order to provide an initial basis for sulfur content detection. It was found that only the dielectric constant was

significantly affected by sulfur content. Figure 5.4 presents dielectric data for diesel #1 and diesel #2 at three different sulfur concentrations.

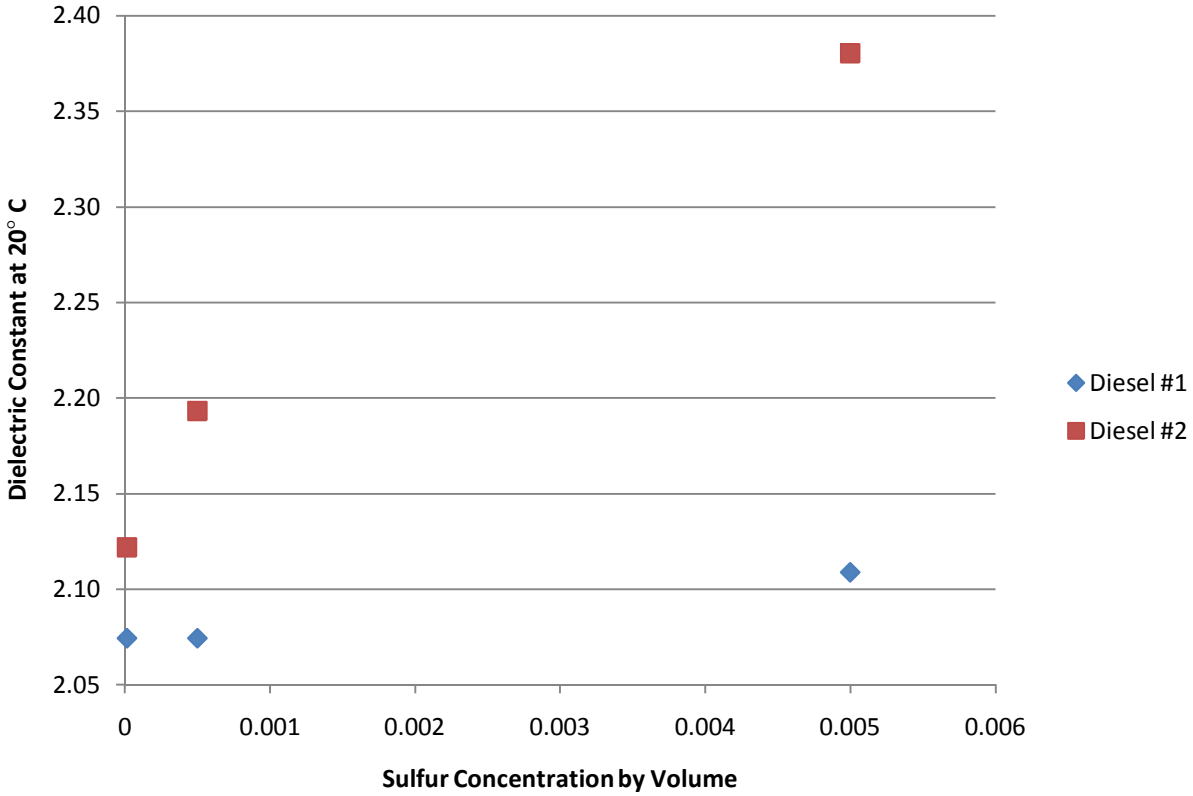

Figure 5.4 Dielectric constant of diesel fuel with varying sulfur content

Figure 5.4 suggests that increasing sulfur content led to an increase in the dielectric constant. However, the effect was much greater in diesel #2 compared to diesel #1. Additionally, this data implied that the MEAS sensor would be able to sense sulfur at concentrations of 500 ppm or greater for diesel #2 but not diesel #1. Diesel fuels were regulated to 15 ppm in the United States so detection to that level would be very desirable. Consequently, more testing was required to determine the effect of sulfur on fuel properties, and to set the lower

concentration limit for detection. Later in this thesis in Section 5.3.2 the effects of sulfur are covered in more detail.

5.1.3 Sensor Outputs for Biodiesels from Different Oil Sources

Biodiesel fuel samples from four plant oil sources were prepared for testing with the MEAS sensor. Figure 5.5 demonstrates the dynamic viscosity output results of experimentation on soybean, rapeseed, false flax, and jatropha methyl esters over a temperature range of 20°-80°C.

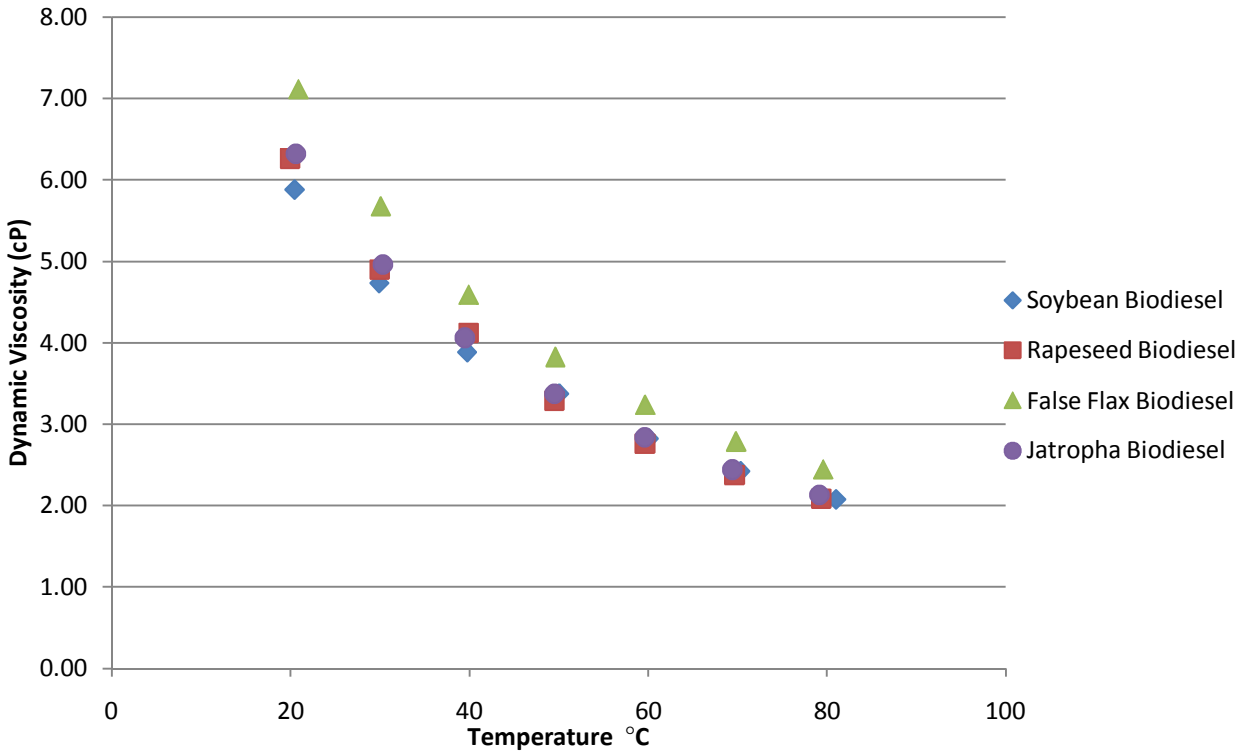

Figure 5.5 Dynamic viscosity of biodiesel from several oil sources

It can be seen that the measured viscosities of soybean, rapeseed, and jatropha biodiesels were very similar with small significant differences between them (variation less than 7.5%).

Moreover, the biodiesel refined from false flax oil was more viscous that the other samples suggesting its fatty acid composition may be different than the other fuels.

Knothe (2005) studied the effect of fatty acid composition on biodiesel properties. Knothe commented that viscosity was affected by both the chain length and degree of saturation of the fatty acids with viscosity increasing with both parameters increasing. Table 4.3 indicates that false flax biodiesel had a significant percentage of its composition made up of highly unsaturated fatty acids. High degrees of un-saturation suggested that this fuel would have a lower viscosity; however, the viscosity of false flax biodiesel was higher. This effect is unexplained except for the possibility that the fuel conversion was not as complete leaving some partially converted fatty acids in the false flax sample.

As was observed with the other fuels tested, viscosity changed non-linearly with temperature. Also, there was more deviation in the measurements between samples at lower temperatures. Of particular interest was the effect that using biodiesel from different sources would have on the accuracy of algorithms developed for SME biodiesel; therefore, calculating the percent difference of the sensor output between the other samples and the soybean biodiesel gave some insight into the problem. Table 5.1 details the percent difference in dynamic viscosity between rapeseed, false flax, and jatropha biodiesels and soybean biodiesel. The percent difference tended to decrease as temperature increases. However, these calculations indicated that rapeseed and jatropha biodiesel were similar to soybean biodiesel from the practical perspective of the sensor.

Table 5.1 Percent change in dynamic viscosity of several biodiesels over soybean biodiesel

Temperature °C	Rapeseed	False Flax	Jatropha
20	6.5	20.9	7.5
30	3.5	19.9	4.8
40	6.1	18.1	4.5
50	-2.8	13.2	-0.2
60	-2.2	14.6	0.5
70	-1.9	15.0	0.7
80	0.4	17.7	2.5

Previous studies also indicated that density was a function of fatty acid composition. Density outputs for the same set of fuels and temperatures are presented in Figure 5.6.

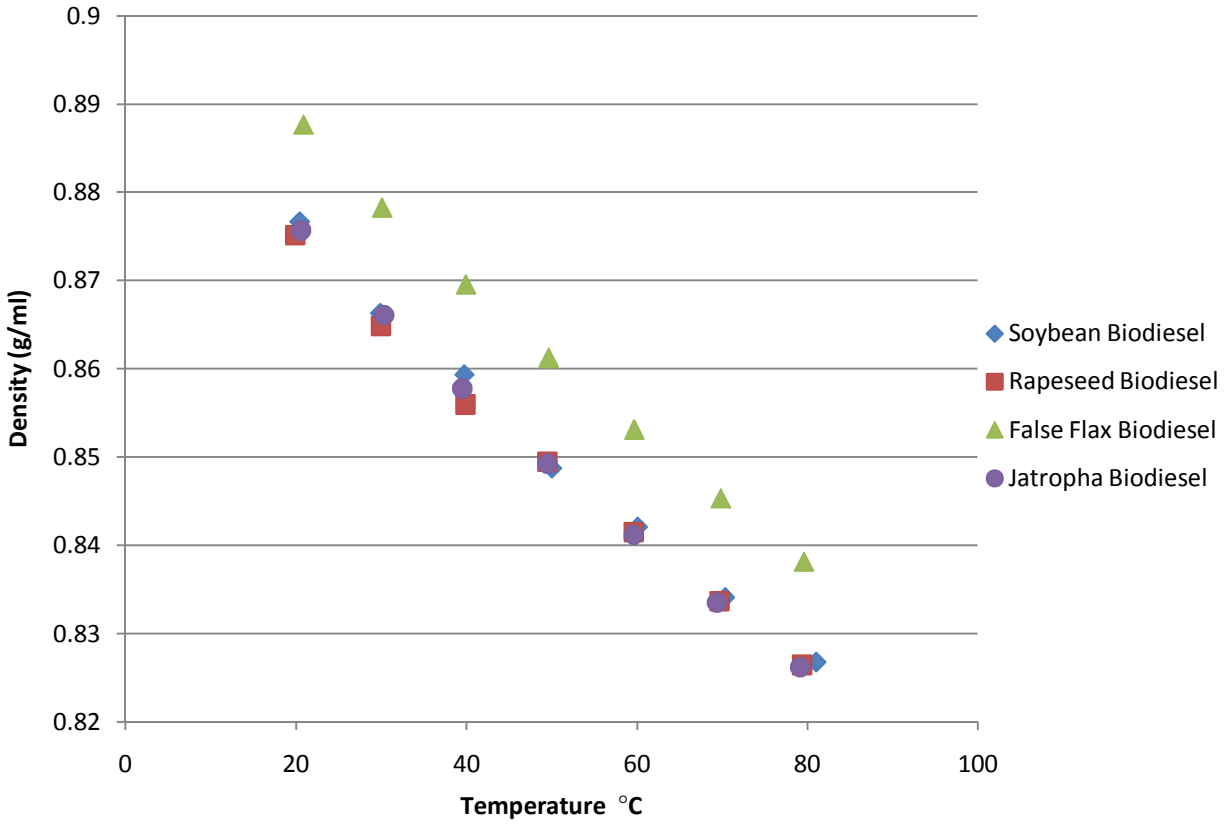

Figure 5.6 Density of biodiesels from several oil sources

Inspection of the plot indicates once again the soybean, rapeseed, and jatropha biodiesels had very similar properties as evidenced by nearly identical densities over the temperature range tested (variation less than 0.5%). Also, false flax had a higher density suggesting its chemical composition could be different from the other samples. Table 3.14 implies that as fatty acids became more unsaturated the density increased. False flax biodiesel's high percentage of poly-unsaturated fatty acids accounted for the higher density. Each fuel's density decreased linearly with temperature as expected from the available literature. With percent differences less than 2%, biodiesel differentiation based on density output by the MEAS was impractical (Table 5.2).

Table 5.2 Percent change in density of several biodiesels over soybean biodiesel

Temperature °C	Rapeseed	False Flax	Jatropha
20	-0.2	1.3	-0.1
30	-0.2	1.4	0.0
40	-0.4	1.2	-0.2
50	0.1	1.5	0.1
60	-0.1	1.3	-0.1
70	0.0	1.3	-0.1
80	0.0	1.4	-0.1

The dielectric constant outputs from the MEAS sensor for these biodiesel samples has also been compiled and graphed. Figure 5.7 details these results.

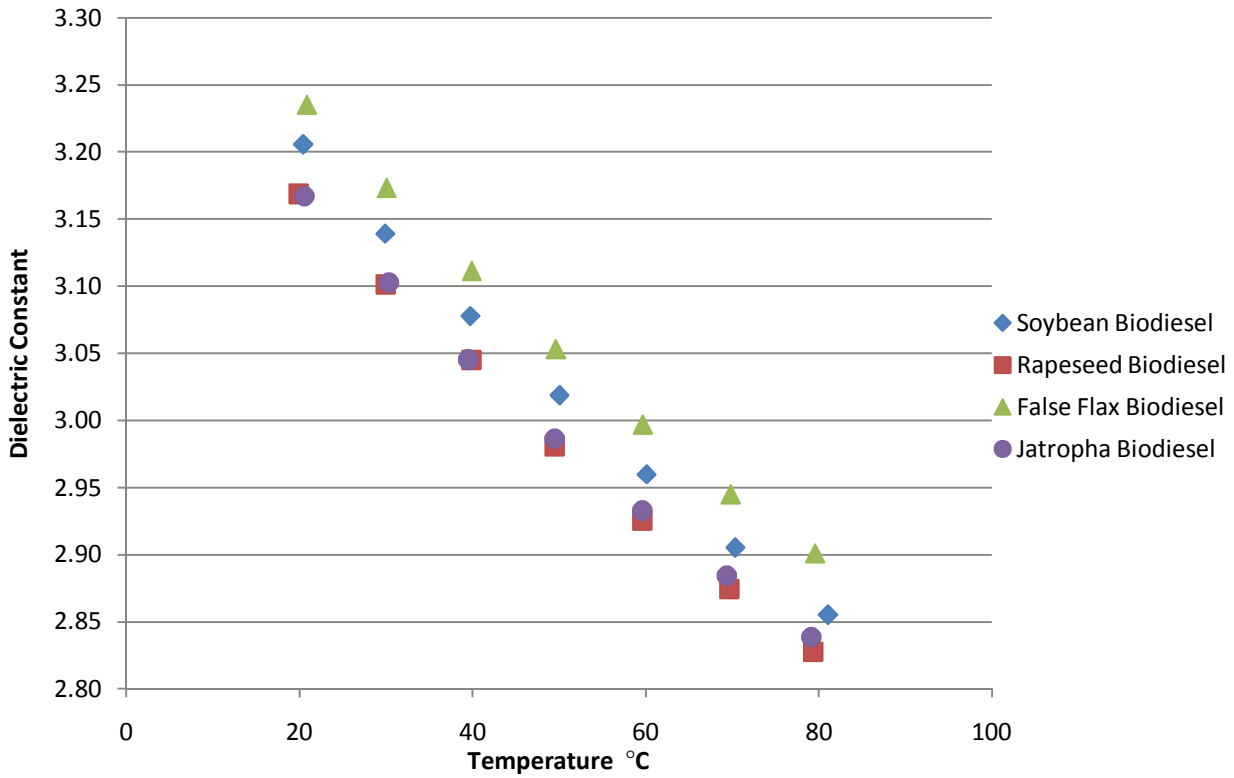

Figure 5.7 Dielectric constant of biodiesels from several oil sources

Jatropha and rapeseed biodiesels had similar dielectric properties while soybean and false flax biodiesels had a higher dielectric constant. The relationship between fatty acid composition and the dielectric constant was not well quantified in previous studies. However, increased un-saturation leads to higher polarity which suggested that the dielectric constant would be highest for false flax biodiesel followed by soybean biodiesel based on the fatty acid compositions presented in Table 4.3. In fact Figure 5.7 agrees with this prediction.

The percent change between each of the fuels and the soybean biodiesel confirmed that an algorithm based on soybean biodiesel dielectric constant introduced only small errors when used with biodiesel from these other sources (Table 5.3).

Table 5.3 Percent change in dielectric constant of several biodiesels over soybean biodiesel

Temperature °C	Rapeseed	False Flax	Jatropha
20	-1.2	0.9	-1.2
30	-1.2	1.1	-1.2
40	-1.1	1.1	-1.1
50	-1.3	1.1	-1.1
60	-1.2	1.3	-0.9
70	-1.1	1.4	-0.7
80	-1.0	1.6	-0.6

5.1.4 Property Measurement of Plant Oils

The MEAS sensor was used to measure the properties of each of the oils from which the biodiesel samples discussed in the previous section were refined. Figure 5.8 gives the dynamic viscosity outputs of soybean, rapeseed, false flax, and jatropha oils over a temperature range of 20°-80°C.

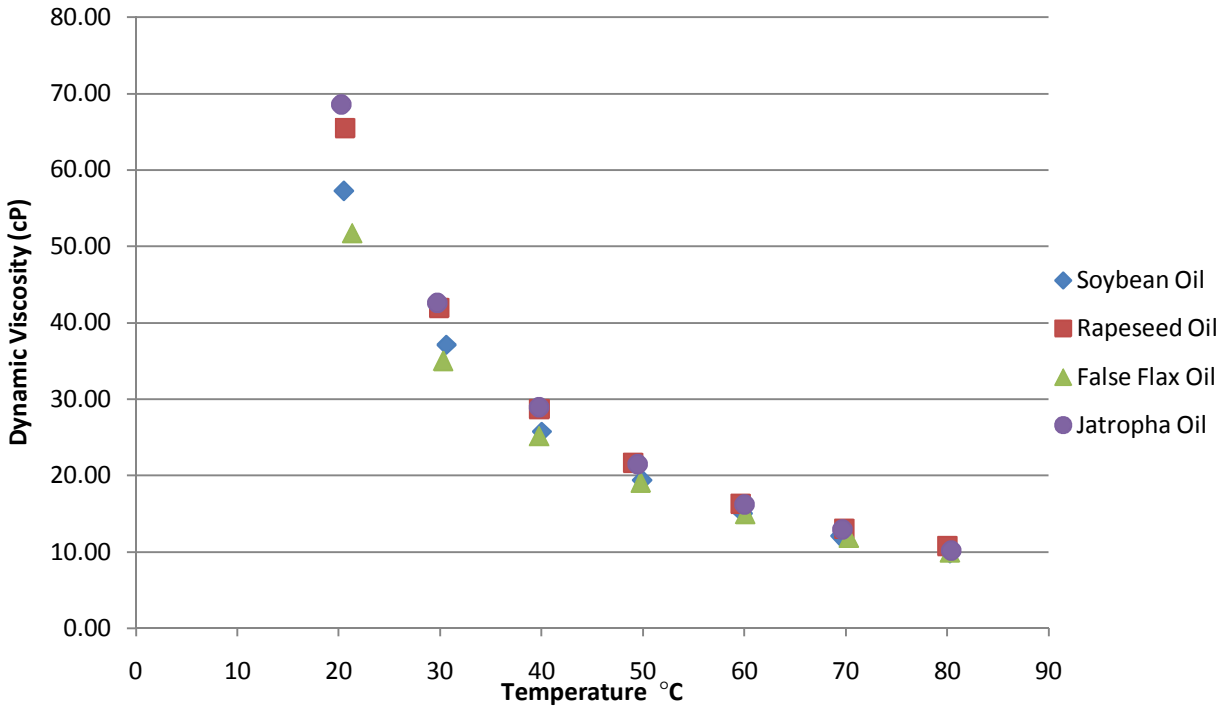

Figure 5.8 Dynamic viscosity outputs for several plant oils

The viscosities of the plant oils were similar for all of the tested samples. The viscosity decreased rapidly and non-linearly with temperature. The difference between measurements for each sample at 20°C and 30°C was much larger than that for the higher temperatures. This was due to the sensor being calibrated for viscosity ranges under 20 cP leading to much larger measurement errors. Therefore, the MEAS sensor would not be accurate in viscosity measurement for oils at low temperatures. Also, the viscosities of the oils were about 10 times larger than that of the methyl ester biodiesels refined from them. The larger viscosity seen in the false flax biodiesel did not manifest itself in the oil properties.

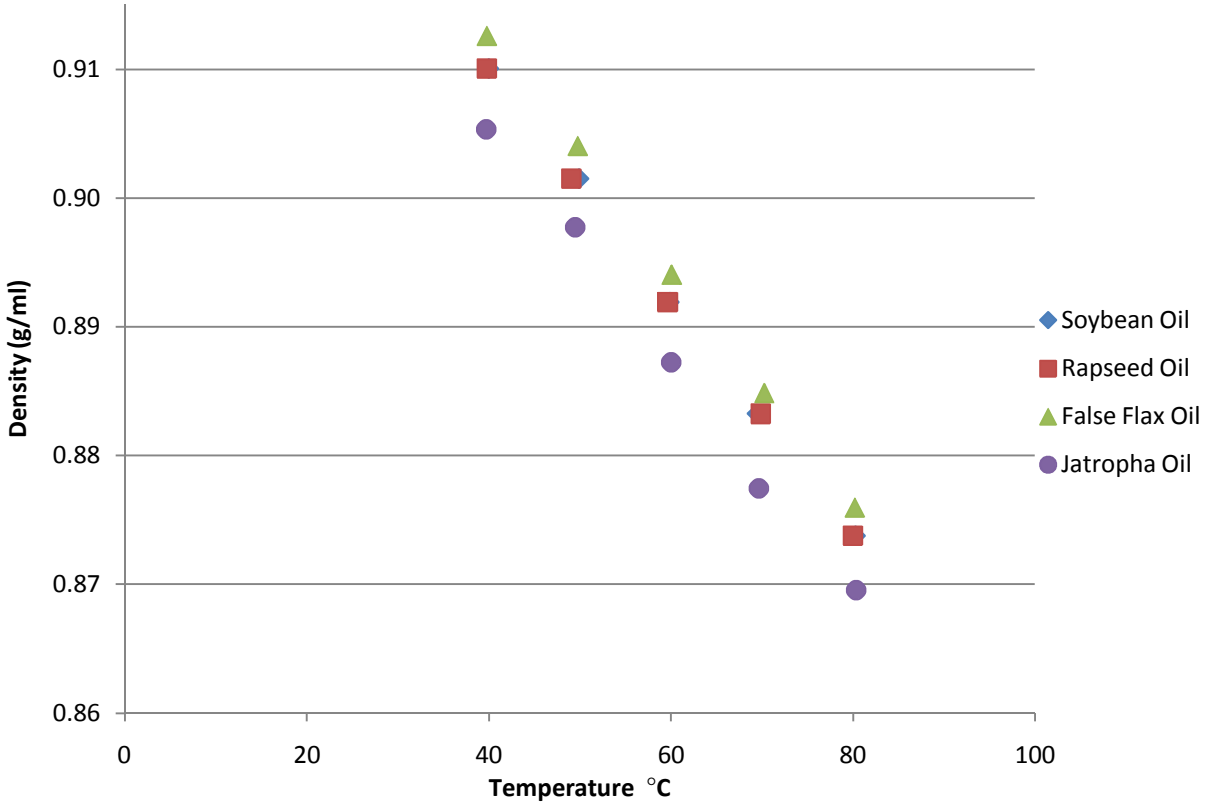

Figure 5.9 Density outputs for several plant oils

Figure 5.9 presents the density measurements taken for this same set of oils. The density measurement did not give reasonable results for any sample below 40°C so data was plotted

from 40° to 80°C. Again, this was due to the measurements being outside the calibration window of the sensor. The density of jatropha oil was the lowest of the measured samples while the other three were similar. Moreover, again the trends in density seen in the biodiesel samples did not necessarily transfer to the corresponding oils. The presence of contaminants such as free fatty acids in the case of jatropha oil would have had some influence. Measurement of density below 40°C resulted in major errors relative to the true values.

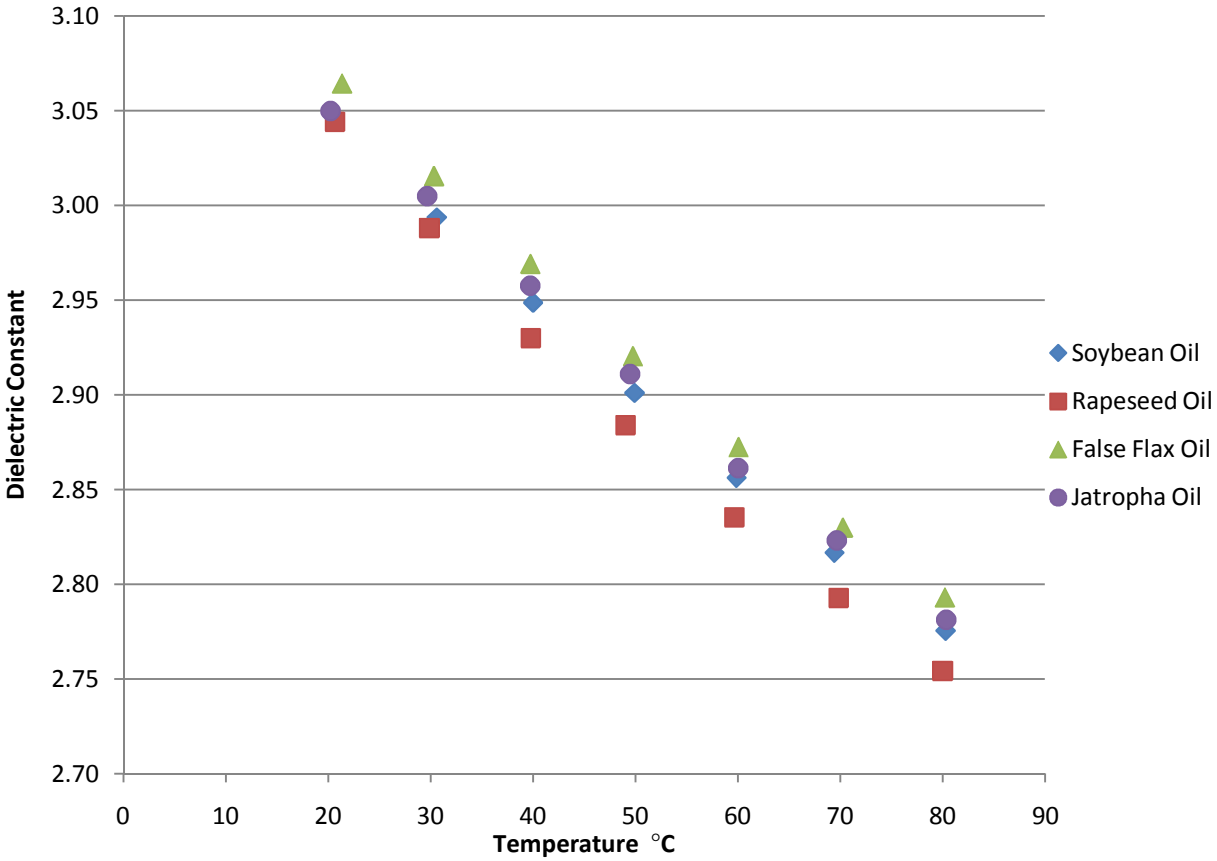

Figure 5.10 Dielectric constant outputs for several plant oils

Dielectric constant measurements are detailed in Figure 5.10. The dielectric constant measurement appeared to be accurate over the entire temperature range measured. This was because dielectric properties of the oils were similar to that of other fuels measured that the

sensor was calibrated for. In addition, there were few differences between the dielectric properties of the four oils (variation less than 7.0%).

5.1.5 Summary of Results

The MEAS sensor was used to measure the properties of several fuels in order to determine its effectiveness in distinguishing between them. The viscosity and density of diesel #1, diesel #2, jet A, and SME biodiesel were found to be diverse enough to be identified by the sensor. The dielectric constant of SME biodiesel was very different from the other petroleum based fuels. In addition the temperature dependence of each property was found to be non-linear, linear, and linear for dynamic viscosity, density, and dielectric constant respectively. Diesel fuel samples with varying sulfur content were measured showing increasing dielectric constant with increasing sulfur content, but the experiments were not conclusive and more testing will be discussed in later sections.

Biodiesels from several sources were tested to evaluate the accuracy that test results from SME biodiesel samples would have when other biodiesels are measured. False flax biodiesel was found to be different from the other samples while soybean, rapeseed, and jatropha biodiesels were similar. This suggested that the sensor results developed would be accurate for most of the US and Europe since the rapeseed and soybean biodiesels were so similar.

The response of the sensors to straight plant oils was also measured. The viscosity of these oils was much higher than the corresponding biodiesel illustrating the difficulties with injecting these oils at low temperatures. The viscosity and density at low temperatures were too large to be accurately measured by this sensor with its current calibration. The trends in seen for the plant oils did not necessarily transfer to the properties of the biodiesels refined from them.

5.2 Fuel Blend Properties Measurement

Fuels are often blended in order to combine between positive characteristics of each of the neat fuels. Blends of diesel #2 and diesel #1 with SME biodiesel are the most common diesel fuels used in the US so MEAS sensor testing was performed on these blended fuels.

5.2.1 SME Biodiesel Blends with Diesel #2

Figure 5.11 contains sensor outputs for blends of SME biodiesel and diesel #2 in 10 percent by volume increments at 30°-80°C. Fuel properties at each temperature were plotted as a function of blend percentage.

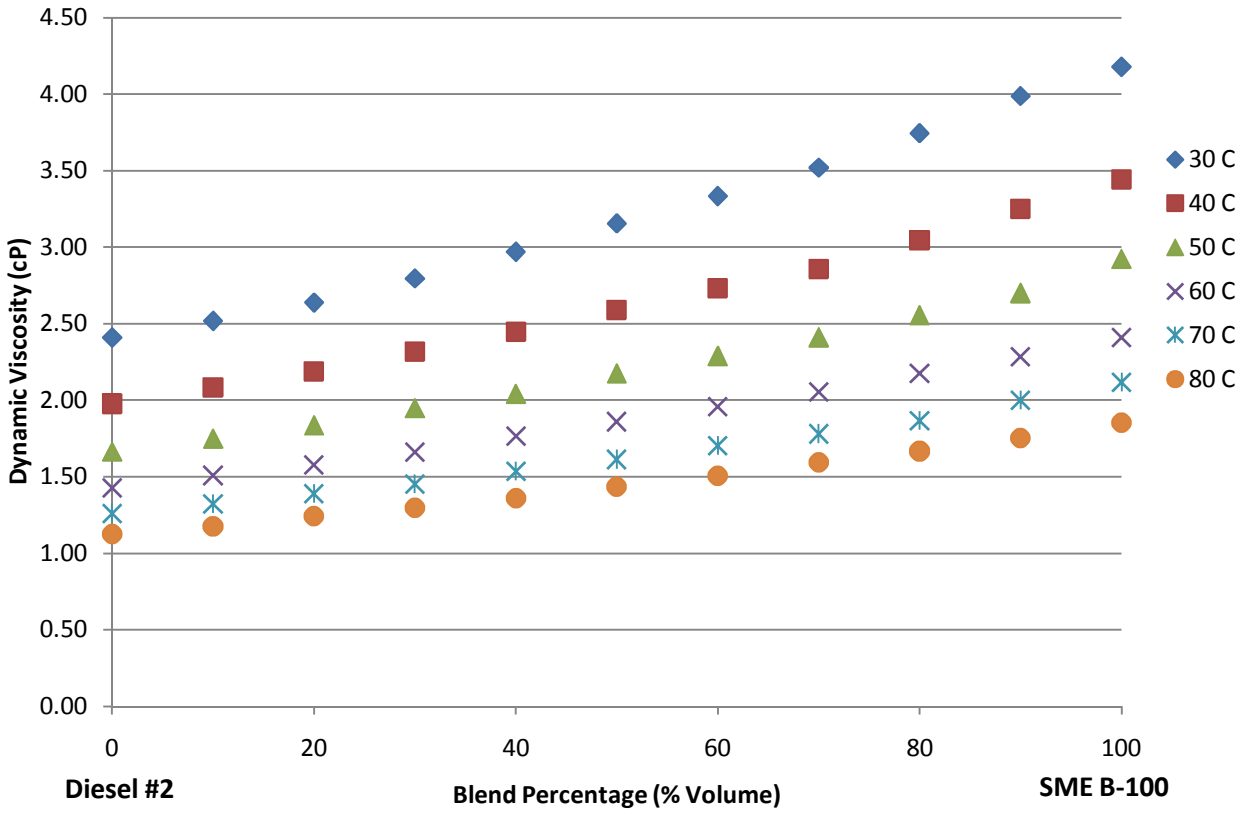

Figure 5.11 Dynamic viscosity of blends of diesel #2 and SME biodiesel

The viscosity varied non-linearly with mixture composition. The degree of non-linearity increased with decreasing temperature. This result was in agreement with other studies. McCrady (2007) commented that the relationship is nearly exponential.

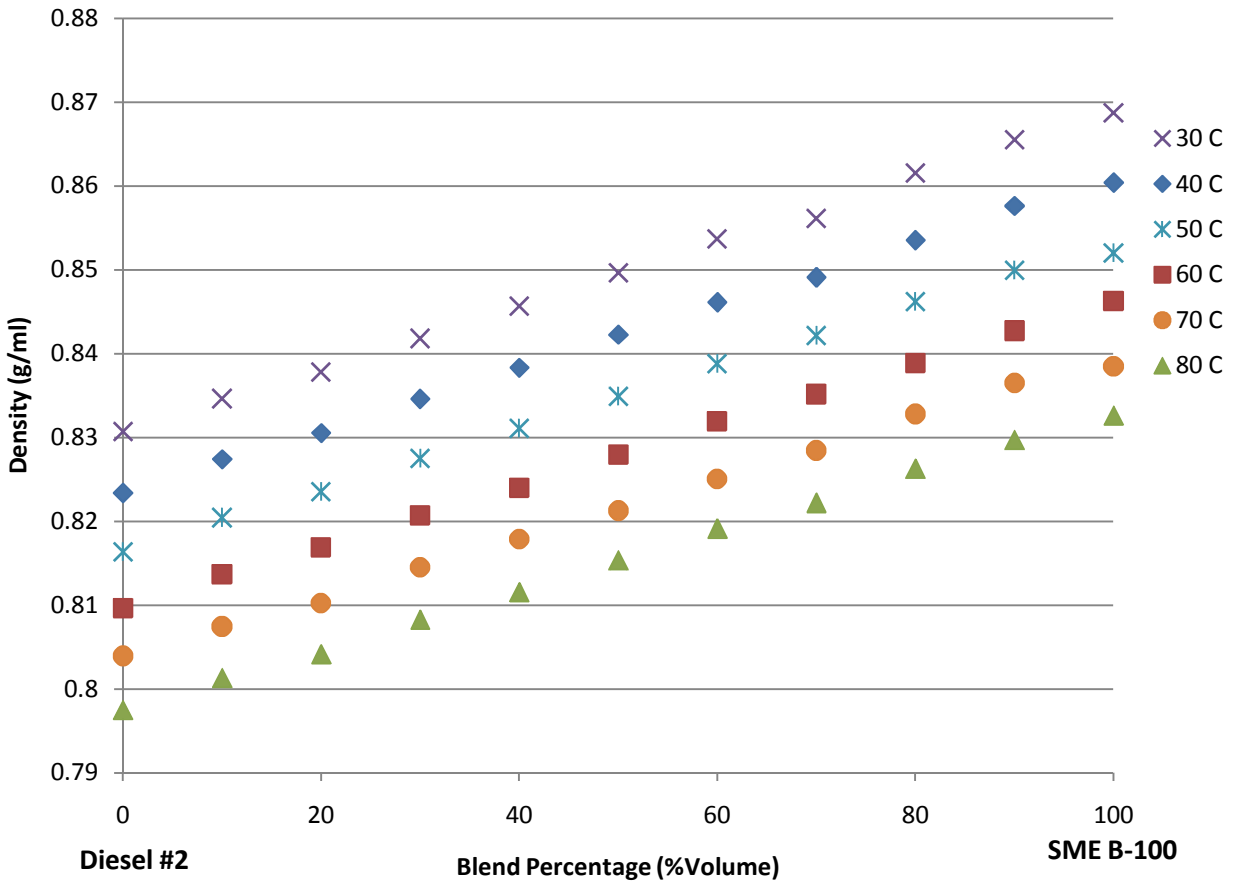

Figure 5.12 Density of blends of diesel #2 with SME biodiesel

The density of fuels varied linearly between the two neat fuels suggesting a simple interpolation between the diesel #2 and SME B-100 was sufficient to predict density at any other blend. Also, the slope of each blend line was the same, independent of temperature (variation less than 0.5%). This followed from the initial fuel study results since the density of all fuels changed at the same rate with temperature.

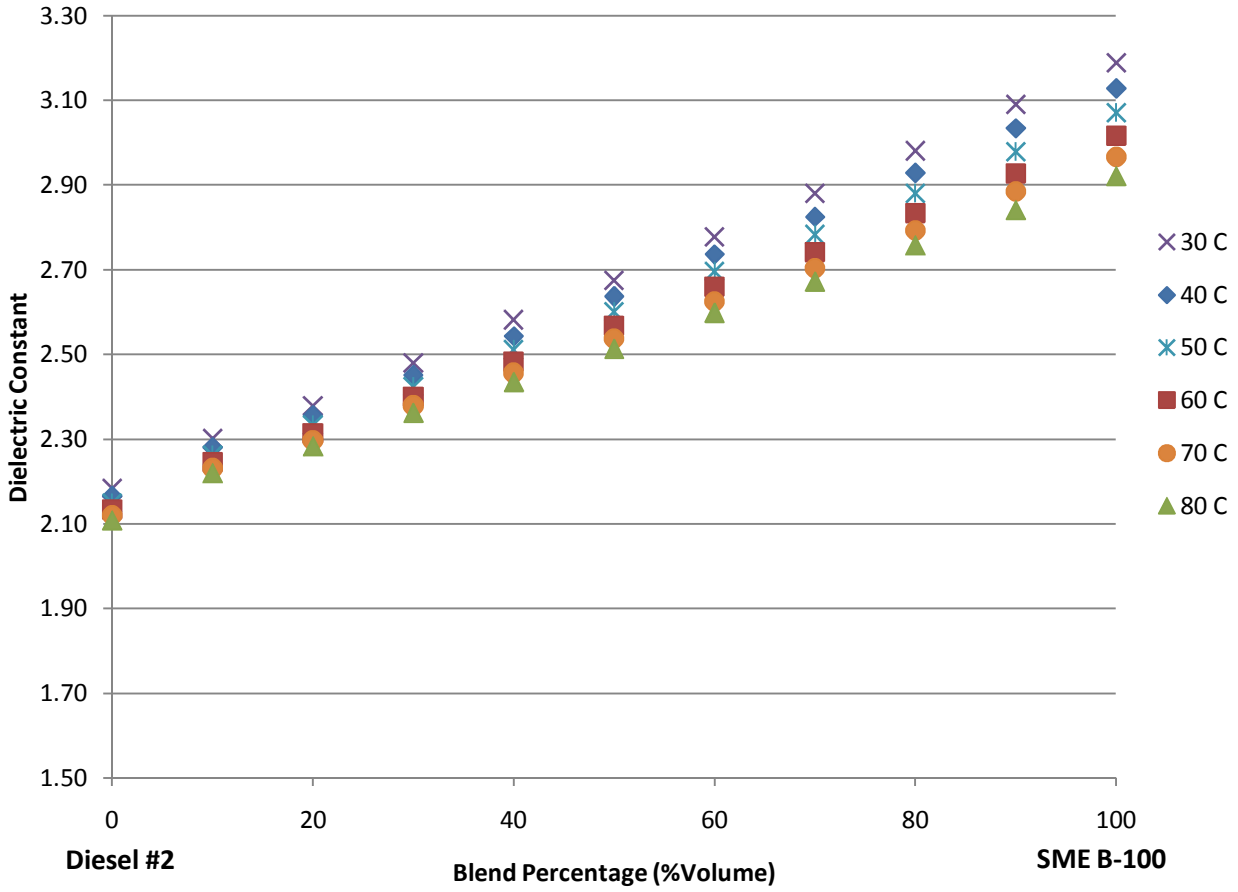

Figure 5.13 Dielectric constant of blends of diesel #2 and SME biodiesel

Dielectric measurements from the sensor for blended fuels have also been recorded (Figure 5.13). The dielectric constant of fuels also varied linearly with blend percentage. The slope of this linear change was dependent on temperature as the difference between the dielectric constant of diesel #2 and SME B-100 increases with decreasing temperature. This was due to the higher polarity of the biodiesel leading to higher temperature dependence.

5.2.2 SME Biodiesel Blends with Diesel #1

Blends with diesel #1 are less common that those with diesel #2; however, at low blend percentages of biodiesel they are commercially used. Consequently, blends of diesel #1 with biodiesel up to B-20 were tested (Figure 5.14).

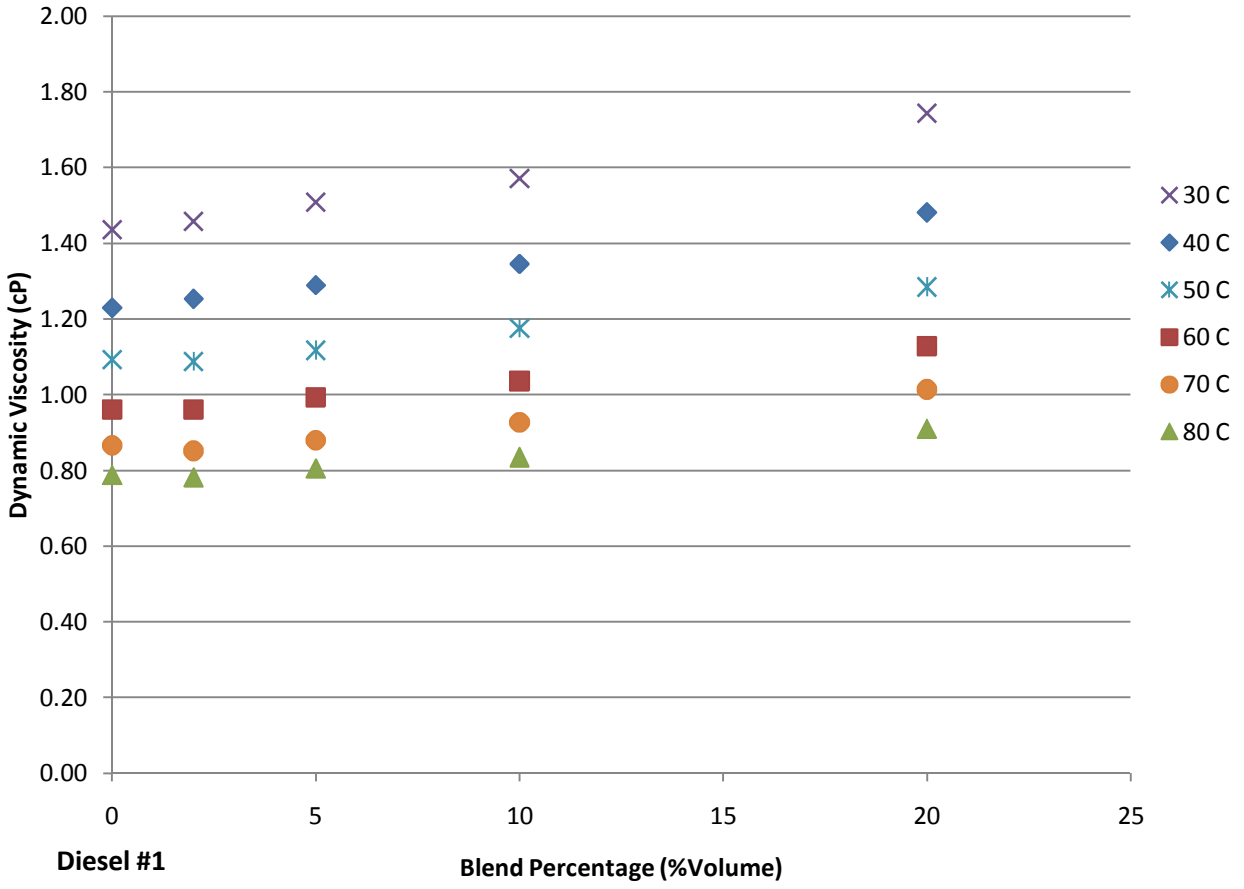

Figure 5.14 Dynamic viscosities of blends of diesel #1 with SME biodiesel

Blends with diesel #1 followed very similar trends as was observed for blends with diesel #2. Again, the viscosity varied non-linearly with blend percentage although the trend was not as apparent at these low blend levels. An exponential fit was expected to model this data closely based on previous studies including McCrady (2007).

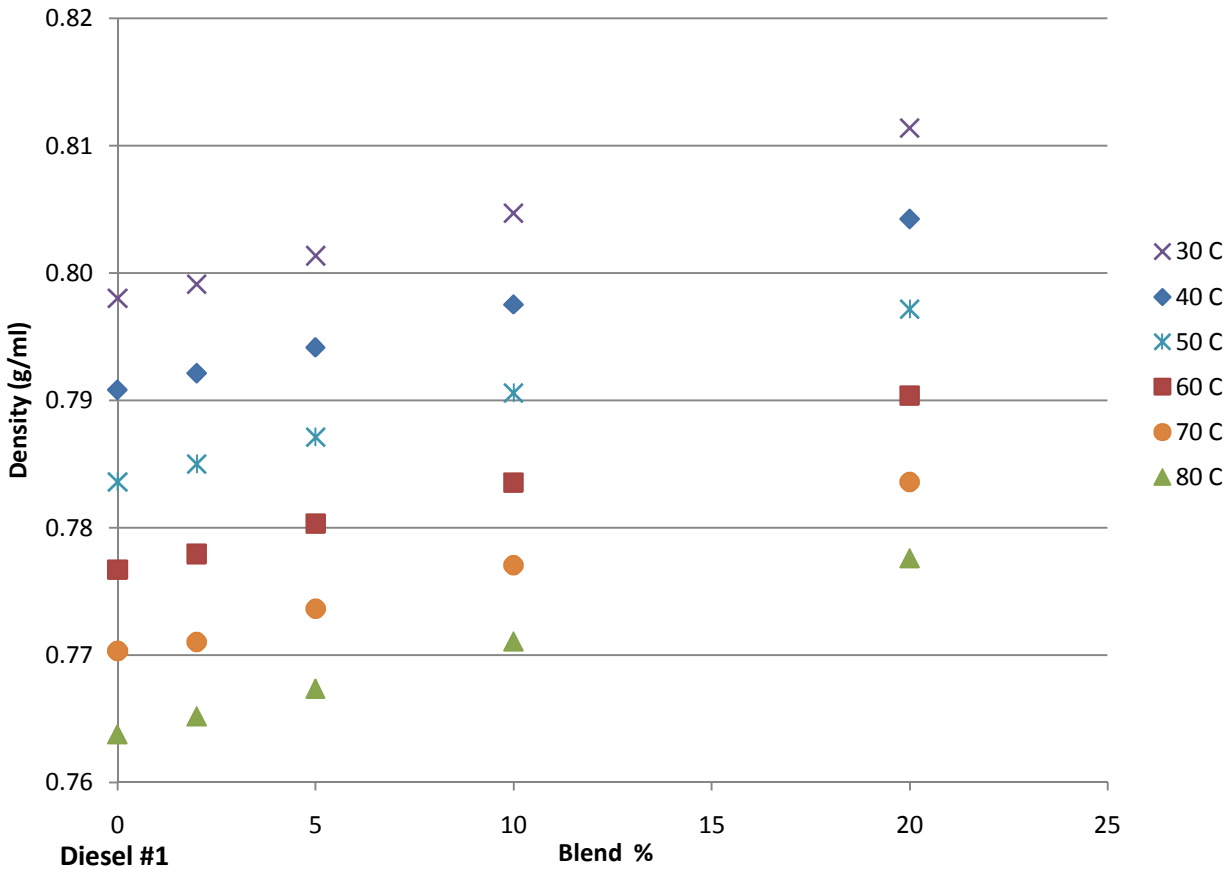

Figure 5.15 Density of blends of diesel #1 with SME biodiesel

Figure 5.15 plots density outputs for blends with diesel #1 and SME biodiesel. Density outputs appeared to fit a linear trend with blend percentage. In addition, the rate of this fit was approximately independent of temperature. These trends were the same as was seen in blends with diesel #2. It was useful to observe that the density of B-20 blends with diesel #1 were well below the density of pure diesel #2. This was a functional characteristic if density was to be used as a determinant between blends from each of diesel #1 and diesel #2 as the maximum density seen from blends with diesel #1 would not overlap with diesel #2 blend densities.

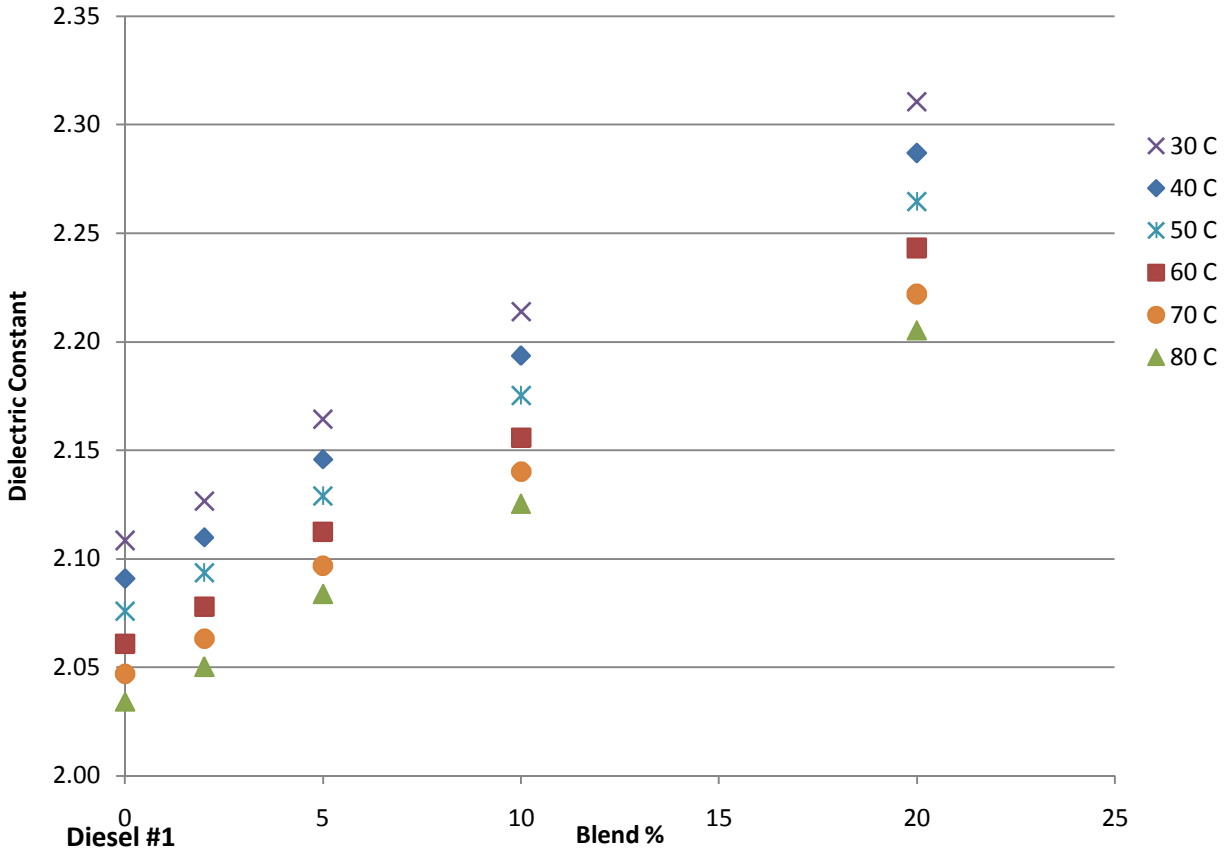

Figure 5.16 Dielectric Constant of blends of diesel #1 with SME biodiesel

The sensor's dielectric constant outputs for the same set of blended fuels are displayed in Figure 5.16. The dielectric constant increased linearly with mixture composition percentage. Also, the slope of these lines was dependent on temperature and had to be accounted for in modeling. In addition, in the same way it was observed that the density measurement of B-20 blends with diesel #1 fell below the density of diesel #2; note that this was not the case with dielectric constant. Blends at levels of greater than B-5 would be indistinguishable from blends with diesel #2 through use of the dielectric constant only.

5.2.3 Summary of Results

The properties of blended fuels have been detailed with the goal of determining the MEAS sensor's ability to discern between blended fuels and to predict blend levels. Results indicate that all three of the sensor outputs could be used for blend calculations.

For blends of biodiesel with both diesel #1 and diesel #2, dynamic viscosities varied in a non-linear way with blend percentage. This non-linearity was nearly exponential, but was also dependent on temperature. Curve fitting this trend will be discussed in Section 5.5.3. The density and dielectric constant measurements showed that these properties changed linearly with blend percentage. This was very convenient from a blend prediction perspective since a simple linear interpolation between the two neat fuel properties at a given temperature would be sufficient.

Another desirable property was for the sensor to be able to distinguish between blends using #1 diesel and blends using #2 diesel. Since the expected maximum blend percentage with diesel #1 was B-20 it was required that at least one of the sensor outputs at B-20 not fall into the range of outputs expected for blends with diesel #2. Density fulfilled this requirement very well and could be the most ideal fuel property for baseline fuel determination.

5.3 Effect of Fuel Contamination on Sensor Outputs

Detection of fuel contamination was a priority of this project as this capability added instant value to engines from both the manufacturer's and consumer's standpoint. The effect of multiple possible contaminants was difficult to quantify and required selection of the most important pollutants fuels might contain. The effect of several contaminants on MEAS sensor outputs follows.

Each of these contaminants (water, urea, glycerol, and methanol) was tested on several fuels or blends; however, for the sake of discussion only data collected on one fuel sample for each contaminant will be presented within this chapter. Figures containing all of the contamination results can be found in appendix B.

5.3.1 Water

The effect of water contamination was measured at four levels of contamination and at three different temperatures. Figure 5.17 gives dynamic viscosity results for diesel #2 fuel with water contamination.

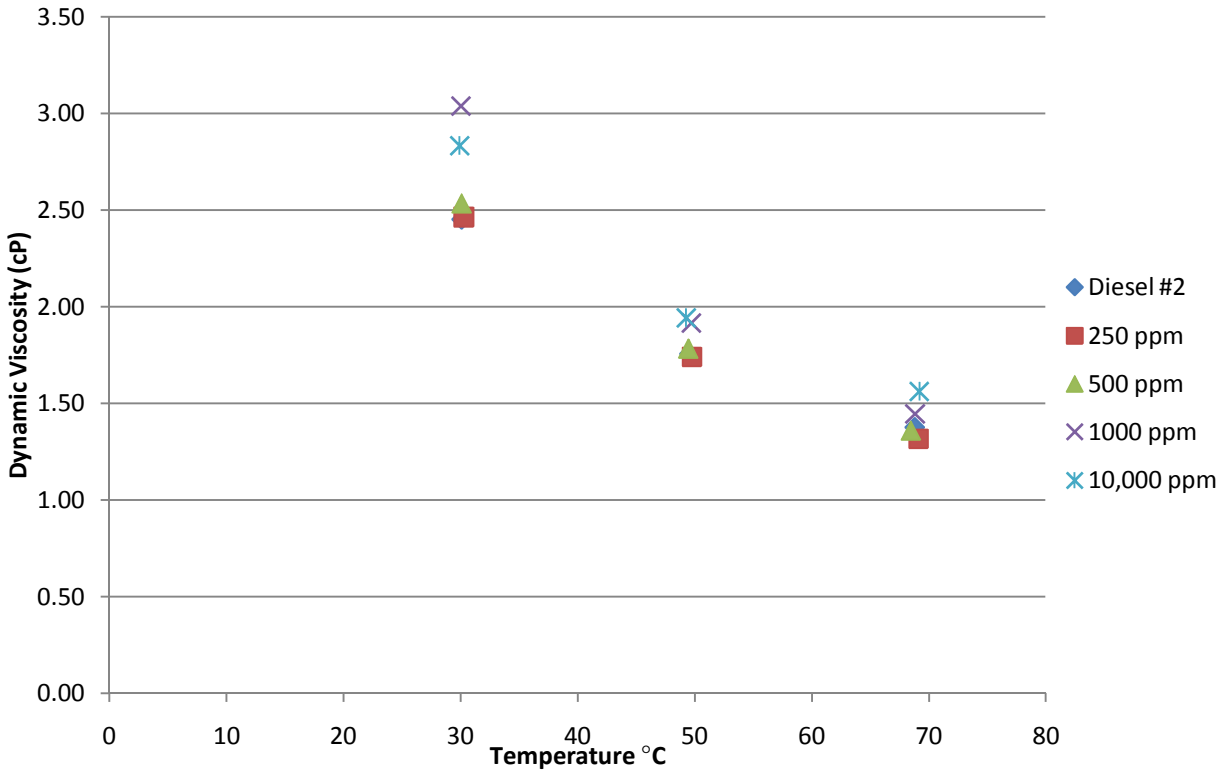

Figure 5.17 Dynamic viscosity of diesel #2 with water contamination

Results indicated that the viscosity of the fuel increased in general as water contamination increased. This effect was apparent at concentrations above 500 ppm while lower

concentrations did not have a large enough effect to be detectable. In addition the viscosity spike was larger at lower temperatures. The results agreed with published data related to water contamination of E-85 fuels (Lee, 2008). The increase in viscosity was also seen in this study, and was noted as being strange since the viscosity of water is lower than fuel.

Table 5.4 summarizes the percent change of viscosity over that of the un-contaminated fuel for diesel #2 over the entire contaminant concentration and temperature range tested.

Table 5.4 Percent change in viscosity from water contamination

	Percent Change from Diesel #2 at 30°, 50°, and 70°C		
Concentration (ppm)	30°C	50°C	70°C
250	0.4	-0.8	-4.2
500	3.2	1.5	-1.1
1,000	23.8	9.1	5.1
10,000	15.4	10.6	13.5

There were significant changes in viscosity due to water contamination at 1,000 ppm or higher concentrations. In addition the effect was larger at lower temperatures. Differences of less than five percent in the viscosity measurement would likely not be detectable in the general case since some error in the sensor's measurement and calibration as well as natural fuel property variation must be accounted for (Section 5.5.4).

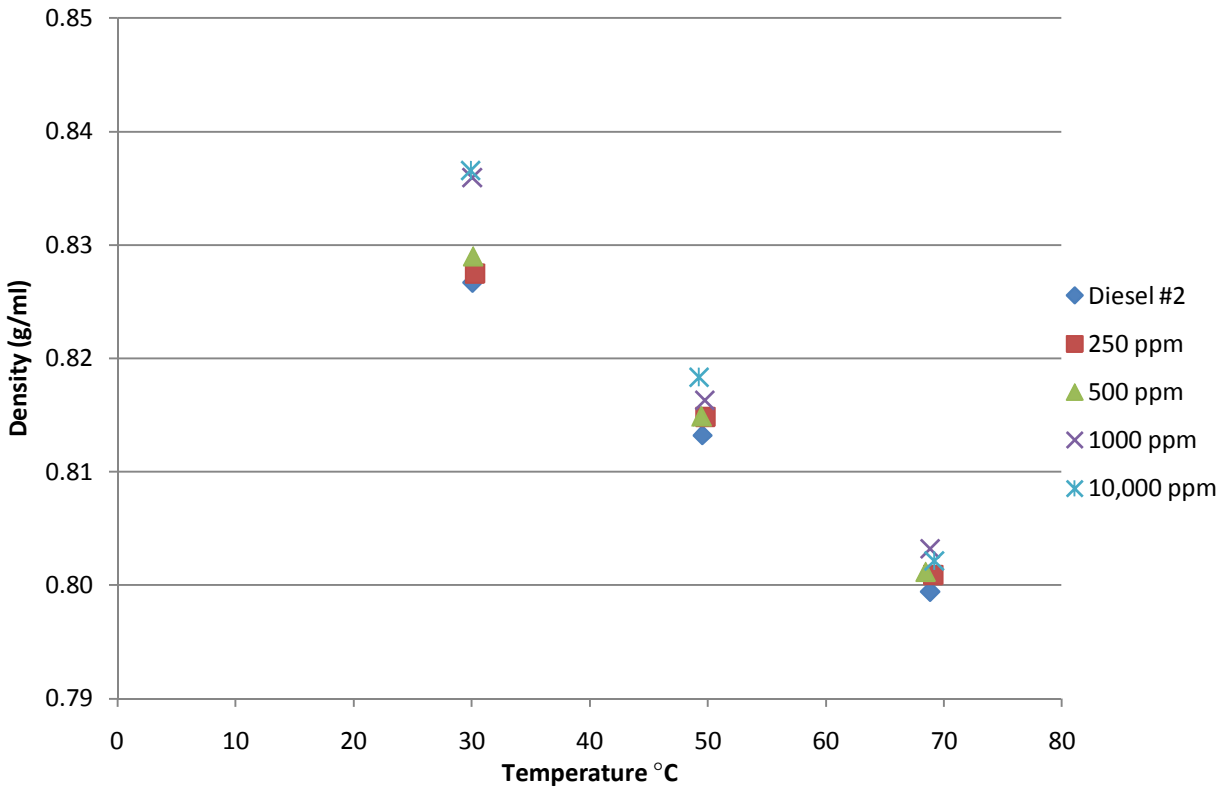

Figure 5.18 Density of diesel #2 with water contamination

The density outputs measured for diesel #2 with water added are presented in Figure 5.18. Density outputs were not largely affected by water contamination. This followed from the fact that blending studies show that density tended to change linearly with blend percentage and water has a density around 1 g/ml compared to fuel (.8-.9 g/ml). Therefore, concentrations of water at less than one percent had a minimal impact on fuel density. At concentrations above 1,000 ppm there was a measurable effect, but it was much less than what was seen for viscosity. In addition the density spike was larger at lower temperatures. Table 5.5 contains percent change results for the contaminated samples over the clean fuel.

Table 5.5 Percent change in density of diesel #2 under water contamination

	Percent Change from diesel #2		
Concentration (ppm)	30°C	50°C	70°C
250	0.1	0.2	0.2
500	0.2	0.2	0.2
1,000	1.1	0.3	0.5
10,000	1.2	0.6	0.3

The change in density due to water contamination was not significant for contamination levels below 1,000 ppm. Again the change was temperature dependent with detection of water more likely at lower temperature. Also, the accuracy of the density measurement for the sensor was much better than that for viscosity with errors less than 0.5%.

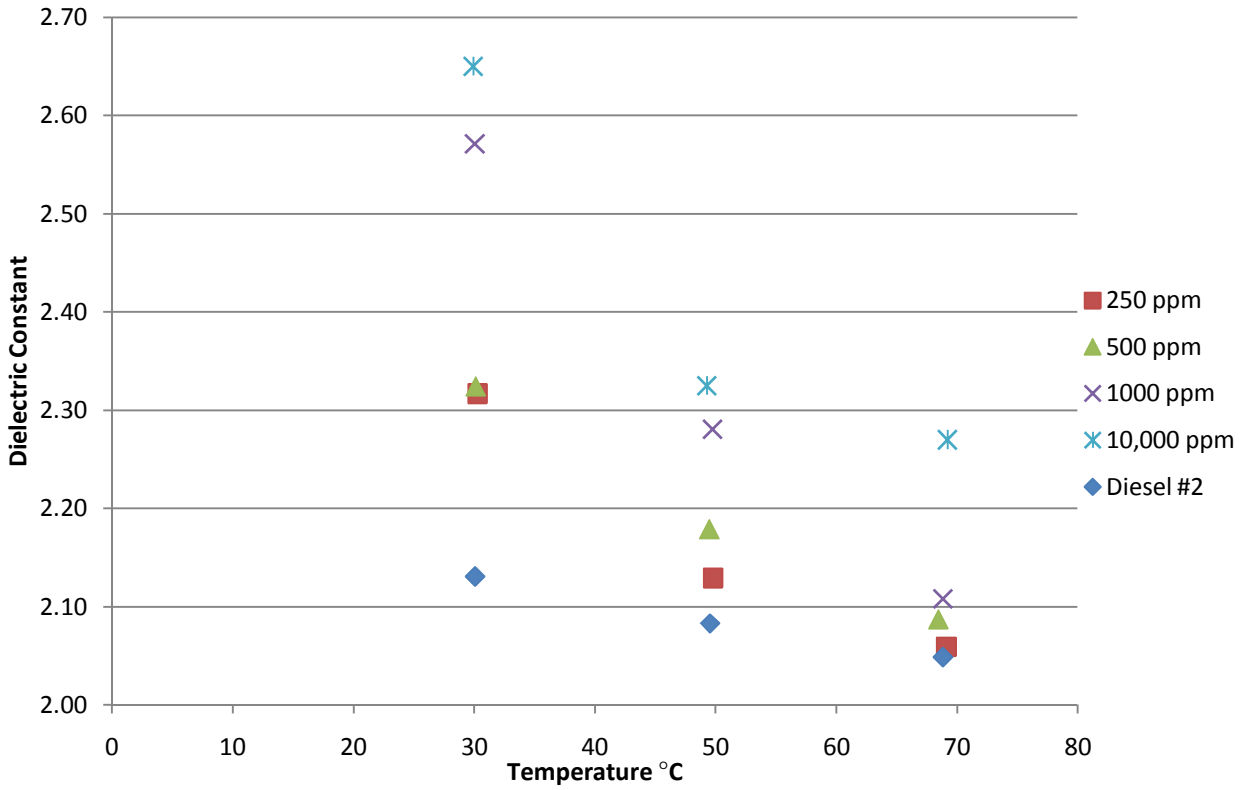

Figure 5.19 Dielectric constant of diesel #2 under water contamination

The dielectric constant data for diesel #2 with water contamination are displayed in Figure 5.19. The dielectric constant of fuel increased significantly with increasing water contamination. Moreover, the change in dielectric constant between 1,000 and 10,000 ppm was not much considering the large jump in added water. This was due to the diesel fuel having reached its solubility limit causing water to separate rather than mix with the fuel. Van Gerpen et al. (1996) estimated this limit at less than 250 ppm for the temperature range considered. Mixing kept more water in suspension during this testing explaining change in dielectric above the solubility limit. The dielectric spike was very dependent on temperature and was much larger at lower temperatures. This was due to the fact that water is a highly polar liquid and therefore has very high dielectric temperature dependence. As temperature decreased the dielectric constant of the fuel remained nearly constant while the dielectric constant of water increased greatly leading to the larger effect of water contamination. The change in dielectric constant with water contamination is summarized (Table 5.6).

Table 5.6 Percent change in dielectric constant of diesel #2 with water contamination

	Percent Change from diesel #2		
Concentration (ppm)	30°C	50°C	70°C
250	8.7	2.2	0.5
500	9.0	4.6	1.9
1,000	20.7	9.5	2.9
10,000	24.4	11.6	10.8

Results confirm observations from Figure 5.20 including the fact that the dielectric spike of water contamination was very dependent on temperature. The detection limits for water were 250 ppm at 30°C, 500 ppm at 50°C, and near 10,000 ppm at 70°C. The measurement errors for

dielectric sensor were less than viscosity but greater than density. Observation led to an estimate of these errors at 2%.

Water contamination data was also collected from blends of diesel and SME biodiesel at levels of B-30, B-50, B-70, and B-100 (Table 5.7). Van Gerpen et al. (1996) studied water contamination of fuels and concluded that biodiesel had much higher water solubility than diesel #2. Therefore, it was expected that the other fuels tested would show larger changes in properties.

Table 5.7 Percent change of viscosity of B-0, B-30, B-50, B-70, and B-100 with water

		Concentration (ppm)			
		250	500	1,000	10,000
	Temperature	Percent Change			
Diesel #2	30°C	0.4	3.3	23.8	15.4
	50°C	-0.9	1.6	9.1	10.6
	70°C	-4.3	-1.1	5.1	13.5
B-30	30°C	-1.2	0.4	1.2	5.3
	50°C	-0.9	1.4	1.6	4.4
	70°C	-3.6	-2.2	-1.5	-0.6
B-50	30°C	-0.5	10.1	6.6	27.3
	50°C	3.2	7.8	6.3	16.4
	70°C	0.9	5.8	5.2	7.3
B-70	30°C	0.2	1.5	2.0	3.5
	50°C	-4.5	-2.4	-2.8	-3.6
	70°C	-1.0	7.7	2.5	-0.8
B-100	30°C	-0.7	4.3	-2.8	-2.8
	50°C	3.3	3.7	-0.4	-1.9
	70°C	3.0	10.5	1.0	4.4
Average	30°C	-0.4	3.9	6.2	9.7
	50°C	0.1	2.4	2.7	5.2
	70°C	-1.0	4.1	2.5	4.8

Table 5.7 contains a great deal of data that might be difficult to interpret, although common trends were apparent. Average changes were tabulated to help provide clarity. At 250 ppm there was no effect on viscosity. At 500 and 1,000 ppm there was a measurable effect; however, at these levels there were as many samples that show no change as that do. At 10,000 ppm there was a larger change in viscosity. In general, the spike in viscosity increased with decreasing temperature as was observed with diesel #2. In addition the data was much more variable and erratic at higher water contamination because of the heterogeneous mixing of water and fuel which caused errors in measurement. The sensor required that the fluid around the sensing element be well mixed for accuracy. This led to the varied effects observed across fuel samples. Furthermore, the addition of more water did not always cause a large spike in viscosity since the solubility limit of the fuel was likely surpassed.

Table 5.8 contains the results of water contamination on density measurements of the same range of blended fuels. The results were much more consistent compared to viscosity and all cases followed very similar trends to the results discussed for diesel #2.

Table 5.8 Percent change of density of B-0, B-30, B-50, B-70, and B-100 under water contamination

		Concentration (ppm)			
		250	500	1,000	10,000
	Temperature	Percent Change			
Diesel #2	30°C	0.10	0.28	1.12	1.19
	50°C	0.20	0.21	0.38	0.63
	70°C	0.18	0.22	0.47	0.33
B-30	30°C	0.37	0.41	0.45	1.38
	50°C	0.22	0.22	0.24	0.49
	70°C	0.20	0.23	0.34	0.57
B-50	30°C	0.26	0.49	0.63	0.49
	50°C	-0.03	0.16	0.29	0.18
	70°C	0.13	0.20	0.40	-0.43
B-70	30°C	0.01	0.03	0.20	0.25
	50°C	0.19	0.22	0.22	0.18
	70°C	-0.04	-0.16	-0.01	-0.01
B-100	30°C	0.16	0.09	0.51	0.61
	50°C	-0.05	0.00	0.25	0.51
	70°C	0.02	0.03	0.11	0.39
Average	30°C	0.18	0.26	0.58	0.79
	50°C	0.11	0.16	0.28	0.40
	70°C	0.10	0.10	0.26	0.17

Inspection of percent change calculations show that there was very little effect on density by water contamination. The property was expected to increase at higher water concentrations because water has a density approximately 25% higher than fuel. Average values showed that density would increase more from water addition at lower temperatures. Also, the senor's ability to accurately measure density did not seem to be affected by heterogeneous mixing in contrast to viscosity.

Table 5.9 Percent change of dielectric constant of B-0, B-30, B-50, B-70, and B-100 under water contamination

		Concentration (ppm)			
		250	500	1,000	10,000
	Temperature	Percent Change			
Diesel #2	30°C	8.73	9.06	20.66	24.36
	50°C	2.22	4.60	9.49	11.62
	70°C	0.51	1.89	2.90	10.81
B-30	30°C	1.84	6.13	6.16	49.17
	50°C	1.77	4.04	2.78	36.63
	70°C	0.27	0.29	0.82	9.23
B-50	30°C	4.19	17.17	13.19	27.38
	50°C	1.55	6.38	11.75	29.64
	70°C	0.59	1.53	2.96	26.54
B-70	30°C	1.59	4.31	6.50	10.95
	50°C	1.06	1.28	3.02	5.02
	70°C	0.51	0.52	1.51	6.80
B-100	30°C	2.55	1.55	5.23	13.31
	50°C	1.24	1.01	6.79	8.27
	70°C	0.45	0.70	0.90	5.52
Average	30°C	3.78	7.64	10.35	25.03
	50°C	1.57	3.46	6.77	18.24
	70°C	0.47	0.99	1.82	11.78

Table 5.9 details the percent change of the dielectric constant output for fuels with water contamination. The dielectric constant was the property most affected by water contamination which was because of the high polarity and dielectric constant of water. In addition, the dielectric constant change due to water addition was also the most temperature dependent as evidenced by the average percent change. Water contamination would be detected by a spike in

the dielectric constant output. The detection limit was 250 ppm at 30°C, 500 ppm at 50°C and somewhere between 1,000 and 10,000 ppm at 70°C. The detection limits were strongly dependent on temperature

5.3.2 Sulfur

Baseline testing on sulfur in fuels was discussed in Section 5.1.2; this experimentation concluded that sulfur might have an effect on the dielectric constant of fuel but that more work was needed to quantify this effect. This section covers more testing of fuel with varying sulfur content. Figure 5.20 shows the dielectric constant of diesel #2 with varying levels of Dibenzothiophene, a sulfur analog in diesel fuels.

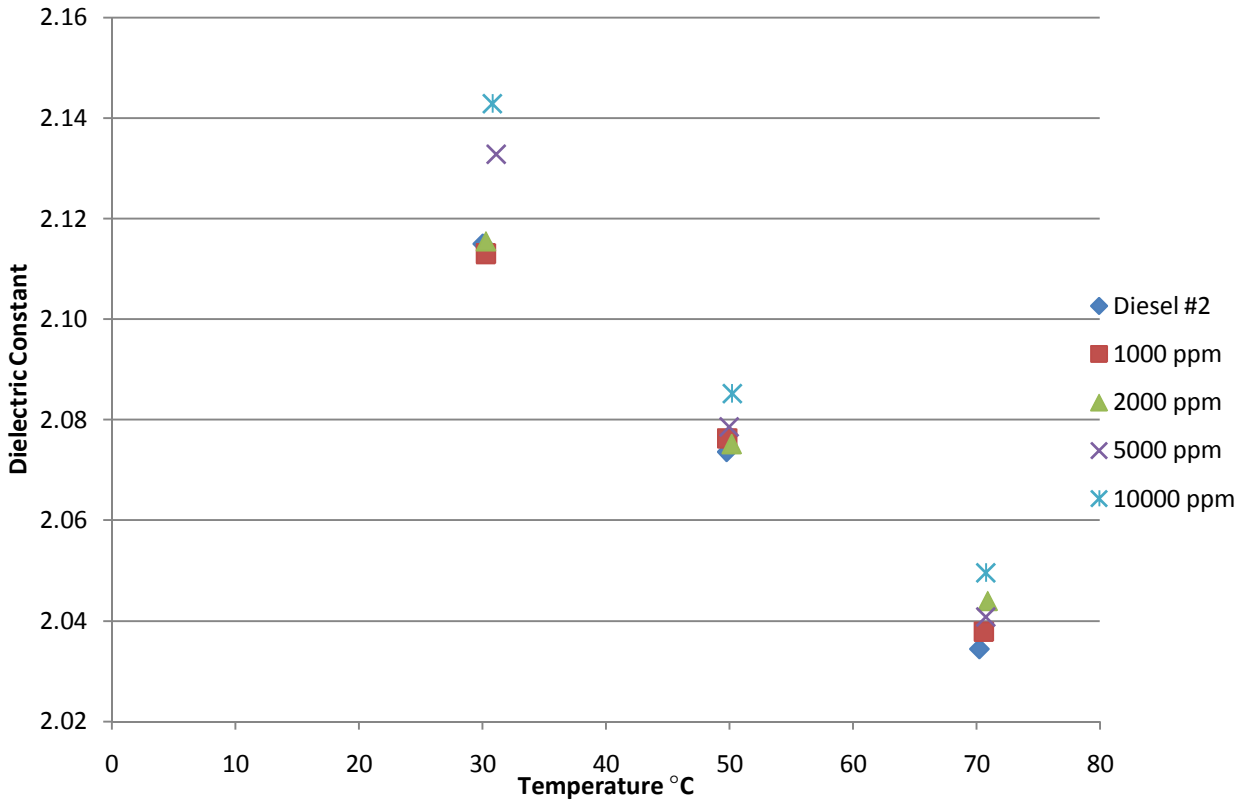

Figure 5.20 Dielectric constant of diesel #2 with sulfur contamination

Figure 5.20 reveals that the dielectric constant of diesel fuel increased as sulfur content increases (variation up to 1.5%); however, this increase was detectable at levels much higher than the 15 ppm regulation. This result was less promising than the initial data taken on sulfur as the dielectric spike was not as significant. Moreover, in the detection limit for sulfur based on the two experiments was in the range of 1,000-5,000 ppm.

To summarize the sulfur effect and provide validation for the assertion that density and viscosity were not significantly changed. Table 5.10 gives percent change data for diesel #2 with sulfur contamination.

Table 5.10 Properties of diesel #2 with sulfur contamination

		Concentration (ppm)			
		Percent Change			
	Temperature	1,000	2,000	5,000	10,000
Viscosity	30°C	0.33	-0.30	-0.68	1.24
	50°C	4.59	2.05	1.98	5.36
	70°C	4.05	1.60	2.26	5.74
		Concentration (ppm)			
		Percent Change			
	Temperature	1,000	2,000	5,000	10,000
Density	30°C	0.03	0.18	0.20	0.25
	50°C	0.04	0.09	0.16	0.10
	70°C	-0.07	0.05	0.04	0.02
		Concentration (ppm)			
		Percent Change			
	Temperature	1,000	2,000	5,000	10,000
Dielectric Constant	30°C	-0.09	0.03	0.84	1.32
	50°C	0.13	0.08	0.24	0.56
	70°C	0.17	0.47	0.31	0.74

There was very little change in density or viscosity of the fuel with added sulfur considering the natural variation in the measurement. Additionally, there was a slight increase in

dielectric constant at high sulfur concentrations, and this dielectric spike was independent of temperature.

5.3.3 Urea

Another contaminant tested was urea in the form of DEF, diesel exhaust fluid. This urea based liquid is used in some exhaust after-treatment systems and must be refilled occasionally. Refilling of fuel and DEF would often occur at the same time allowing for the possibility of cross contamination due to operator error. This set of tests evaluated the sensor for protection against accidental addition of DEF to the fuel tank (Figures 5.21, 5.22, and 5.23).

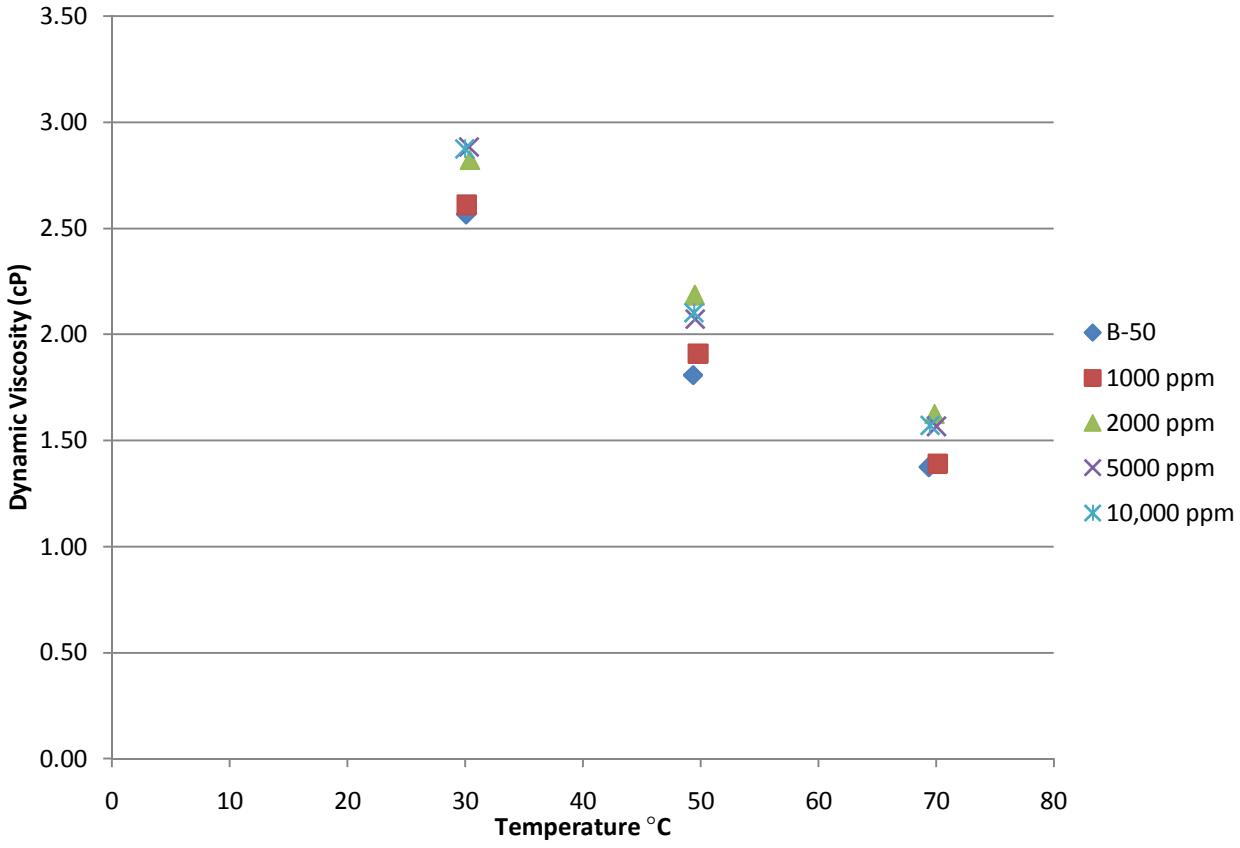

Figure 5.21 Dynamic viscosity of diesel #2 with urea contamination

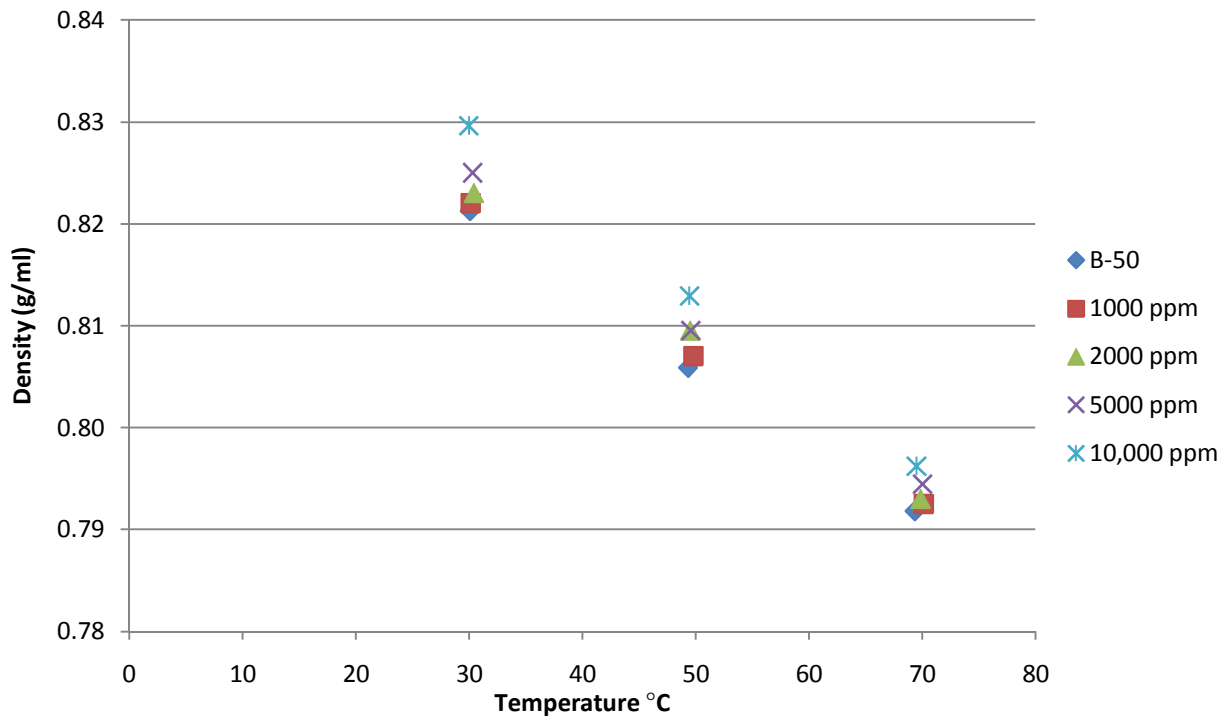

Figure 5.22 Density of diesel #2 with urea contamination

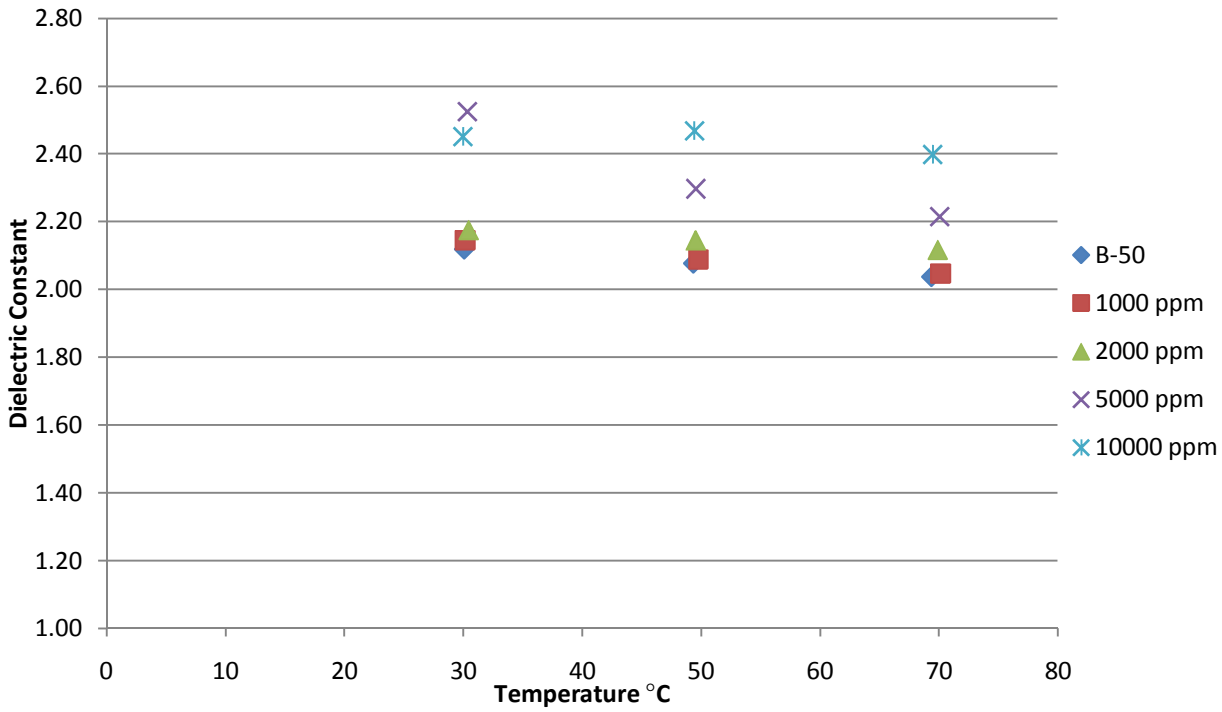

Figure 5.23 Dielectric constant of diesel #2 with urea contamination

Figures 5.21, 5.22, and 5.23 suggest that the addition of urea to fuel had an effect on all three of the sensor outputs, although the change in dielectric was much larger than that of viscosity and density.

Blends of SME biodiesel and diesel #2 at levels of B-30 and B-50 were also tested for urea contamination. Tables 5.11, 5.12, and 5.13 summarize the percent change due to contamination for each of viscosity, density, and dielectric constant respectively over this range of fuels.

Table 5.11 Percent change of dynamic viscosity with urea contamination

		Concentration (ppm)			
		1,000	2,000	5,000	10,000
	Temperature	Percent Change			
Diesel #2	30°C	1.73	9.98	12.36	12.01
	50°C	5.68	20.89	14.70	16.35
	70°C	1.09	18.28	13.92	14.30
B-30	30°C	1.81	0.98	3.69	5.00
	50°C	7.38	8.01	6.63	9.07
	70°C	2.25	14.62	8.59	16.52
B-50	30°C	0.89	7.02	5.07	-4.52
	50°C	5.67	6.78	7.22	-3.25
	70°C	6.69	8.74	8.13	-0.15

Table 5.12 Percent change of density with urea contamination

		Concentration (ppm)			
		1,000	2,000	5,000	10,000
	Temperature	Percent Change			
Diesel #2	30°C	0.09	0.21	0.46	1.01
	50°C	0.14	0.45	0.45	0.87
	70°C	0.08	0.15	0.33	0.55
B-30	30°C	0.23	0.08	0.59	0.77
	50°C	0.24	0.20	0.49	0.95
	70°C	0.03	-0.21	0.37	0.23
B-50	30°C	0.48	2.31	3.04	0.69
	50°C	1.39	3.00	3.08	0.39
	70°C	0.89	2.75	2.70	0.27

Table 5.13 Percent change of dielectric constant with urea contamination

		Concentration (ppm)			
		1,000	2,000	5,000	10,000
	Temperature	Percent Change			
Diesel #2	30°C	1.29	2.70	19.18	15.74
	50°C	0.49	3.22	10.57	18.82
	70° C	0.45	3.83	8.69	17.67
B-30	30°C	5.58	8.53	19.11	22.63
	50°C	4.68	3.66	21.79	32.80
	70°C	2.13	2.38	25.70	48.60
B-50	30°C	1.13	6.28	11.95	16.07
	50°C	0.52	7.64	10.51	11.35
	70°C	0.42	5.24	9.12	13.89

Analysis of the urea contamination results showed few consistent trends. Although the addition of urea tended to increase the dielectric constant significantly and the viscosity and density to a lesser level it was difficult to use this data for algorithm development. The high variability of the effect of urea was a product of the urea tending to crystallize into small solids in the fuel. These solids would stick to the sensing element and caused very inaccurate measurements. Urea contamination could be detected by the sensor but at high concentrations it would introduce considerable error into the prediction capability of the sensor.

5.3.4 Glycerol

SME biodiesel and blends with diesel #2 were tested with varying glycerol amounts added. Figure 5.24 gives dynamic viscosity results for SME B-100.

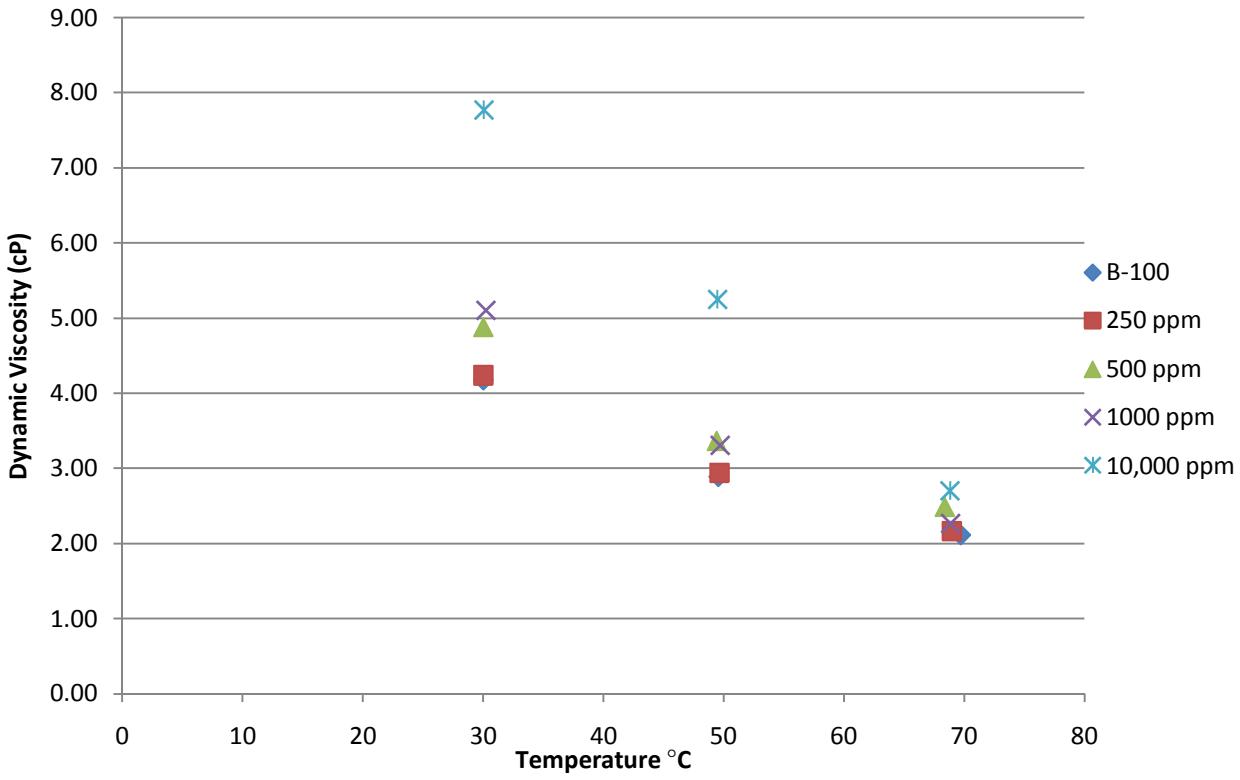

Figure 5.24 Dynamic viscosity of SME B-100 with glycerol contamination

Viscosity was affected considerably by the addition of free glycerin to the fuel sample at concentrations above 1,000 ppm. However, the effect was small at levels below 1,000 ppm. The viscosity of pure glycerol is approximately one hundred times greater than that of fuel so this increase in viscosity was not surprising. The phenomenon was very temperature dependent with the viscosity increase largest at low temperatures. These results agreed with Van Gerpen et al. (1996) whose experiments also showed significant increases in viscosity with glycerin addition.

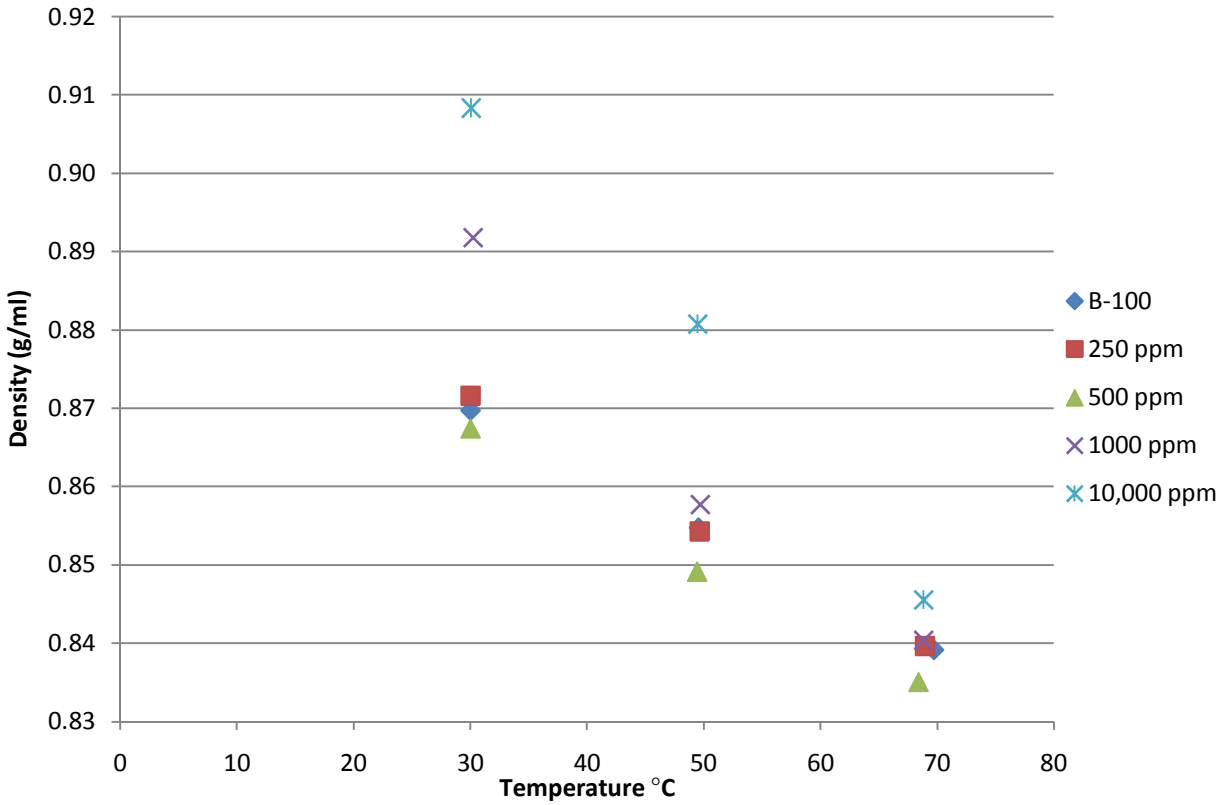

Figure 5.25 Density of SME B-100 with glycerol contamination

The density of SME B-100 under the same glycerol addition is plotted in Figure 5.25. Glycerol contamination had a larger effect on density measurements than any of the other contaminants tested in this study. Moreover, pure glycerol has a density of 1.261 g/ml which is also the highest of any of the contaminants. The change in density was largest at lower

temperatures. This suggested that the temperature dependence of density for glycerol was greater than for fuel samples. In cases of high glycerol contamination the density measurement was affected sufficiently to make fuel type determination by use of this sensor output very inaccurate.

The dielectric constant was also increased in the case of glycerol addition. Figure 5.26 details the results.

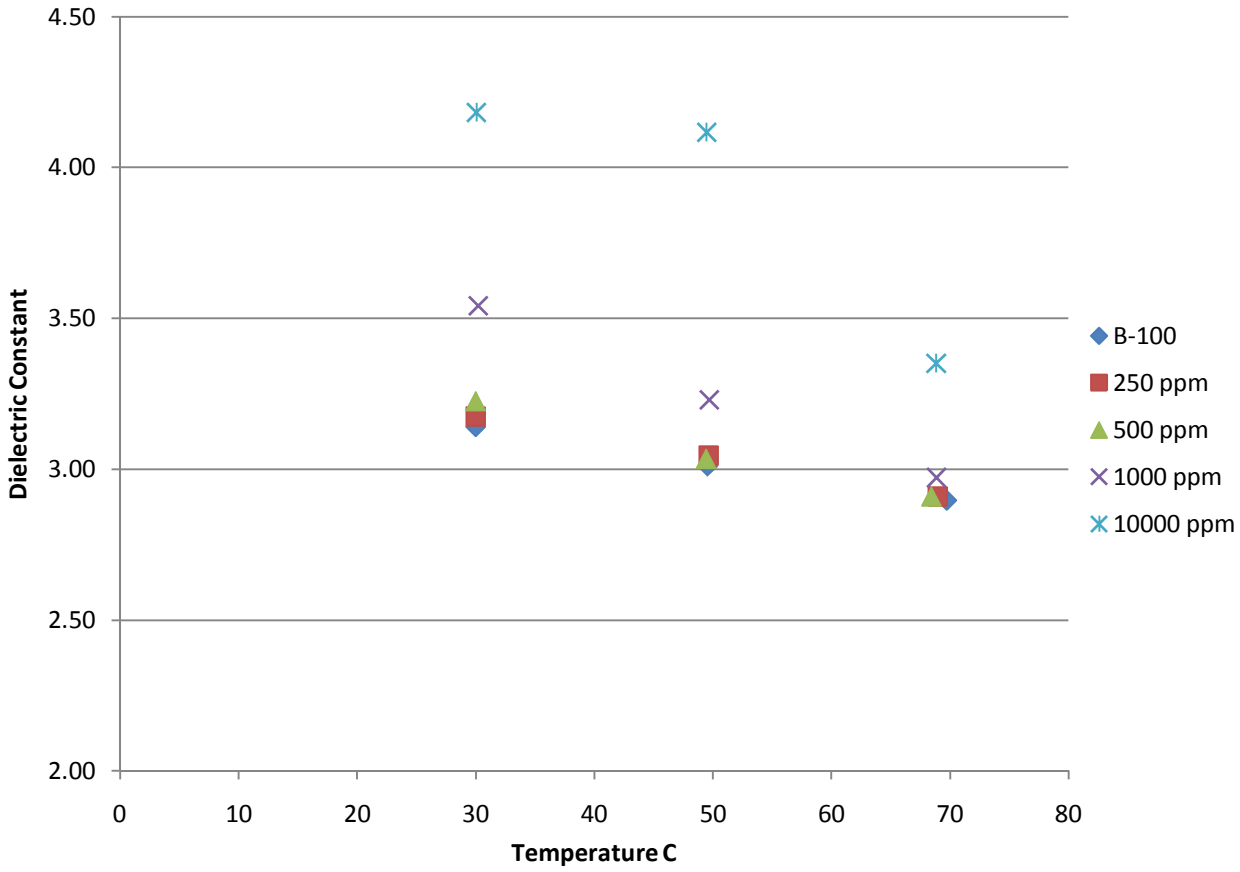

Figure 5.26 Dielectric constant of SME B-100 with glycerol contamination

The dielectric constant was moderately changed with glycerol addition. Concentrations below 1,000 ppm seemed to have little effect. In general, the amount of dielectric spike increased with decreasing temperature.

Several blends were also tested for glycerol pollution. Tables 5.14, 5.15, and 5.16 summarize the percent change of each of viscosity, density, and dielectric constant respectively for blends of SME B-100 with diesel #2 under several glycerol contamination concentration levels.

Table 5.14 Percent change in dynamic viscosity for fuels with glycerol contamination

		Concentration (ppm)			
		250	500	1,000	10,000
	Temperature	Percent Change			
B-100	30°C	1.5	16.9	22.3	86.0
	50°C	1.9	16.6	14.5	81.9
	70°C	2.3	17.9	7.3	27.8
B-70	30°C	9.2	10.3	20.4	24.3
	50°C	8.3	9.6	18.3	25.1
	70°C	8.7	11.3	22.5	16.7
B-50	30°C	9.4	5.2	30.7	101.1
	50°C	5.4	2.4	23.2	92.8
	70°C	0.5	1.6	10.9	45.1
B-30	30°C	17.4	16.4	30.6	30.5
	50°C	13.0	13.8	31.2	-2.2
	70°C	2.7	3.6	8.4	0.2
Average	30°C	9.4	12.2	26.0	60.5
	50°C	7.2	10.6	21.8	49.4
	70°C	3.6	8.6	12.3	22.4

Table 5.15 Percent change in density for fuels with glycerol contamination

		Concentration (ppm)			
		250	500	1,000	10,000
	Temperature	Percent Change			
B-100	30°C	0.21	-0.27	2.53	4.44
	50°C	-0.06	-0.66	0.33	3.03
	70°C	0.05	-0.49	0.14	0.75
B-70	30°C	0.95	1.12	2.65	2.32
	50°C	0.76	0.83	1.06	1.33
	70°C	0.89	0.95	0.67	1.10
B-50	30°C	-0.05	0.37	2.36	4.71
	50°C	-0.08	0.16	1.12	3.83
	70°C	-0.11	0.04	0.39	1.81
B-30	30°C	1.95	2.13	2.76	2.41
	50°C	1.25	1.60	2.89	0.43
	70°C	1.07	1.05	1.02	0.14
Average	30°C	0.76	0.84	2.57	3.47
	50°C	0.47	0.48	1.35	2.16
	70°C	0.47	0.39	0.55	0.95

Table 5.16 Percent change in dielectric constant for fuels with glycerol contamination

		Concentration (ppm)			
		250	500	1,000	10,000
	Temperature	Percent Change			
B-100	30°C	1.1	2.7	12.8	33.2
	50°C	1.1	0.8	7.3	36.7
	70°C	0.4	0.5	2.6	15.6
B-70	30°C	6.6	7.3	15.8	15.8
	50°C	6.5	6.6	10.3	12.6
	70°C	6.4	6.4	7.2	9.0
B-50	30°C	0.3	2.3	17.2	41.6
	50°C	0.4	0.9	17.7	40.5
	70°C	-0.1	0.4	6.2	37.9
B-30	30°C	1.4	5.9	7.1	9.0
	50°C	3.1	7.1	10.1	9.6
	70°C	1.5	1.7	4.5	9.4
Average	30°C	2.3	4.6	13.2	24.9
	50°C	2.8	3.9	11.4	24.9
	70°C	2.0	2.2	5.1	18.0

Percent change calculations show that viscosity was the property impacted the most by glycerol addition followed by dielectric constant and then density. All three sensor outputs showed more change at lower temperatures. Glycerol contamination would not be as easily interpreted by basic algorithms because all three outputs were significantly affected leaving no outputs to determine fuel type prior to detecting contamination. However, glycerol contamination above the ASTM standard of 1,900 ppm should be measurable. No trends were evident with changing blend level. The most important variable defining the deviations in change between fuel samples was likely heterogeneous mixing.

5.3.5 Methanol

Methanol was another potential contaminant of biodiesel, and consequently was used to dope fuel samples for testing with the MEAS sensor. Sensor outputs under various levels of contamination for SME B-100 were measured, and dielectric constant was found to be the only output appreciably altered (on average, viscosity variation under 3.0% and density variation under 0.25%). Figure 5.27 contains dielectric measurements for SME B-100 under methanol contamination.

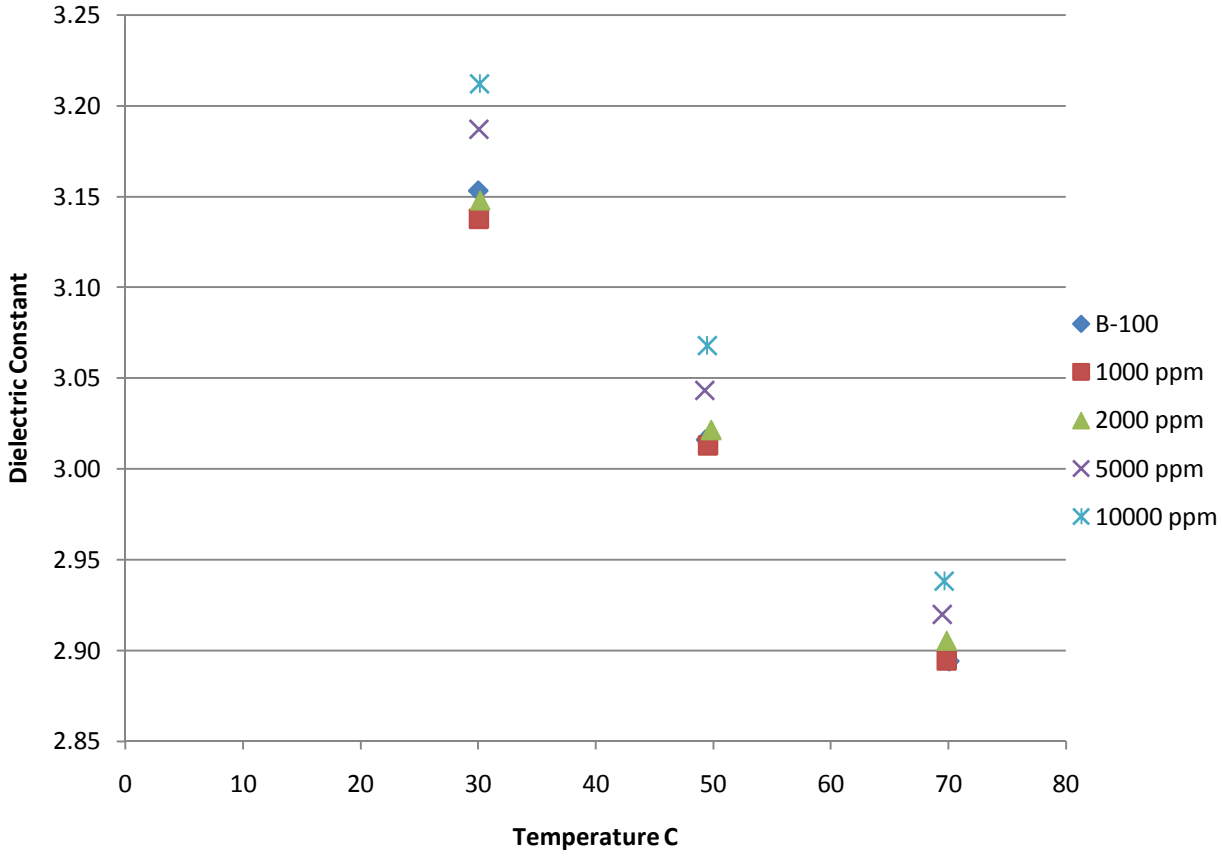

Figure 5.27 Dielectric constant of SME B-100 with methanol contamination

Dielectric constant increased with methanol addition as would be expected because the dielectric constant of pure methanol is 32.5. Methanol addition below 5,000 ppm was not

detectable. Tat and Van Gerpen (2003b) reported the dielectric spike with methanol addition to be much less than what is suggested by Figure 5.27. The discrepancy was tied to the difference between sensors used for measurement.

Tables 5.17, 5.18, and 5.19 contain viscosity, density, and dielectric changes for several fuels with methanol contamination.

Table 5.17 Percent change in dynamic viscosity of fuels with methanol contamination

		Concentration (ppm)			
		1,000	2,000	5,000	10,000
		Percent Change			
B-100	30°C	1.9	-7.5	-6.2	-7.1
	50°C	-2.4	-4.3	-3.7	-8.7
	70°C	-0.2	-0.5	4.6	-3.4
B-70	30°C	-6.9	-3.5	-7.1	-6.2
	50°C	-3.8	-1.9	-3.9	-3.9
	70°C	0.9	0.6	2.1	0.1
B-30	30°C	-2.6	2.1	4.5	11.0
	50°C	-4.8	-0.7	-0.8	5.5
	70°C	-2.6	4.9	1.7	6.9
Average	30°C	-2.5	-3.0	-2.9	-0.8
	50°C	-3.6	-2.3	-2.8	-2.4
	70°C	-0.6	1.6	2.8	1.2

Table 5.18 Percent change in density of fuels with methanol contamination

		Concentration (ppm)			
		1,000	2,000	5,000	10,000
		Percent Change			
B-100	30°C	0.01	0.15	0.21	0.33
	50°C	0.18	0.16	0.08	0.26
	70°C	0.10	0.00	0.00	0.13
B-70	30°C	0.26	-0.06	0.32	0.09
	50°C	0.33	0.23	0.37	0.27
	70°C	0.02	0.06	0.06	0.06
B-30	30°C	0.09	-0.13	0.04	-0.23
	50°C	0.20	0.19	0.26	-0.01
	70°C	0.20	0.05	0.21	0.23
Average	30°C	0.12	-0.01	0.19	0.06
	50°C	0.24	0.19	0.24	0.17
	70°C	0.11	0.04	0.09	0.14

Table 5.19 Percent change in dielectric constant of fuels with methanol contamination

		Concentration (ppm)			
		1,000	2,000	5,000	10,000
		Percent Change			
B-100	30°C	-0.5	-0.2	1.1	1.9
	50°C	-0.1	0.2	0.9	1.7
	70°C	0.0	0.4	0.9	1.5
B-70	30°C	0.4	0.7	1.5	3.1
	50°C	0.3	0.5	1.2	2.5
	70°C	0.2	0.4	0.9	1.7
B-30	30°C	-0.7	-0.4	0.9	11.3
	50°C	-0.2	0.2	0.9	5.9
	70°C	0.0	0.3	0.6	1.4
Average	30°C	-0.2	0.0	1.1	5.4
	50°C	0.0	0.3	1.0	3.4
	70°C	0.1	0.4	0.8	1.5

Tables 5.17 through 5.19 confirm that the density and viscosity of fuels were not largely changed by methanol addition. Also, the dielectric constant was affected measurably at methanol concentrations greater than 5,000 ppm. Furthermore, methanol contamination had the largest effect at low temperatures.

5.3.6 Summary of Results

Five contaminants of fuel were experimented with in order to determine the effect these contaminants have on the properties of fuels, and to gauge whether the MEAS sensor would be able to discern contaminated fuels from clean fuels. Results showed that for all of the contaminants tested if concentrations in the fuel were high enough there would be a measurable effect on fuel properties (Table 5.20).

Table 5.20 Summary of contamination effects

Fuel Situation	Viscosity	Density	Dielectric Constant
Water contamination	small increase	small increase	large increase
Urea contamination	small change/ erratic	small change/erratic	large change/erratic
Glycerol contamination	large increase	small increase	large increase
Methanol contamination	no change	no change	medium increase
Sulfur contamination	no change	no change	small increase

For each contaminant an approximate detection limit with the MEAS sensor could be set. Taking into account the natural variation in fuel properties table it is possible to provide estimates the detection limits for each contaminant (Table 5.21).

Table 5.21 Detection limits for various contaminants

Contaminant	Water	Sulfur	Urea	Glycerol	Methanol
Temperature °C	30-70	30-70	30-70	30-70	30-70
Detection Limit (ppm)	250-1,000	5,000-10,000	2000	1,000-10,000	5,000
ASTM Standard	500 ppm	15 ppm	NA	1,900 ppm	2,000 ppm

Detection limits meet ASTM standards at most temperatures for water and glycerol. Methanol and urea were also detectable but must be present in higher concentrations. Furthermore, detection limits were very temperature dependent. Lower temperatures led to more effective contaminant detection in all cases (below 50°C). This suggested that the sensor should be placed closer to the fuel tank in order to measure fuel near ambient conditions. When fuel was contaminated sensor outputs were more variable and less accurate because of the effect of heterogeneous mixing. If the fluid surrounding the sensing element contained a droplet of contaminant the sensor's outputs were greatly changed. It was expected that fuel type and blend prediction algorithms would be less accurate in the case of contaminated fuels. Moreover, while contaminants were easily discerned from observation of sensor outputs when fuel type was known, it was a much more complicated problem to detect contamination when fuel type was also unknown which was the case faced by fuel composition sensors in real applications. Section 5.6 discusses the development of algorithms that provide solutions to this issue.

5.4 Effect of Fuel Degradation on Sensor Outputs

As fuel degrades its properties change, allowing this condition to be detectable to the MEAS sensor. Although the exact consequences of combusting degraded fuel are not well defined, it is less than ideal to use degraded fuel. Engine manufacturers feel that identifying

degraded fuel could add value to engines despite conflicting literature on how detrimental combusting degraded fuel actually is. The effects of degradation on sensor response for several fuel samples are summarized in the following figures. Results for open container samples of diesel #1, diesel #2, and SME B-100 were plotted (Figure 5.28).

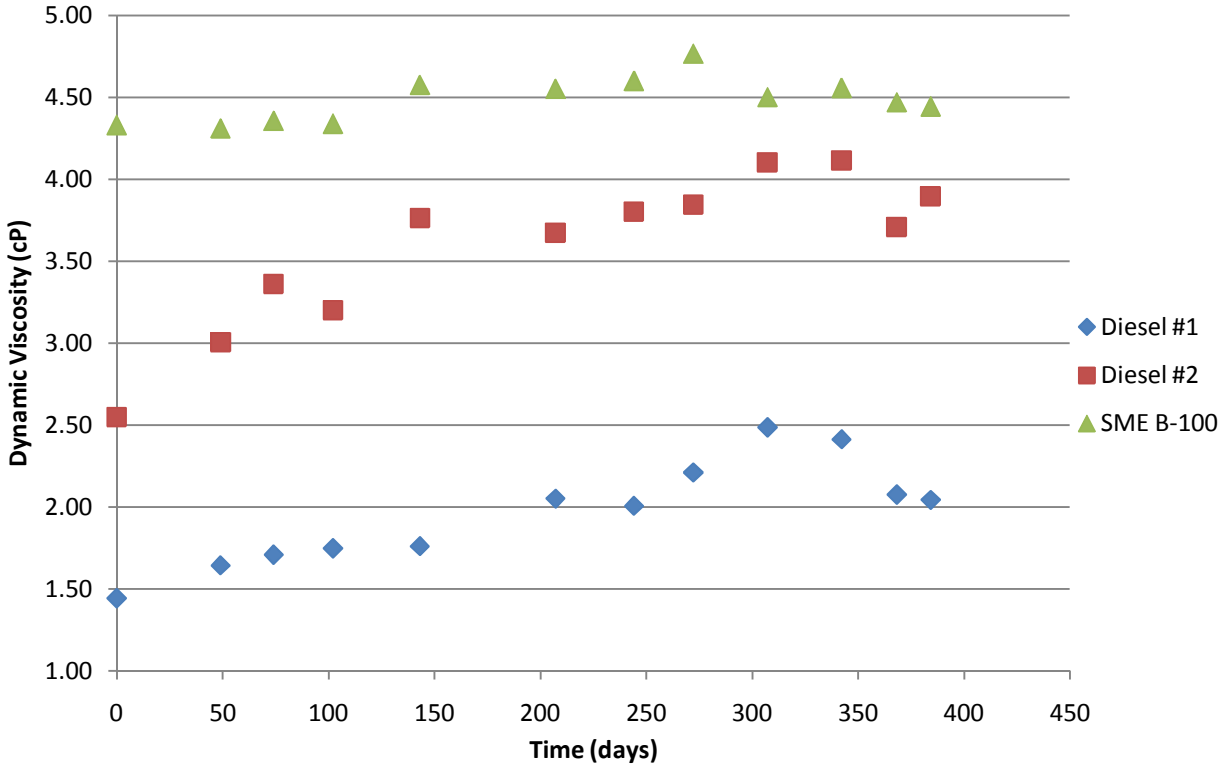

Figure 5.28 Effect of time on the dynamic viscosity of several fuels

It can be seen that the viscosity of all three fuels increased with time. The result was very dramatic for diesel #1 and diesel #2 with viscosity increasing by more than 50% of the original value. The literature review suggested that biodiesel would be more susceptible to degradation than petroleum based fuels. However, these results indicated the degradation of the petroleum based fuels was much more observable by the MEAS sensor than for biodiesel. The change in viscosity for biodiesel was in a similar range to findings from Bondioli et al. (2003). The

variation observed in the trends was partially due to changes in the temperature at time of measurement between each case.

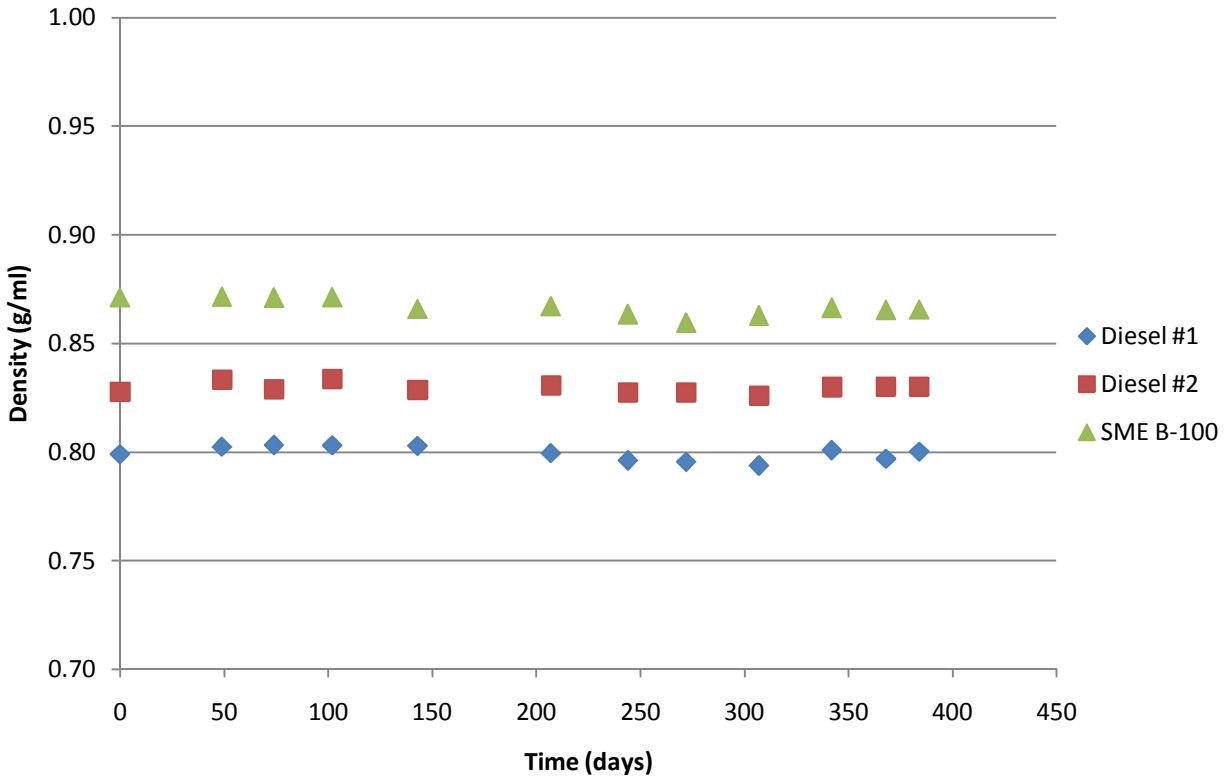

Figure 5.29 Effect of time on the density of several fuels

Figure 5.29 summarizes the density of open container fuels samples with time. The density of the fuels was nearly constant over the entire measurement time period. Moreover, a comparison of the density measurement to the viscosity measurement would be an effective way to detect degraded fuel.

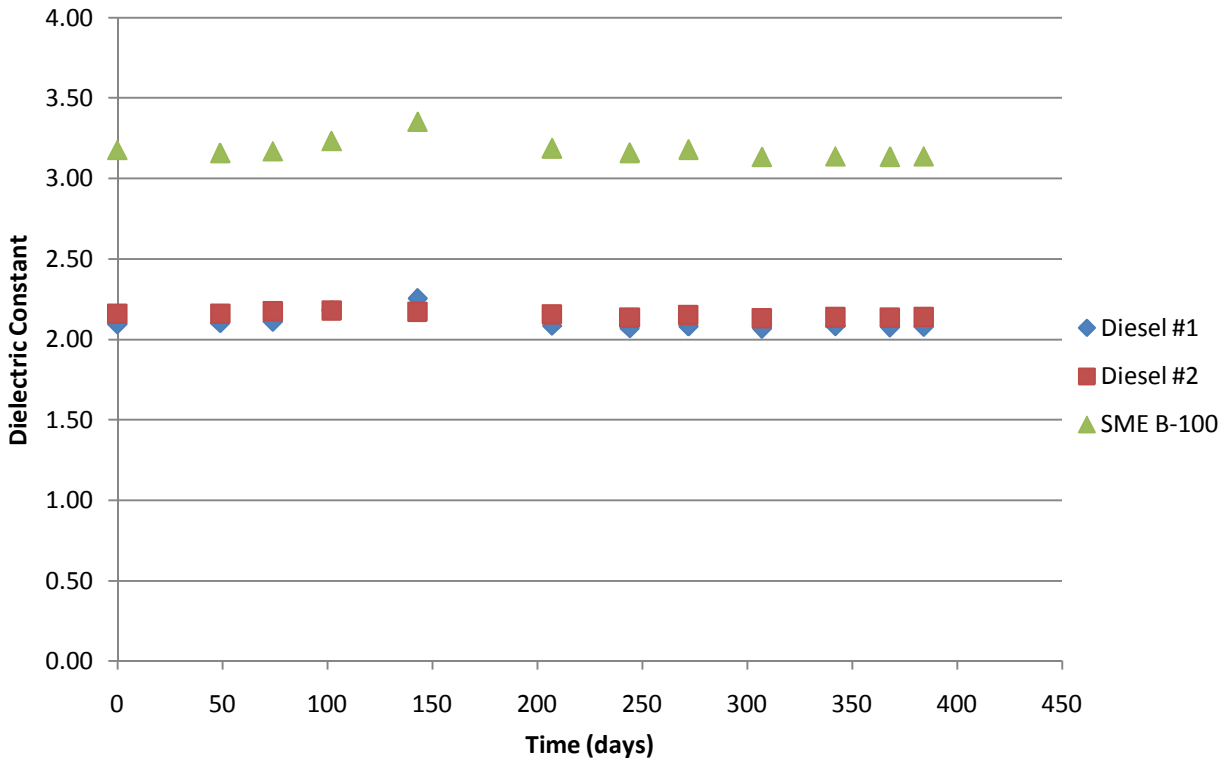

Figure 5.30 Effect of time on the dielectric constant of several fuels

Figure 5.30 presents the dielectric constant output against time. As with the density output, the dielectric constant measurement from the MEAS sensor did not appear to change as fuel samples age.

Figures 5.31 through 5.33 present results for measurements from closed container fuel samples over a 580 day time period. Data was not available for a several month period near the beginning of the study.

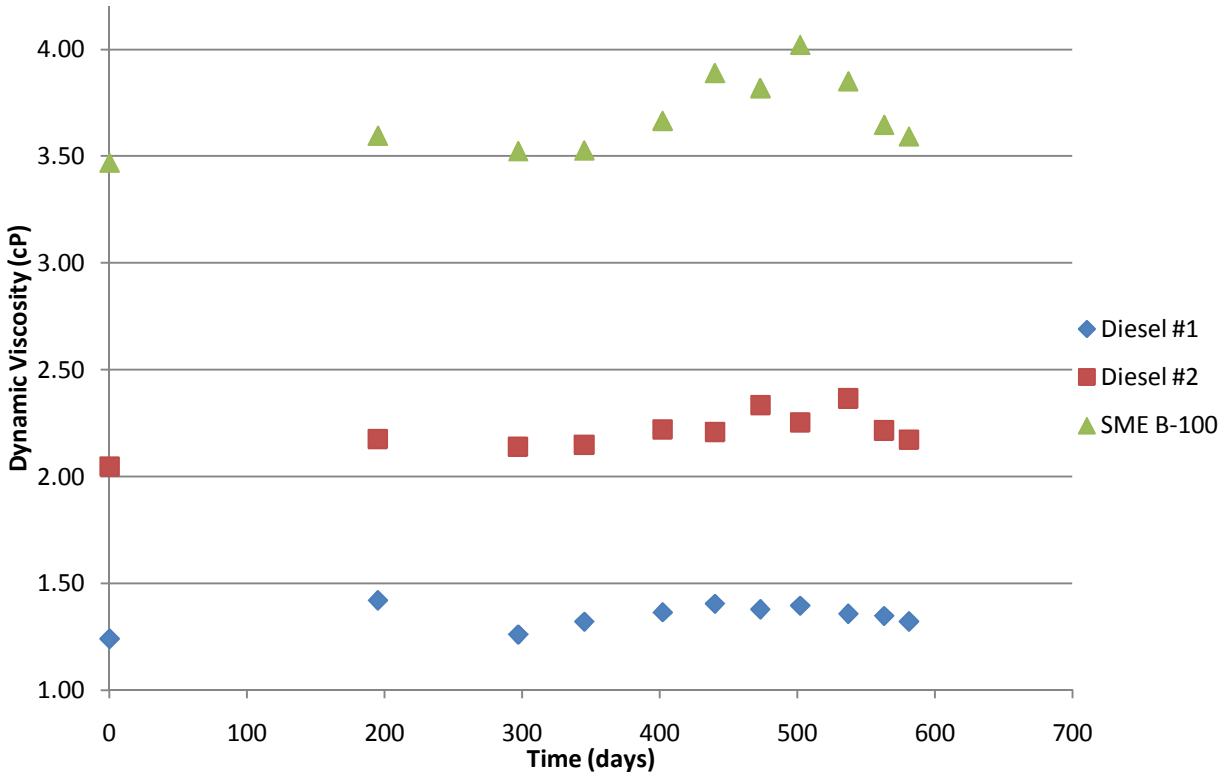

Figure 5.31 Effect of time on the dynamic viscosity of several fuels

The viscosity once again increased with age for the closed container samples although the effect was not as pronounced as indicated in Figure 5.31. The change was approximately the same for each of the three fuels and was in the range of 6-12%. A peak in viscosity measurements was observed late in the time period for unknown reasons

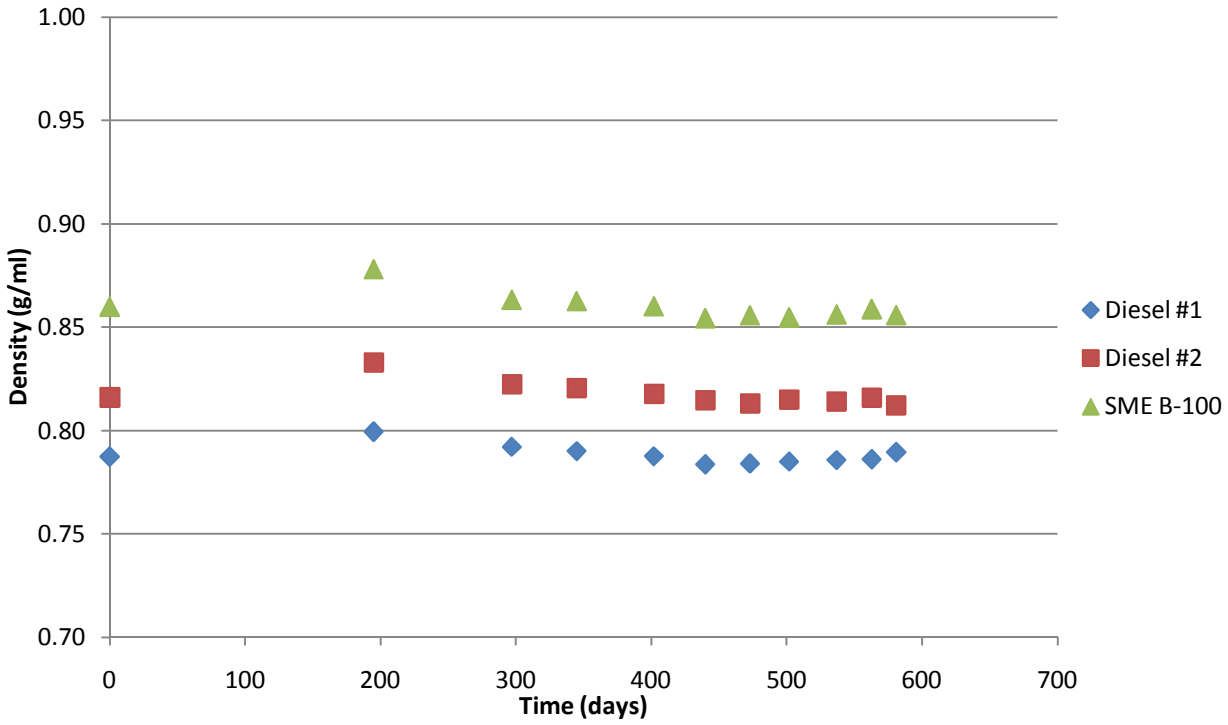

Figure 5.32 Effect of time on the density of several fuels

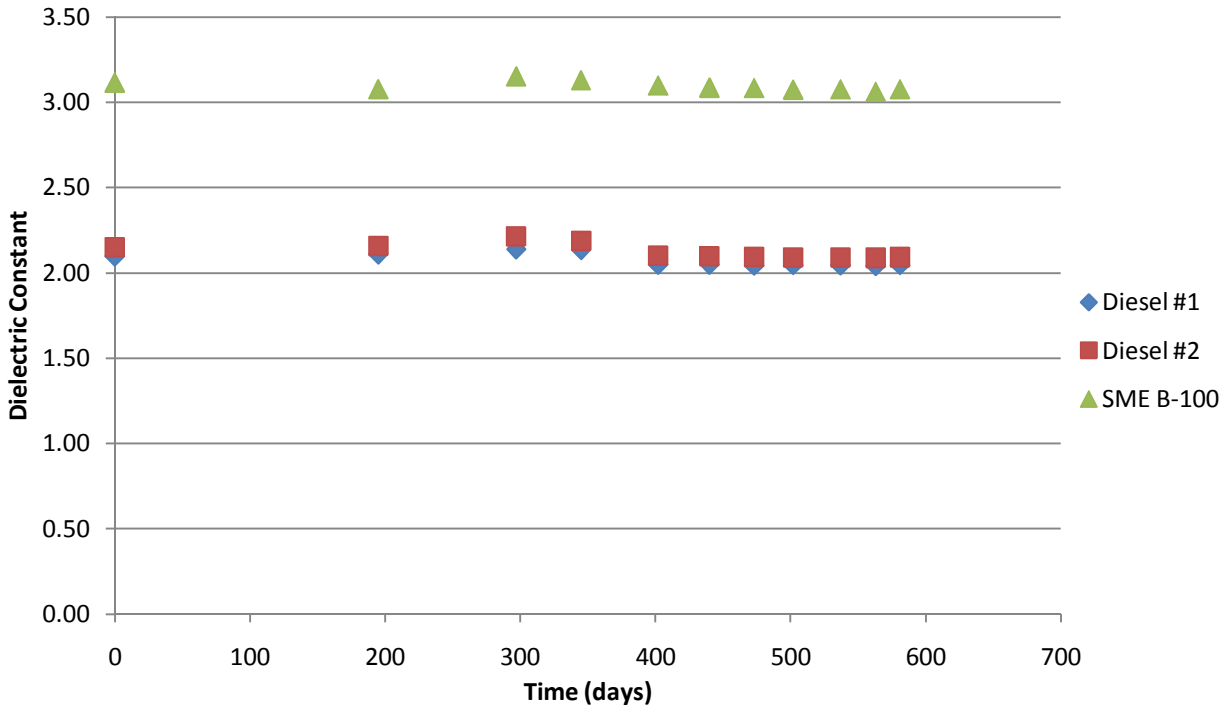

Figure 5.33 Effect of time on the dielectric constant of several fuels

Figures 5.32 and 5.33 display sensor results for the density and dielectric constant outputs. It can be seen that the density and dielectric constant were nearly constant with ageing for these fuels samples. Based on the above results degraded fuel would show an increased viscosity over fresh fuels while having unchanged density and dielectric properties. Moreover, an algorithm employing a comparison of either the density or dielectric constant measurement with the viscosity measurement would be successful at identifying degraded fuels.

5.5 Development of a Fuel Classification Model

General results for the form and accuracy of models applied to the data are conveyed in this chapter. In addition the use of these models in the design of an algorithm for fuel type and quality detection is described.

5.5.1 Algorithm Format

The base algorithm proposed for use in the MEAS sensor involved a series of decisions based on sensor outputs. This series of logic sought to determine the type of diesel fuel that was being used, the level to which this fuel was blended with biodiesel, the contamination level of the fuel, and the degradation level of the fuel.

The first step in fuel type determination was to decide if diesel #1 or diesel #2 is the primary fuel. As was seen in Section 5.2.3 density is the ideal output to use for this since it was minimally affected by contaminants and it did not overlap for diesel #1 blends up to B-20 and diesel #2 blends. Therefore, the algorithm used a linear split on the density scale dependent on temperature to determine within which blending regime the fuel fell (Figure 5.34).

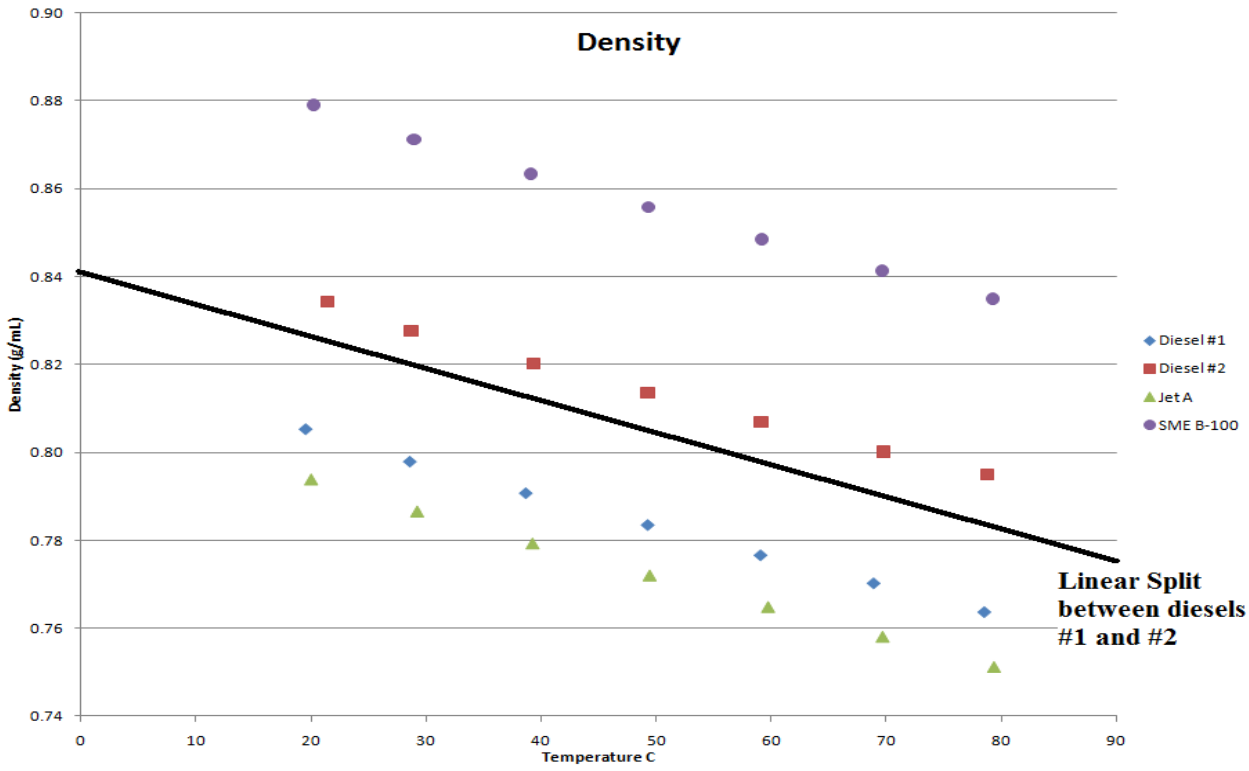

Figure 5.34 Base fuel determinations relative to density output

Once the base fuel had been set the blend percentage was calculated. The algorithm first calculated the properties of the neat fuels at the measured temperature. For example, if the base fuel was diesel #2, six properties (the dynamic viscosity, density, and dielectric constant of pure diesel #2 and SME B-100) were calculated using temperature regression models. Next, the algorithm took the measured density and dielectric outputs and linearly interpolated between the two calculated values for neat fuels and returned two estimates for blend percentage. The viscosity output was also interpolated but it was not linear as described in Table 4.8. Finally, there were three estimates for blend percentage. The three results were averaged to give the final blend approximation. Testing of this part of the algorithm for uncontaminated fuels gave blend prediction accuracy at three percent or better.

For contaminated fuels blend prediction gave errors up to 30% if no other compensation was included. Water contamination and degradation were the most important of the fuel conditions studied so the algorithm development focused on these effects. The algorithm provided the predicted dielectric constant of the fuel based on the measured viscosity. This value was compared to the measured dielectric constant. As is shown in more detail in Section 5.5.5 a relationship had been developed for the difference between these two values over varying temperature and contamination levels. If the difference was close to zero the algorithm indicated that the fuel was clean and the original blend estimate was specified. If the difference was positive this indicated that there was water contamination at some level. If it was negative the fuel was considered degraded. The average change of each output over the clean fuel output for varied temperature and contamination had also been compiled so the estimated contamination level could give an adjusted property that was close to that of the clean fuel. Finally, this adjusted value was entered into the blend prediction interpolations. This method would decrease blend prediction error to 10% or less.

5.5.2 Regression Models for Fuel Properties with Temperature

Inspection of the plots created for sensor outputs discussed in Section 5.1.1 gave some information about the type of models that may describe the dependence of each output on temperature. Furthermore, the MEAS sensor's temperature measurement was an essential output for accurate prediction of fuel composition. Temperature was used to estimate uncontaminated properties of possible fuels which could then be used to compare with the measured outputs. Section 4.7.2 summarizes the models used to fit the data. Figure 5.35 shows dynamic viscosity data with curve fitting for several fuels.

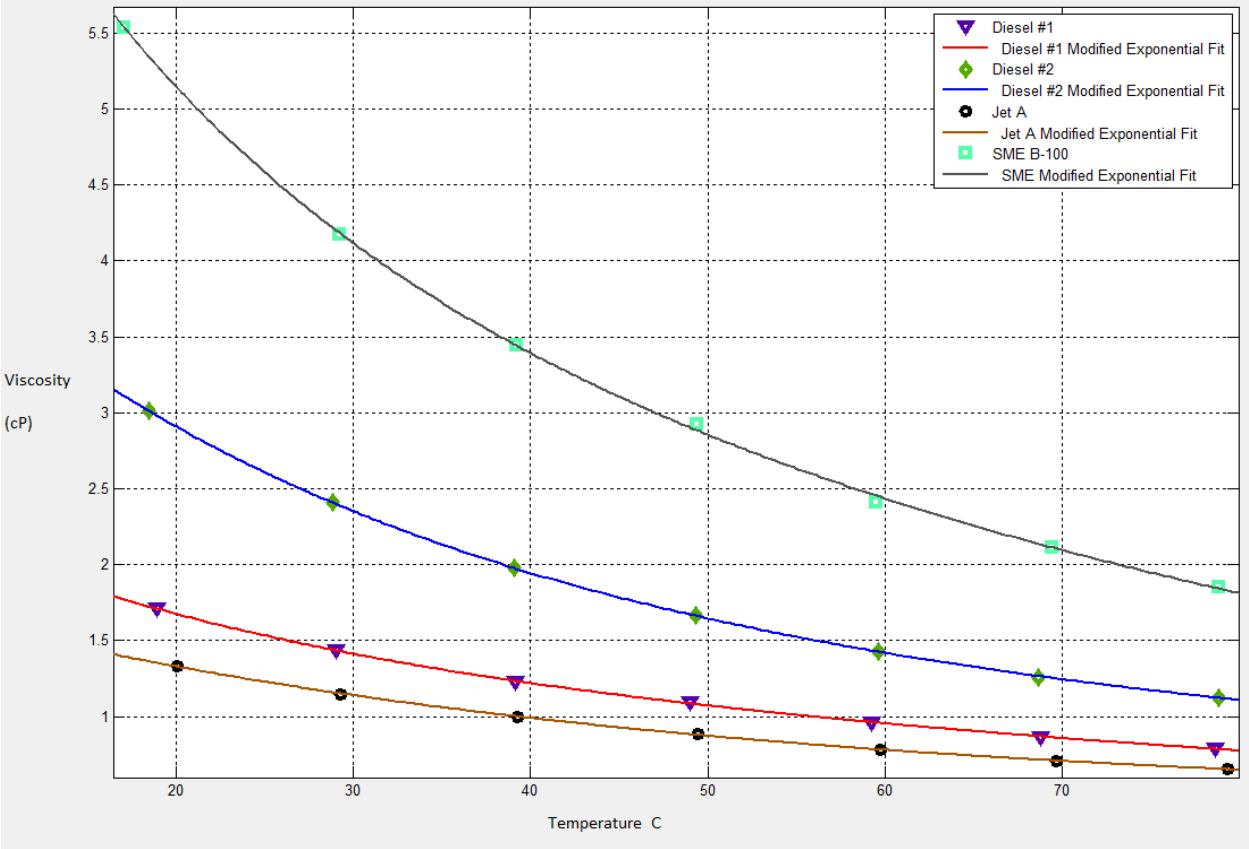

Figure 5.35 Dynamic viscosity curve fits

Data fits for viscosity with temperature were developed using the model described in Table 4.8. The model fit very well giving minimum R^2 = .9996.

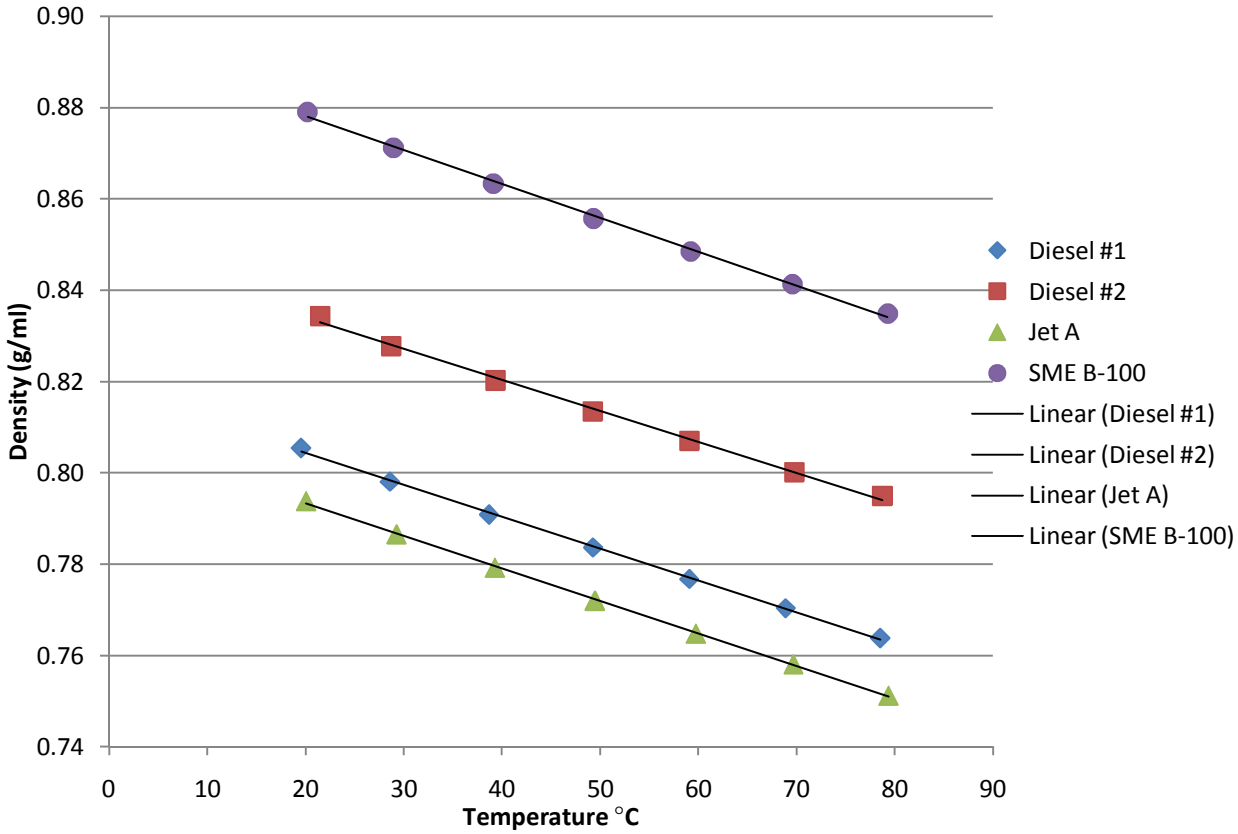

Figure 5.36 Density curve fits

The density outputs were also modeled as shown in Figure 5.36. Density was predicted with a linear relationship with temperature. Each of the fuels had a linear fit with approximately the same slope (less than 0.5% variation). Accuracy of the fits was a minimum $R^2 = .9972$.

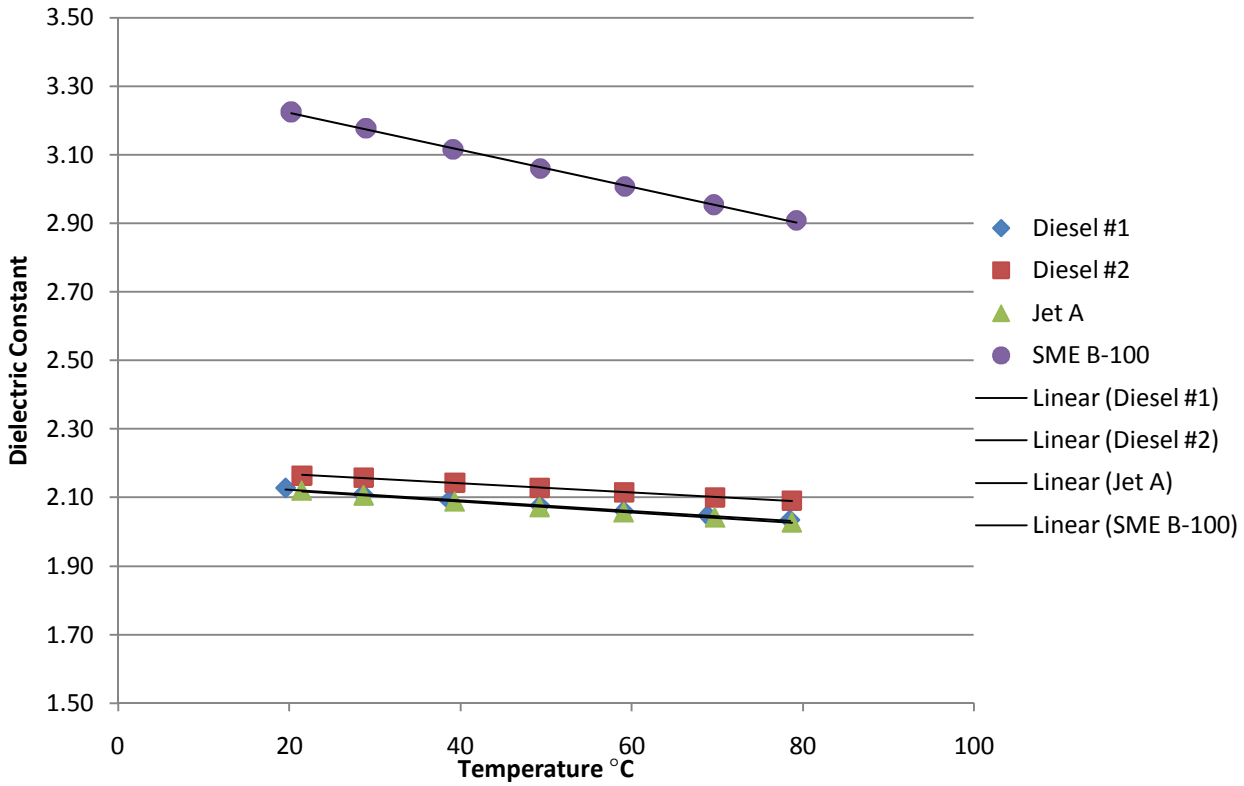

Figure 5.37 Dielectric constant curve fits

Figure 5.37 contains the data for dielectric constants of the same fuels and temperature range. The dielectric constant was also very accurately modeled by a simple linear model. The slope of this model did vary for the type of fuel. The accuracy was apparent from R^2 >.9971.

5.5.3 Regression Models for Fuel Properties with Blend

In order to interpolate between the calculated values of the two pure fuels in a blend a model must be established for the way each property changes with blend percentage. Models used for this purpose are described in Table 4.8 (Tat and Van Gerpen, 1999; Tat and Van Gerpen, 2000). This section gives figures showing the accuracy of fits for blends of diesel #2 and SME B-100. Figure 5.38 details both the actual data and values predicted by the model for dynamic viscosity of blends at two different temperatures.

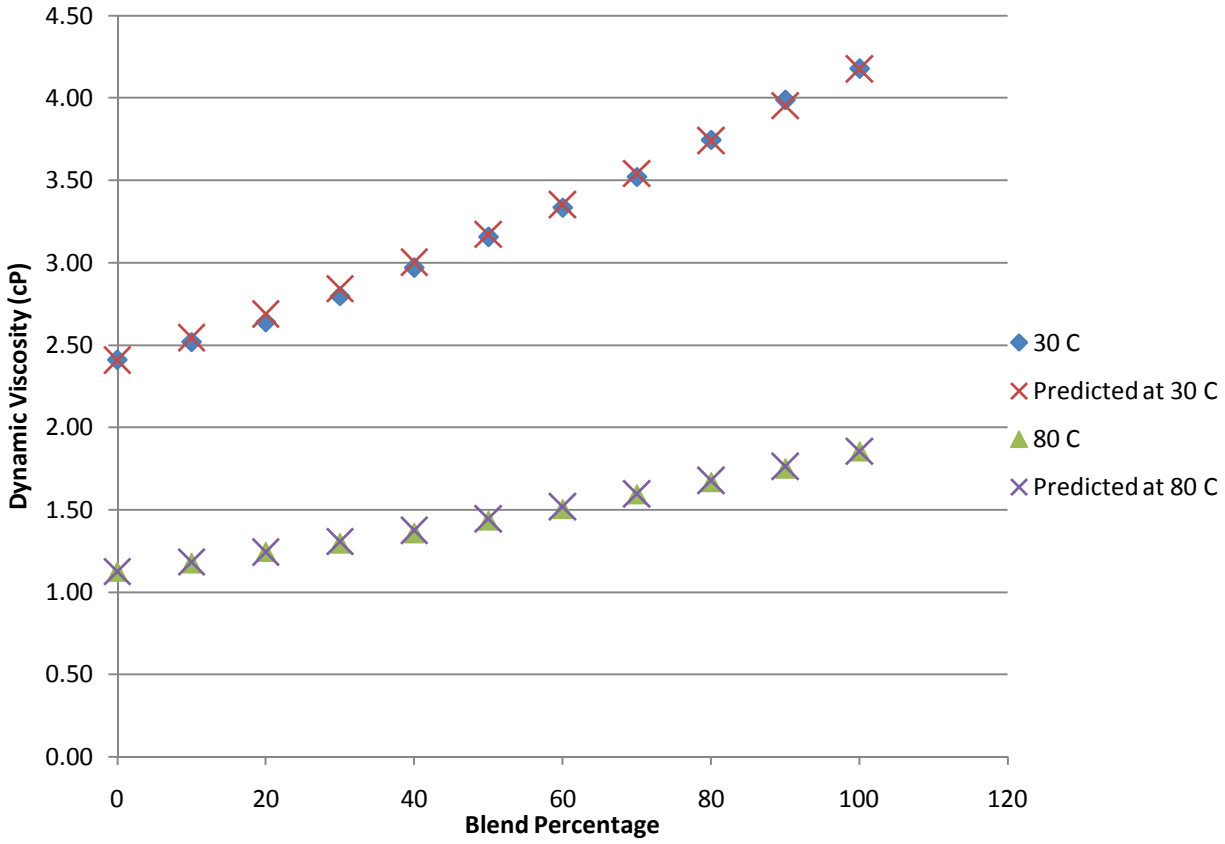

Figure 5.38 Measured and predicted dynamic viscosity for blends of fuel

The Grunberg-Nissan model was very accurate with errors of less than two percent. The exponential shape of the viscosity blending trend was well described by the model.

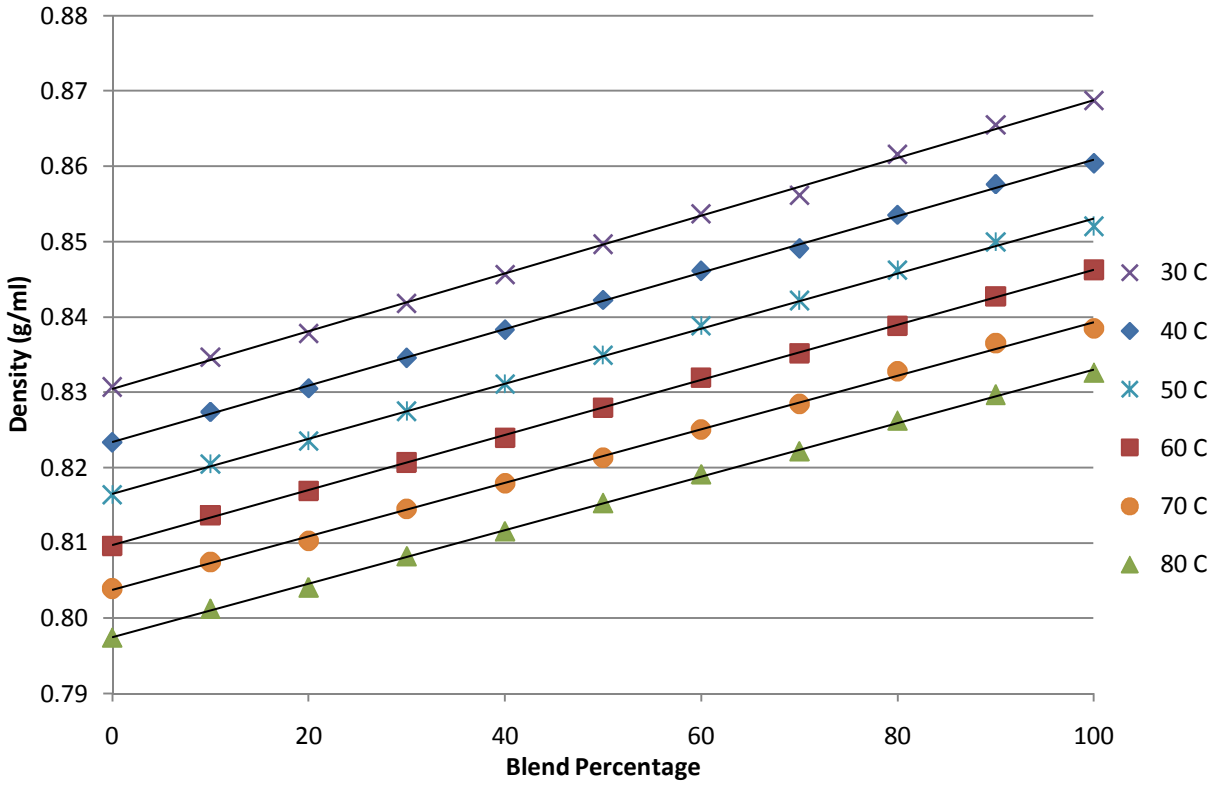

Figure 5.39 Density of diesel #2 and SME B-100 data fitting

Figure 5.39 illustrates the model fit for density. Linear models provided a close fit to the blended fuels at each of the plotted temperatures. In addition the slope of each fit was approximately the same (variation less than 0.5%). The accuracy of the linear model for density of blended fuels was very high with R^2 values of at least .9991.

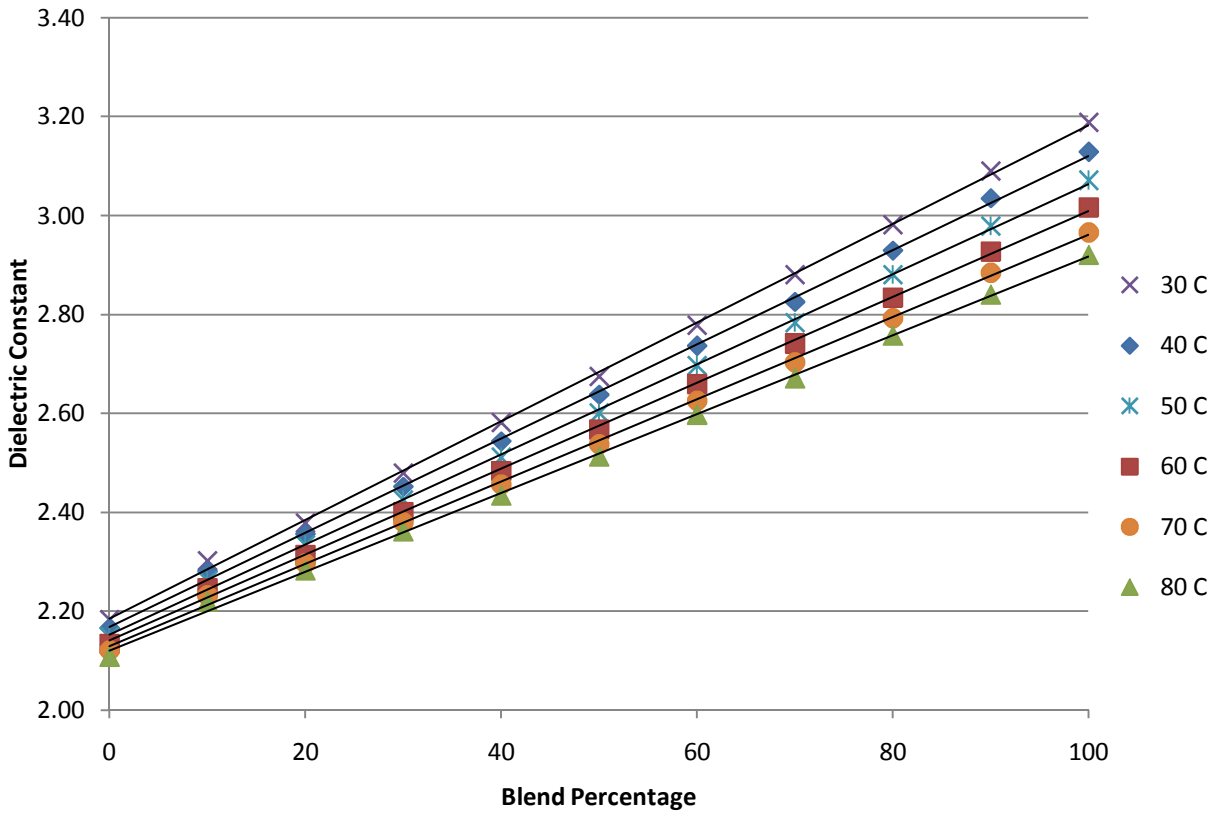

Figure 5.40 Dielectric constant of diesel #2 and SME B-100 data fitting

Figure 5.40 displays the models and data for dielectric constant with changing blend percentage for several temperatures. For dielectric constant a simple linear model was once again sufficient for very accurate prediction of fuel properties given the properties of the two components in the blend. The slope of each line was not the same, however, due to the difference in rates of change of diesel #2 and SME B-100 with temperature. R^2 values were at a minimum .9984.

5.5.4 Sensitivity and Limits of Regression Models

Another important factor in the success of the algorithm was defining the limits of its validity and its sensitivity. This section details the limits of the algorithm with respect to

temperature. In addition the appropriate sensitivity for the algorithm as defined by the natural variation in fuel properties is discussed.

Testing was carried out through the upper temperature range that fuels would likely encounter in a fuel system. Moreover, the models developed should be accurate up to this upper temperature limit. However, the lower temperature limit that fuels would reach in cold climates was not tested. The cloud point was the limit to which the sensor will accurately read fuel properties so this also was set as the lower limit of the algorithm (Figure 5.41). The cloud point for blended fuels was estimated by linearly interpolating between measured cloud points for diesel #2 and SME B-100 found in the literature (Tables 3.4 and 3.5).

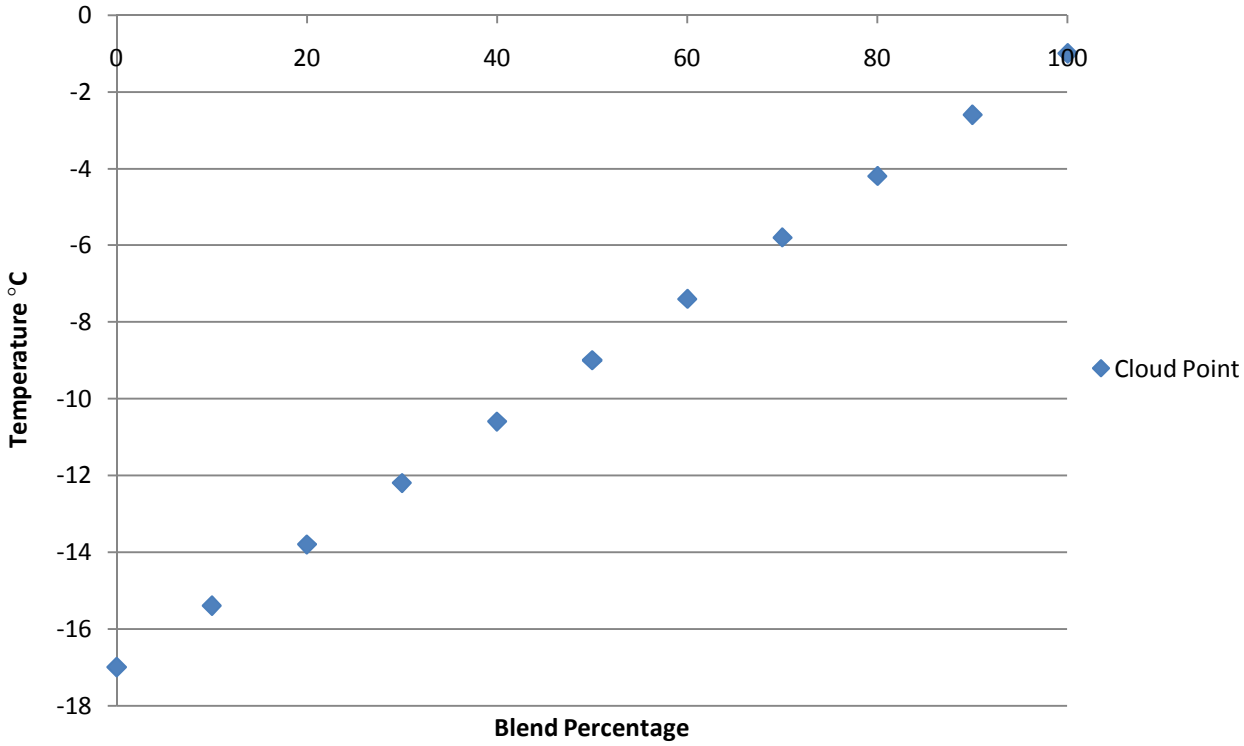

Figure 5.41 Cloud point of blends of diesel #2 and SME B-100

The lower limit of the algorithm was detected when the sensor gave erratic results at temperatures lower than shown in Figure 5.41. At temperatures above 0°C the algorithm should always be accurate. At temperatures below -17°C sensor results must be ignored since the results would not fall within the valid range of the algorithm.

The algorithm also relied on the measured properties from the sensor being relatively similar to the properties measured for fuels in this study. Moreover, the detection of contamination or degradation should not be so sensitive as to falsely detect fuels due to normal variation of properties from those measured in this work. Some analysis was conducted on the natural variation of biodiesel viscosity and density. Table 5.22 summarizes results for predictions of biodiesel viscosities for the natural ranges of fatty acid compositions.

Table 5.22 BDProp predicted natural range of viscosities for SME and RME (rapeseed methyl ester) biodiesel

		Dynamic Viscosity cP		
Biodiesel	Temperature °C	Upper Limit	Lower Limit	Percent Range
SME	17	6.68	6.13	9.0
	37	4.05	3.77	7.4
	57	2.72	2.56	6.2
	77	1.97	1.88	5.1
RME	17	9.41	8.48	11.0
	37	5.61	5.12	9.6
	57	3.63	3.36	8.0
	77	2.50	2.35	6.4

Table 5.22 predicted similar viscosities as to what was measured for SME biodiesel; however, it predicted higher viscosities for rapeseed biodiesel. The important conclusion was

that the natural variation for viscosity in biodiesel was temperature dependent and ranged from about 5% to 10%.

Table 5.23 details the results of similar computations for the density of SME and RME biodiesel. The natural variation in density was much less than that of viscosity. Also, the predicted densities were very similar to what was measured for each type of biodiesel.

Table 5.23 BDProp predicted natural range of densities of SME and RME biodiesel at 20°C

	Upper Limit	Lower Limit	Percent range
SME	0.888	0.883	0.481
RME	0.884	0.881	0.370

Based on the assumption that petroleum based fuels have less variation in properties due to more consistent refining technologies and source compositions it could be assumed that the ranges established for biodiesel were the worst case scenarios for variation in blended fuels. Therefore, the sensitivity of the sensor would be in part based off of the ranges calculated above. In addition, there existed no way of predicting dielectric constant based on fatty acid content so an estimate would be made according to the variation observed during experimentation.

5.5.5 Identification of Contaminants or Degradation

Comparison of how fuel properties changed with added contaminants was a criterion that would be used for contamination identification. Moreover, as discussed in Section 5.5.1 comparison of the dielectric constant predicted from the viscosity measurement to the measured dielectric constant was the basis for both water contamination and degradation condition. This choice is apparent from the blend prediction error calculated from equations 4.1 through 4.3 (Table 5.24).

Table 5.24 Calculated blend prediction error *E*

		$E_{Viscosity}$					$E_{Density}$					$E_{Dielectric\ Constant}$			
		250 ppm	500 ppm	1000 ppm	10000 ppm		250 ppm	500 ppm	1000 ppm	10000 ppm		250 ppm	500 ppm	1000 ppm	10000 ppm
T °C	30	0.02	7.00	10.07	11.91		4.14	6.01	13.24	17.76		9.13	18.97	25.21	62.24
	50	1.36	5.63	6.22	7.42		2.46	3.70	6.40	9.27		4.16	8.99	18.24	48.23
	70	0.55	10.78	7.29	9.99		2.16	2.27	5.75	3.84		1.35	2.74	5.09	33.37

Inspection of the table showed that calculation of the blend level became more inaccurate with increased water addition and decreased temperature for all three outputs. Use of the dielectric constant for blend prediction with contamination introduced the most error. Moreover, the viscosity output was the best predictor of blend level in most cases. Therefore, the comparison of the viscosity and dielectric constant was the best basis for contamination detection.

Degradation was also considered in the algorithm, and a similar calculation was undertaken to find the blend prediction error for degraded fuel as a function of fuel age. The increase in viscosity associated with degradation caused the $E_{viscosity}$ to be much higher than the other two calculated values for density and dielectric constant.

A plot of the difference between the predicted dielectric constant from the viscosity output and the actual dielectric constant could be used to identify both the water contamination and degradation conditions. Figure 5.42 gives this difference for water contamination at four concentrations over three temperatures in addition to degradation at four ages (Eqn. 4.4).

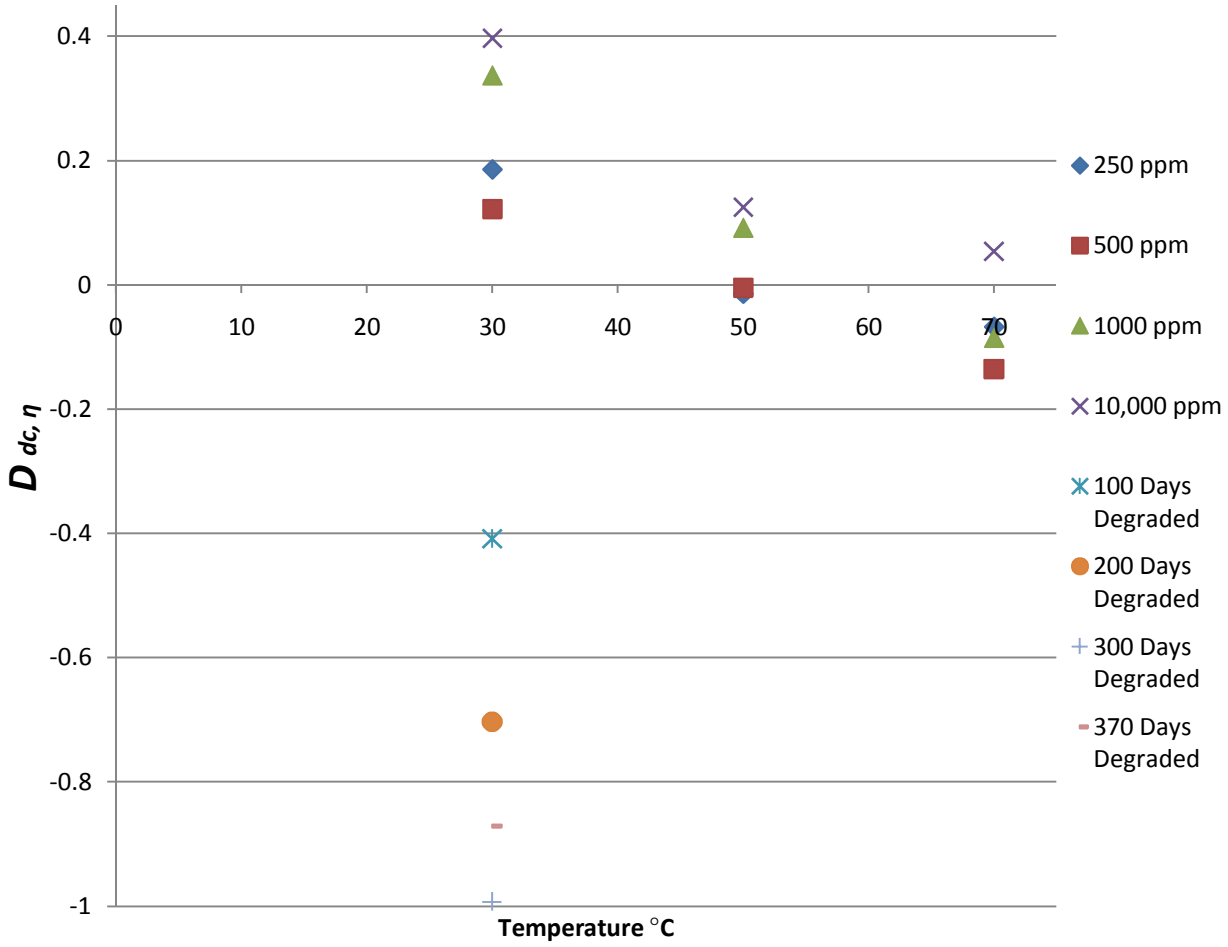

Figure 5.42 Calculated $D_{dc,\eta}$ for water contaminated and degraded fuel

Figure 5.42 shows that water contamination caused the calculated difference to be positive and increase with decreasing temperature. Values that were near zero indicated clean, fresh fuel. In contrast as the value became more positive this indicated higher water contamination. Large negative values were indicative of degraded fuel. At 30°C, 250 ppm water contamination was detectable. At 50°C the detection limit rose to 1,000 ppm while at 70°C the detection limit was near 10,000 ppm. The effect of degradation was very apparent from this plot.

Using Figure 5.42 the water contamination or degradation condition for any fuel sample could be estimated. Once the level of contamination was known the percent change data presented in Section 5.3.1 could be used to approximate the actual values of the fuel if it had not been contaminated. Finally, these approximate clean fuel values could be placed into the interpolation equations to give the blend percentage.

5.5.6 Neural Network to Identify Fuel Composition and Contamination

An alternative method for algorithm development for both blend percentage and contamination identification was the use of a neural network. Neural networks have proven to accurately develop models for many engine and sensor applications, and they provided a second option for fuel composition sensing. Data from one sensor over a range of blends between diesel #2 and SME B-100 and several water contamination levels was used to create and train a neural net algorithm in MATLAB. MATLAB software divided the data into three sets placing 70% of the data vectors into training, 15% into validation, and 15% into testing. The software then automatically optimized training of the network and tested the predictive ability on the testing data. Figure 5.43 shows the algorithms predicted blend percentage values vs. the actual values. Contamination levels 0.0, 0.25, 0.5, 1.0, and 2.0 referred to water concentrations of 250 ppm, 500 ppm, 1,000 ppm, and 10,000 ppm respectively.

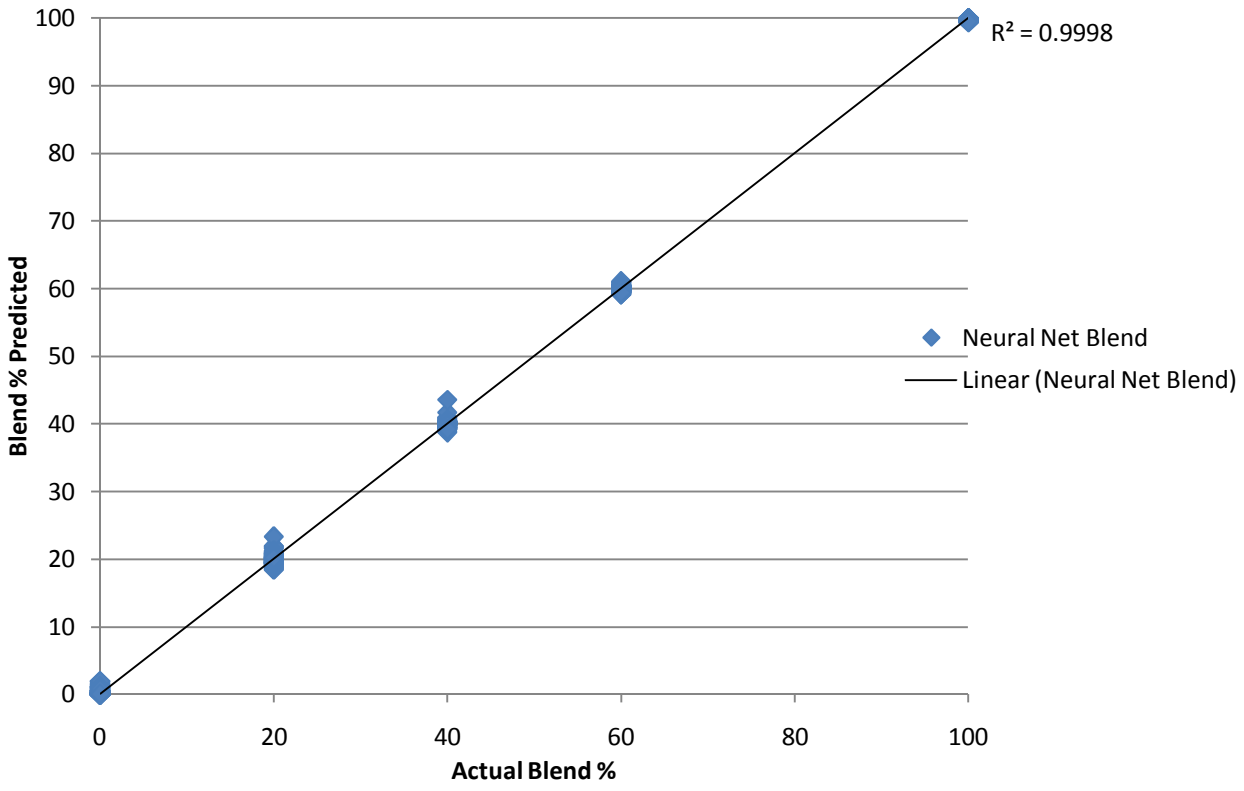

Figure 5.43 Neural network prediction of blend percentage

The neural network generated accurate predictions for blend percentage in the case of using one sensor to develop the algorithm and the same sensor's outputs to test it. The mean square error was less than 3.1 for training, validation, and test data for this case, and the R^2 value was above .99. Moreover, errors of less than 4% were predicted by the network.

In addition the actual values and predicted values for contamination condition were plotted. Figure 5.44 presents these results.

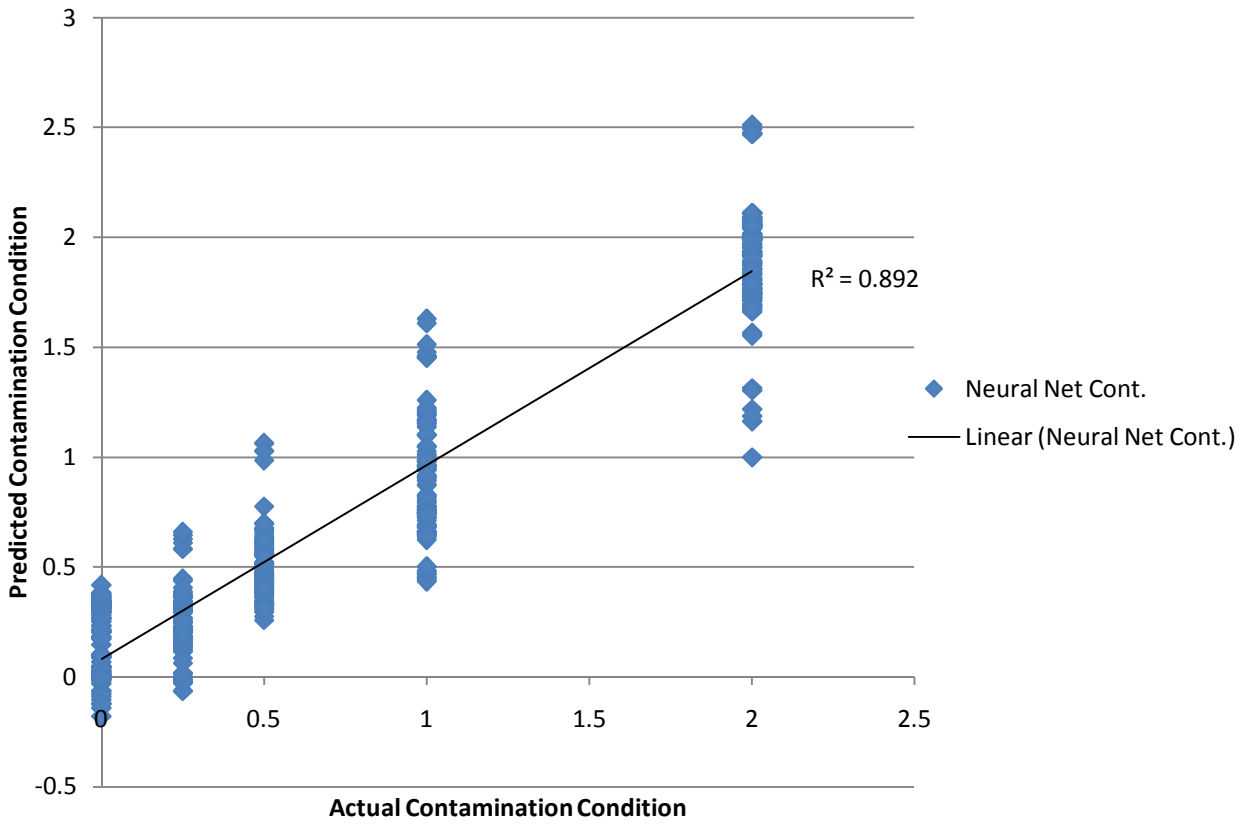

Figure 5.44 Neural network prediction of contamination conditions

The network was less accurate at predicting contamination level, particularly at higher blend percentages. The mean square error for this case was below 8.0 and the R^2 = .892. Addition of water added variability to the data resulting in less accurate results. Also, higher contamination levels led to greater variability. This was still a positive result however since contamination levels of 1 and 2 were entirely distinguishable from clean fuel samples. It was desirable that at the minimum the algorithm could identify the higher contamination levels and not give false positive readings for clean fuel.

Figures 5.43 and 5.44 represent ideal conditions in which the same sensor was used for both algorithm development and testing. Observation of contamination results for several

different sensors indicated that each sensor showed different magnitude of changes from a given contamination concentration. Therefore, a more accurate assessment of neural network software's ability to predict fuel conditions was to develop the model based on data from several sensors. Figure 5.45 shows actual blend percentage vs. predicted blend percentage for a neural network model using three sensors for both development and testing.

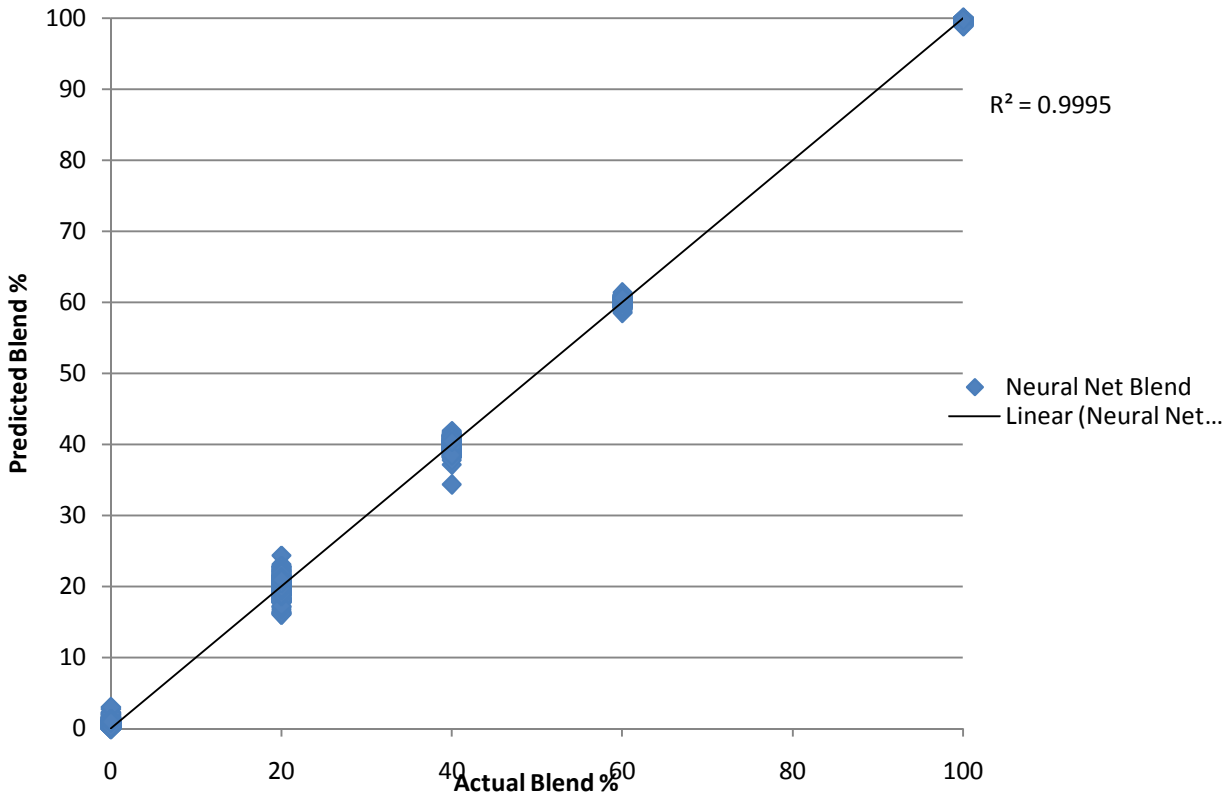

Figure 5.45 Neural network predictions for blend percentage with multiple sensor data

Again, the network accurately predicted blend percentage in the case of multiple sensor data. The mean square error and R^2 values were similar to figure 5.43. Moreover, errors of less than 5% would be expected from this model.

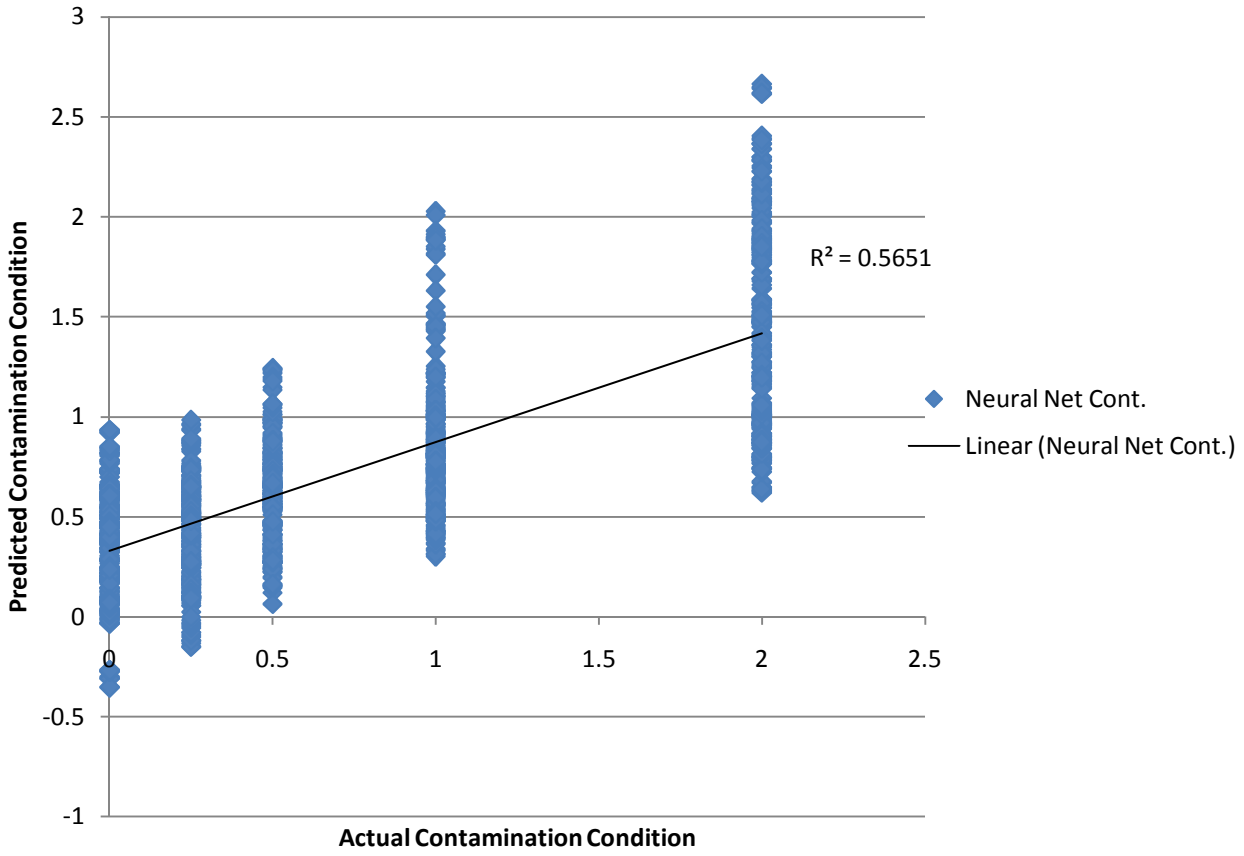

Figure 5.46 Neural network predictions for contamination condition with multiple sensor data

Figure 5.46 shows the contamination prediction results for multiple sensor data. As expected the performance of the neural network approach with respect to predicting contamination condition decreased considerably when including the effect of multiple sensors. The R^2 value for this plot was much lower at .565. More importantly, there was overlap between the predicted conditions of clean fuel and the highest contamination level. This result indicated that the model would not be sufficiently accurate, and would potentially identify clean fuel as being contaminated.

5.5.7 Summary of Results

An algorithm for the detection of water contaminated and degraded fuel in addition to blend percentage determination was developed based on models fitted to fuel data taken over a wide range of temperatures and blends. Linear models were applied to the behavior of the density and dielectric constant outputs with both temperature and blend percentage. Non-linear models were needed to describe the behavior of the dynamic viscosity for both temperature and blend percentage. Furthermore, the density output was employed to distinguish between blends of diesel #1 and blends of diesel #2. All three outputs were used to estimate the blend percentage for clean fuels. In addition contamination by water and degradation was detected by comparison of the viscosity and dielectric outputs from the MEAS sensor. In the condition that the measured dielectric constant was higher than the dielectric constant predicted by the viscosity water contamination was present. For degraded fuel the predicted dielectric constant would be higher than the actual value.

Neural networks were also used to develop and algorithm based on fuel data. Data from a single sensor were consistent enough to create an accurate model for both blend percentage and contamination condition. However, this model had to be accurate for all MEAS sensors, and the added variability due to the inconsistent response of each sensor to water contamination led to decreased performance by neural network models based off of three sensor's data. The model still predicted blend percentage with good accuracy, but the contamination condition was not well identified.

A combination of the two algorithms might be an optimal solution. Using the density determination blends of diesel #1 and blends of diesel #2 would be separated. Then the sensor

outputs could be placed into two separate neural network models separately developed for blends of the two fuels. The neural network model would be very accurate at predicting the fuel blend percentage, but not the contamination condition. Therefore, the blend percentage output of the network would be used to determine the appropriate properties for that fuel which could then be compared to the temperature and blend regression data. Finally, based on this comparison contamination and degradation conclusions would be inferred.

CHAPTER 6: SUMMARY AND CONCLUSIONS

Diesel engines cannot fully optimize their ability to combust many forms of fuel without real-time measurement of fuel composition. Moreover, engine manufacturers seek to add value to engines through addition of fuel contamination and degradation identification. This research sought to apply a commercially developed fluids property sensor for the purpose of fuel composition and quality detection.

The properties of several base fuels were measured using the MEAS sensor over a wide temperature range. It was determined that biodiesel and petroleum based fuels have significantly different density, dynamic viscosity, and dielectric properties over the entire applicable temperature range. Moreover, the sensor should be able to distinguish between any of diesel #1, diesel #2, Jet A, and SME biodiesel fuels. Methyl ester biodiesels from several oil sources were refined to test the properties of each in comparison to soybean biodiesel. Results suggested that algorithms developed from the data using SME biodiesel will apply to both rapeseed and jatropha biodiesels with minimal error. Also, un-refined vegetable oils were tested indicating that the sensor would accurately measure the properties of oils. All fuels displayed similar trends in properties with temperature. The density and dielectric constant decreased linearly with increasing temperature while dynamic viscosity decreased non-linearly with temperature. The change in dielectric constant with temperature was attributed to the corresponding density effect since fuels tend to be non-polar liquids.

Experiments carried out with blended fuels showed definable trends for each of the sensor's three outputs with blend percentage between diesel and biodiesel fuels. Linear models accurately quantified the behavior of density and dielectric constant with changing blend

percentage. Viscosity measurements fit the Grunberg-Nissan model which exhibited a near exponential shape.

Several contaminants of interest for diesel fuels were water, sulfur, urea, glycerol, and methanol. Experimentation was undertaken to quantify the effects of contamination as a function of contaminant concentration and temperature. Water, glycerol, and methanol were all detectable by the MEAS sensor through increases in the dielectric constant, viscosity, or density. Sulfur was found to be undetectable to the sensor at concentrations below several thousand ppm, which was not sufficient for the purposes of protecting exhaust after-treatment systems. It was found that the dielectric constant was sensitive to most contaminants since each of the contaminants was a much more polar liquid than fuels are. Additionally, this effect was more easily deciphered at low temperatures where the difference between the dielectric constant of the fuel and the contaminant was greater. This was because of the higher temperature dependence of the dielectric constant of polar liquids. Consequently, placing the fuel sensor further away from the engine to obtain ambient conditions would be advantageous for contaminant detection. The solubility of the contaminant was found to be important as judged from the fact that additions of 10,000 ppm did not yield results nearly ten times greater than the data for 1,000 ppm contamination. Most contaminants were more soluble in biodiesel than in diesel fuel. However, the effect of contaminants was similarly or more easily detected for diesel #2 and low blends than for B-100.

Long term tests on SME biodiesel, diesel #1, and diesel #2 showed that the viscosity of fuels increased significantly with age. The density and dielectric constants were unchanged with time. The literature review indicated that biodiesel would degrade more quickly than petroleum based fuels; however, results suggested that the viscosity change was larger for the petroleum

based fuels than for biodiesel. The chemical mechanism describing these changes was discussed in the literature review, but the cause of the larger effect for diesel fuel was unexplained.

All of the data collected was used to develop an algorithm for interpreting sensor outputs into useful information about fuel type or quality. Using temperature and blend regression models fitted to the data, the properties of all fuels were successfully predicted over the applicable temperature range. Models for each property with blend percentage interpolated between the base fuel properties for a given temperature to estimate composition for diesel biodiesel blends. Contamination by water and degradation could be detected by comparison of the viscosity and dielectric outputs. This method differentiated between blends of diesel #1 with biodiesel up to 30% from blends of diesel #2 with biodiesel from 0-100%. Within each blend range accuracy of the model should be within 3-4% of the actual value for clean fuel. Contamination could be detected at concentrations above 500 ppm for water, although blend prediction became less accurate with water addition and should be under 10%. Degraded fuel could be detected since two of the sensor outputs remained constant while the viscosity increased.

A neural network approach was also applied to the fuel data with moderate success. Data from a single sensor produced a model that was very accurate for blend prediction and reasonably accurate for contamination condition prediction. However, data from several sensors was much more variable with added water content causing the corresponding neural network model to be less precise. The blend prediction was accurate, but prediction of the contamination condition was not sufficient. A combination of regression models and neural networks might be the optimal approach.

In conclusion, use of the MEAS sensor for diesel fuel composition and quality sensing produced accurate information on fuel type and blend level for each of the fuels studied. In addition the sensor was able to successfully detect water, glycerol, and methanol contamination as well as degraded fuel. Unfortunately the MEAS sensor was unable to detect sulfur at the desired concentrations. By and large, application of this fluid properties sensor to fuel sensing for diesel engines was a promising endeavor.

CHAPTER 7: RECOMMENDATIONS FOR FUTURE WORK

The following recommendations are made for continued study on fuel composition and quality sensing for diesel engines:

1. Measure the properties of fuels from a wide range of locations, refineries, and sources to gain a better understanding of the natural variation in fuel properties.
2. Perform additional testing on the effect of contaminants in order to increase the accuracy of contamination models.
3. Apply algorithm development techniques to add glycerin, methanol, and urea contamination to the water and degradation detection algorithm.
4. Acquire data with a larger set of MEAS sensors over temperature ranges reaching the cloud point of diesel fuel with the intention of creating more accurate neural networks.
5. Test and verify to a higher degree both algorithm techniques proposed in this study. Measure fuels of known type, blend, and contamination condition and compare predicted and actual results.
6. Quantify the effects of combusting degraded fuel on performance and emissions.
7. Find an alternative method of identifying sulfur in diesel fuel at concentrations down to 15 ppm.
8. Apply the MEAS sensor to an engine and verify accuracy of the blend identification and contaminant detection algorithm.
9. Integrate the MEAS sensor into engine controls for injection timing to demonstrate ability to optimize performance and emissions based on fuel type.
10. Measure the properties of multi-component blends of diesel fuel, biodiesel, and alcohols.

REFERENCES

AACL, 2011. Fuel sample composition analysis from American Analytical Chemistry Laboratories. 711 Parkland Ct. Champaign, IL 61821.

ASTM D6751-10. 2010a. Standard specification for biodiesel fuel (B100) blend stock for middle distillate fuels. American Society for Testing and Materials: Philadelphia, PA.

ASTM D975-10c. 2010b. Standard specification for diesel fuel oils. American Society for Testing and Materials, Philadelphia, PA.

BAFF. 2009. Bought ethanol cars. BioAlcohol Fuel Foundation. http://www.baff.info/english/rapporter.cfm. Retrieved 23 May, 2009.

Bondioli, P., A. Gasparoli, L. Della Bella, S. Tagliabue, and G. Toso. 2003. Biodiesel stability under commercial storage conditions over one year. *European Journal of Lipid Science Technology* 105: 735–741

Bonhorst, C.W., P.M. Althouse, and H.O. Triebold. 1948. Esters of naturally occurring fatty acids - physical properties of methyl, propyl, and isopropyl esters of C6 to C18 saturated fatty acids. *Industrial and Engineering Chemistry* 40(12): 2379-2383.

Bouaid, A., M. Martinez, and J. Aracil. 2007. Long storage stability of biodiesel from vegetable and used frying oils. *Fuel* 86: 2596–2602

Chuck, C.J., C.D. Bannister, J.G. Hawley, and M.G. Davidson. 2010. Spectroscopic sensor techniques applicable to real-time biodiesel determination. *Fuel* 89: 457–461

Clipper Controls. 2011. Dielectric Constant Values. Available at https://www.clippercontrols.com/pages/dielectric-constant-values#D. Accessed 18 January, 2011.

Dubovkin, N.F. and V. G. Malanicheva. 1981. Density and Viscosity of Jet Fuels *Chemistry and Technology of Fuels and Oil* 16(8): 543-547.

Fischer, C.H. 1995. n-Fatty Acids: Comparison of Published Densities and Molar Volumes. *Journal of the American Oil Chemists' Society 72:* 681-685

Foster, M. 2010. Personal Communication, 26 May.

Gouw, T. H., and J. C. Vlugter. 1964. Physical properties of fatty acid Methyl Esters. V. dielectric constant. *Journal of the American Oil Chemists' Society* 41(10): 675-678.

Graboski, M.S. and R.L. McCormick. 1998. Combustion of fat and vegetable oil derived fuels in diesel engines. *Progress in Energy and Combustion Science* 24: 125-164.

Hossain, A.K. and P.A. Davies. 2010. Plant oils as fuels for compression ignition engines: A technical review and life-cycle analysis. *Renewable Energy* 35: 1–13.

Jain, S. and M.P. Sharma. 2010. Stability of biodiesel and its blends: A review. *Renewable and Sustainable Energy* Reviews 14: 667–678.

Johnson, K.J., R.E. Morris, and S.L. Rose-Pehrsson. 2006. Evaluating the Predictive Powers of Spectroscopy and Chromatography for Fuel Quality Assessment. *Energy & Fuels* 20: 727-733.

Joshi, R.M. and M. J. Pegg. 2007. Flow properties of biodiesel fuel blends at low temperatures. *Fuel* 86: 143–151.

Kopera, J. J. C., M. E. McMackin, and R. K. Rader. 1993. Methanol concentration smart sensor. SAE Paper No. 930354. Warrendale, Pa.: Society of Automotive Engineers.

Knothe, G. 2005. Dependence of biodiesel fuel properties on the structure of fatty acid alkyl esters. *Fuel Processing Technology*, 86(10), 1059-1070.

Lee, K.Y. 2008. Viscosity of high-alcohol content fuel blends with water: Subsurface contaminant transport implications. *Journal of Hazardous Materials* 160: 94–99.

Lizhi, H., K. Toyoda, and I. Ihara. 2008. Dielectric properties of edible oils and fatty acids as a function of frequency, temperature, moisture and composition. *Journal of Food Engineering* 88: 151–158.

Mays, L.W. 2001. *Water Resources Engineering*. John Wiley & Sons Inc., New Jersey, USA.

McCrady, J.P. 2007. Biodiesel Property Definition for Fuel Atomization and Combustion Modeling. Master's thesis. University of Illinois at Urbana-Champaign, Department of Agricultural and Biological Engineering, Urbana, IL

McCrady, J. 2010, Personal communication, 15 December.

Measurement Specialties. 2009. Preliminary Specification; FPS2800B12C4 – Fluid Property Sensor Module. Toulouse, France.

Seeton, C.J. 2006. Viscosity-temperature correlation for liquids. *Tribology Letters* 22(1): 67-78.

Segur, J.B., and H.E. Oberstar. 1951. Viscosity of Glycerol and Its Aqueous Solutions. *Industrial and Engineering Chemis*try 43(9): 2117-2120.

Sen, D., V. G. Anicich, and T. Arakelian. 1992. Dielectric Constant of Liquid Alkanes and Hydrocarbon Mixtures. *Journal of Applied Physics* 25: 516-521.

Sparks, D., R. Smith, D. Riley, N. Tran, J. Patel, A. Chimbayo, and N. Najafi. 2010. Monitoring and Blending Biofuels Using a Microfluidic Sensor. *Journal of ASTM International* 7(8): Paper ID JAI102473.

Swern, D. 1979. *Bailey's industrial oil and fat products.* 4th ed. Vol. 1. Wiley, New York, NY. Pgs. 34-122

Tat, M. E., and J. H. Van Gerpen. 1999. The kinematic viscosity of biodiesel and its blends with diesel fuel. J*ournal of the American Oil Chemists' Society* 76(12): 1511-1513.

Tat, M.E., and J.H. Van Gerpen. 2000. The specific gravity of biodiesel and its blends with diesel fuel. *Journal of the American Oil Chemists' Society* 77(2): 115-119.

Tat, M.E., and J.H. Van Gerpen. 2003a. Fuel Property Effects on Biodiesel. ASAE Paper No. 2003-6034, St. Joseph, MI.

Tat, M.E., and J.H. Van Gerpen. 2003b Biodiesel blend detection with a fuel composition sensor. *Applied Engineering Agriculture* 19:125–31.

Technical Information & Safe Handling Guide for Methanol Version 3.0. 2006. Methanex Corporation. Available at http://www.methanex.com/products/documents/TISH_english.pdf. Accessed 10 January, 2011.

Tiwari, A.K., A. Kumar, and H. Raheman. 2007. Biodiesel production from jatropha oil (Jatropha curcas) with high free fatty acids: An optimized process. *Biomass and Bioenergy* 31: 569–575.

Valeri, D., and A.J.A. Meirelles. 1997. Viscosities of Fatty Acids, Triglycerides, and Their Binary Mixtures. *Journal of American Oil Chemists' Society* 74: 1221–1226.

Van Gerpen, J.H., E.G. Hammond, L.A. Johnson, S.J. Marley, l. Yu, I. Lee, and A. Monyem. 1996. Determining the Influence of Contaminants on Biodiesel Properties. Iowa State University. Ames, IA.

Yang, H., Y. Briker, R. Szynkarczuk, and Z. Ring. 2004. Prediction of Density and Cetane Number of Diesel Fuel from GC-films and Piona Hydrocarbon by Neural Network. Preprint Papers - American Chemical Society, Division of Fuel Chemistry 49 (1): 81.

Yuan, W. 2005. Computational modeling of NOx emissions from biodiesel combustion based on accurate fuel properties. PhD dissertation. University of Illinois at Urbana-Champaign, Department of Agricultural and Biological Engineering. Urbana, IL.

APPENDIX A: 3-D PLOTS OF SENSOR OUTPUTS

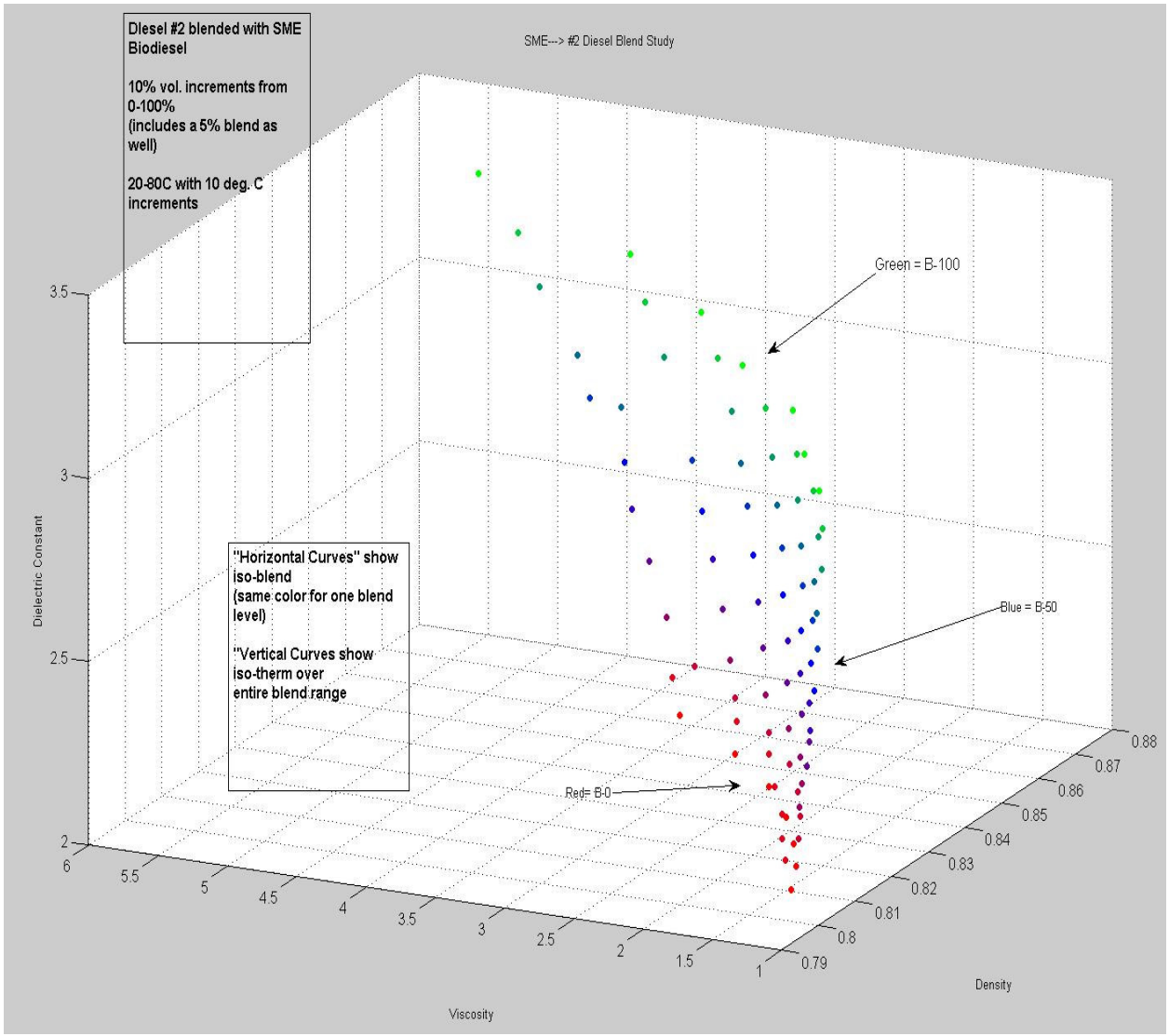

Figure A.1. Sensor outputs for blends of diesel #2 and SME B-100

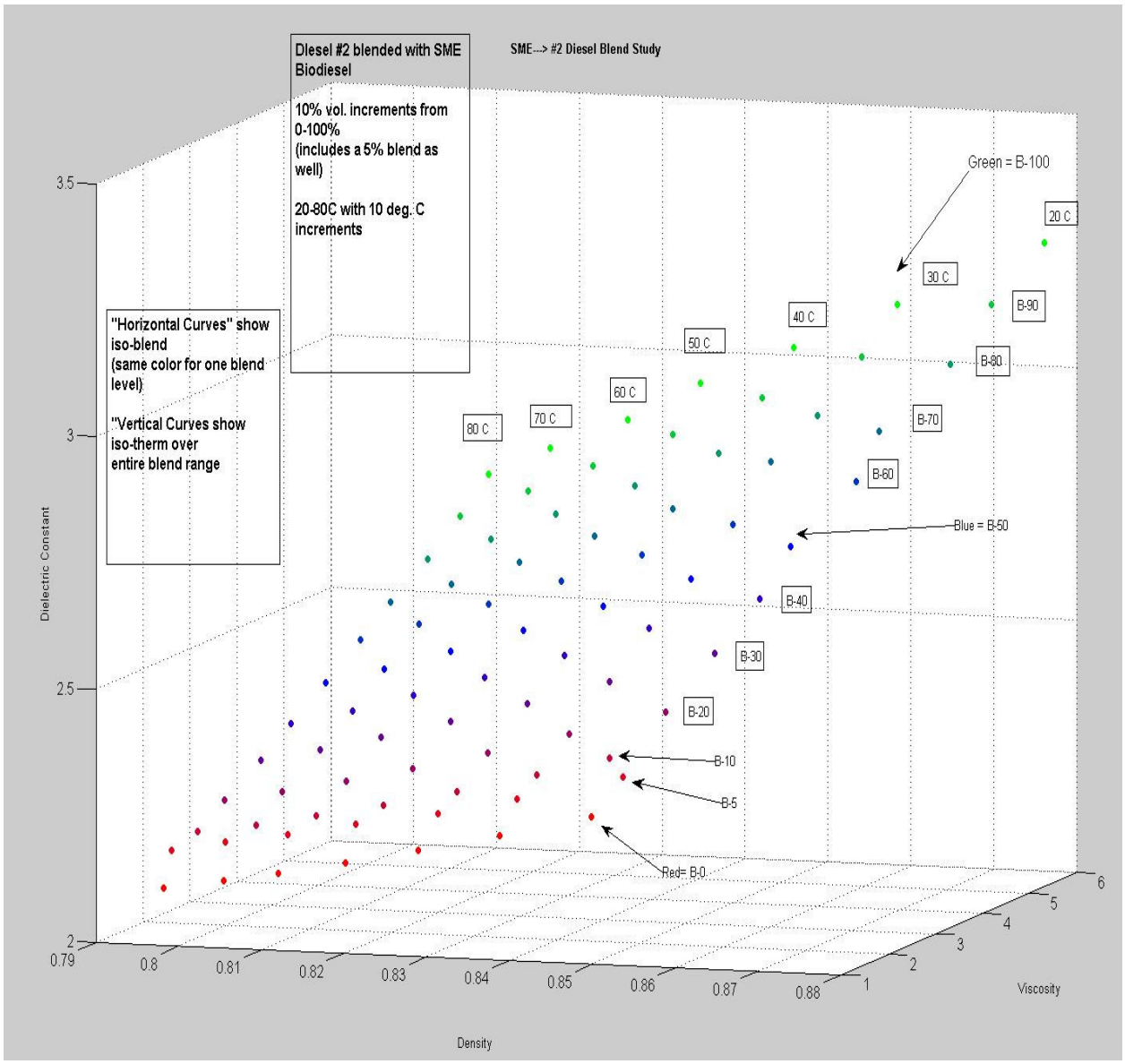

Figure A.2. Sensor outputs for blends of diesel #2 and SME B-100

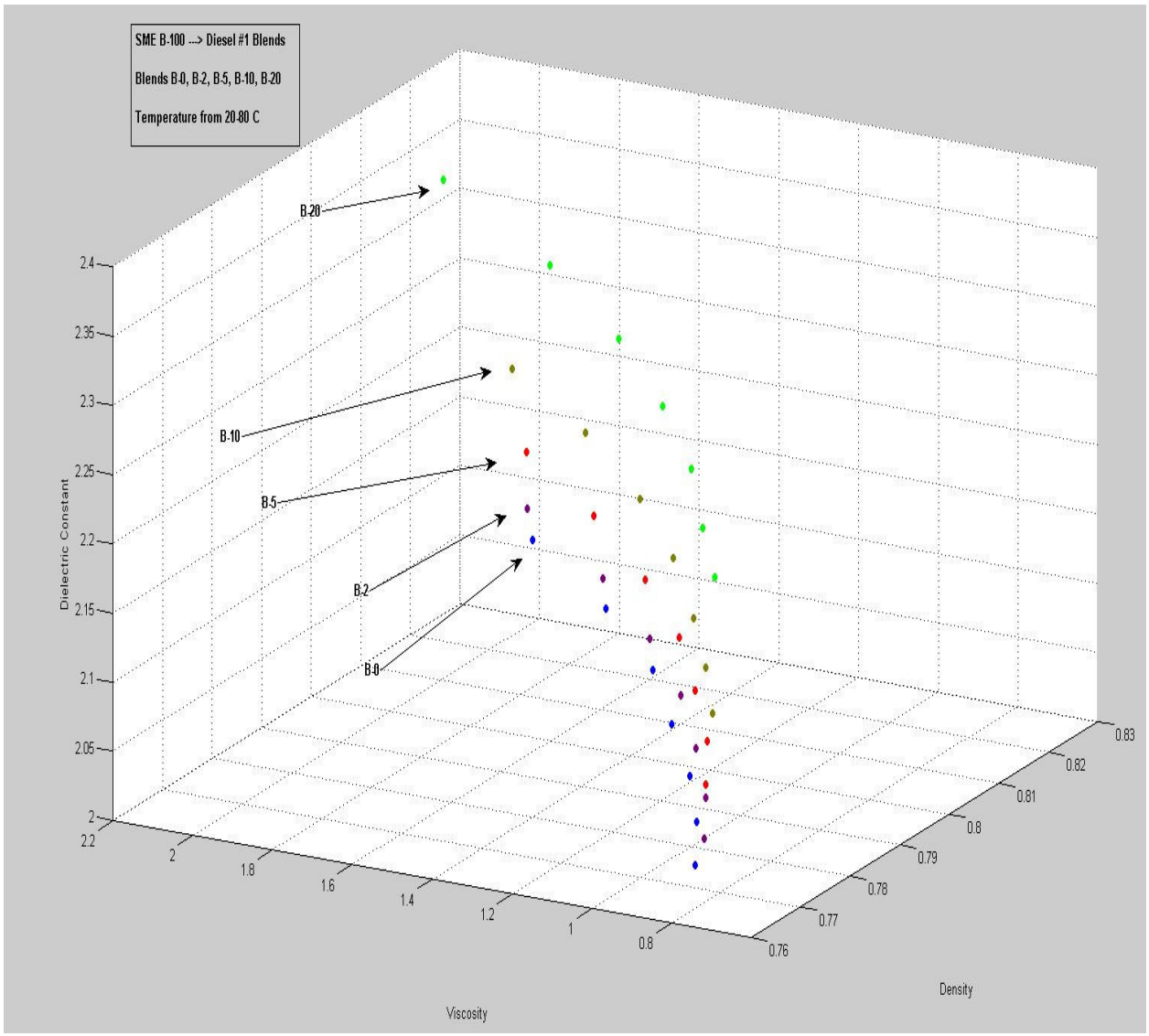

Figure A.3. Sensor outputs for blends of diesel #1 and SME B-100

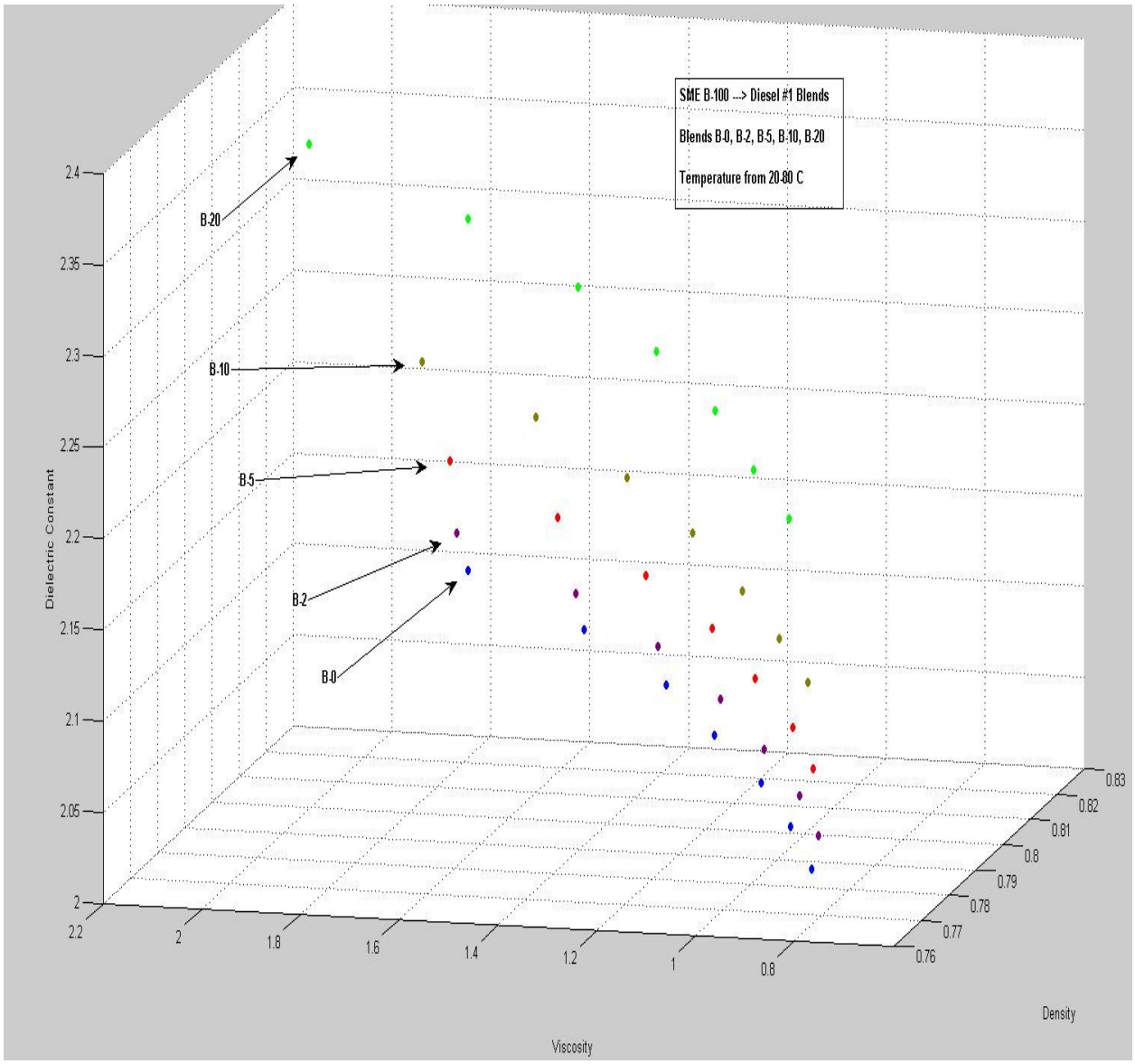

Figure A.4. Sensor outputs for blends of diesel #1 and SME B-100

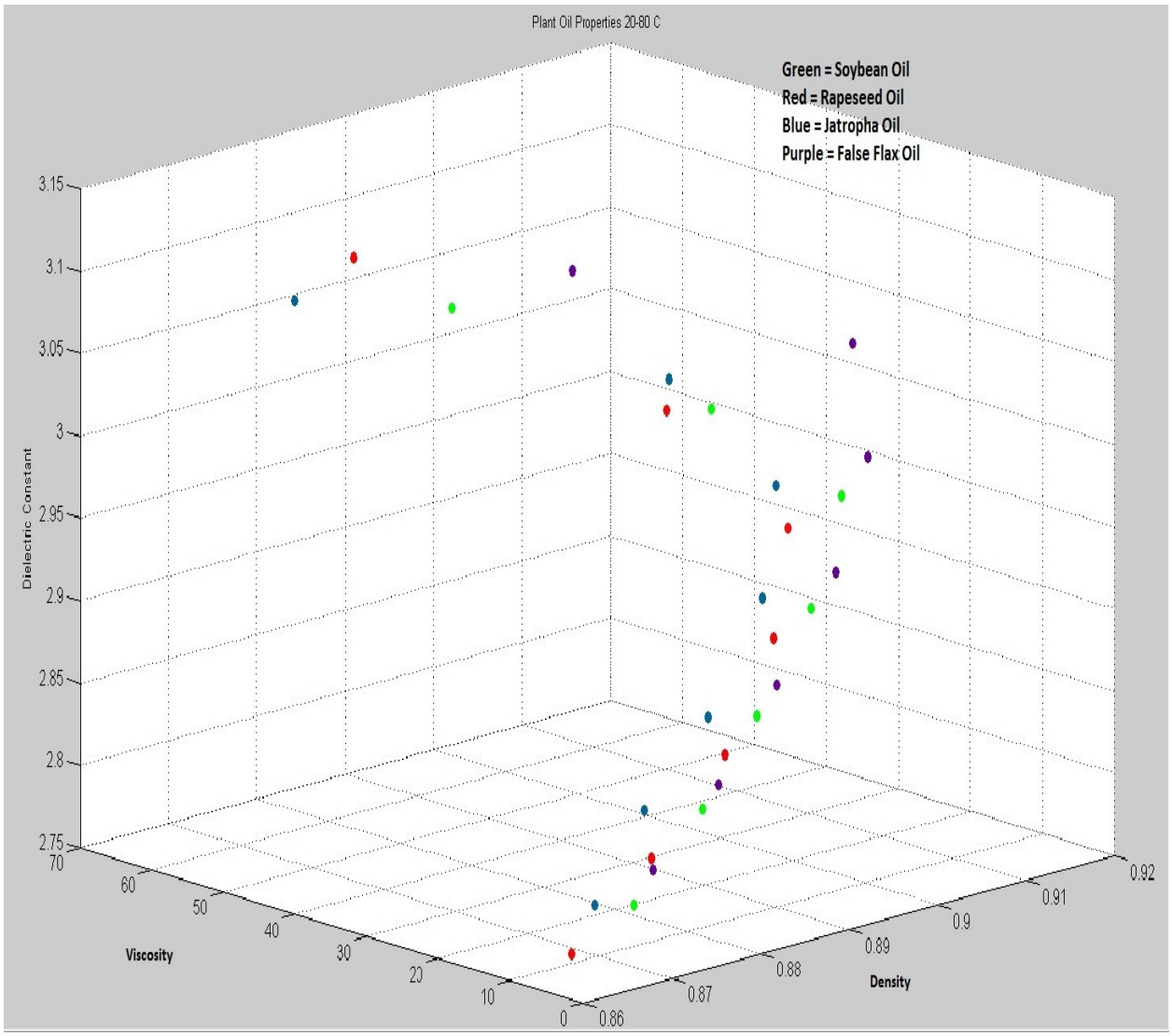

Figure A.5. Sensor outputs for plant oils

APPENDIX B: PLOTS OF CONTAMINATION EFFECTS

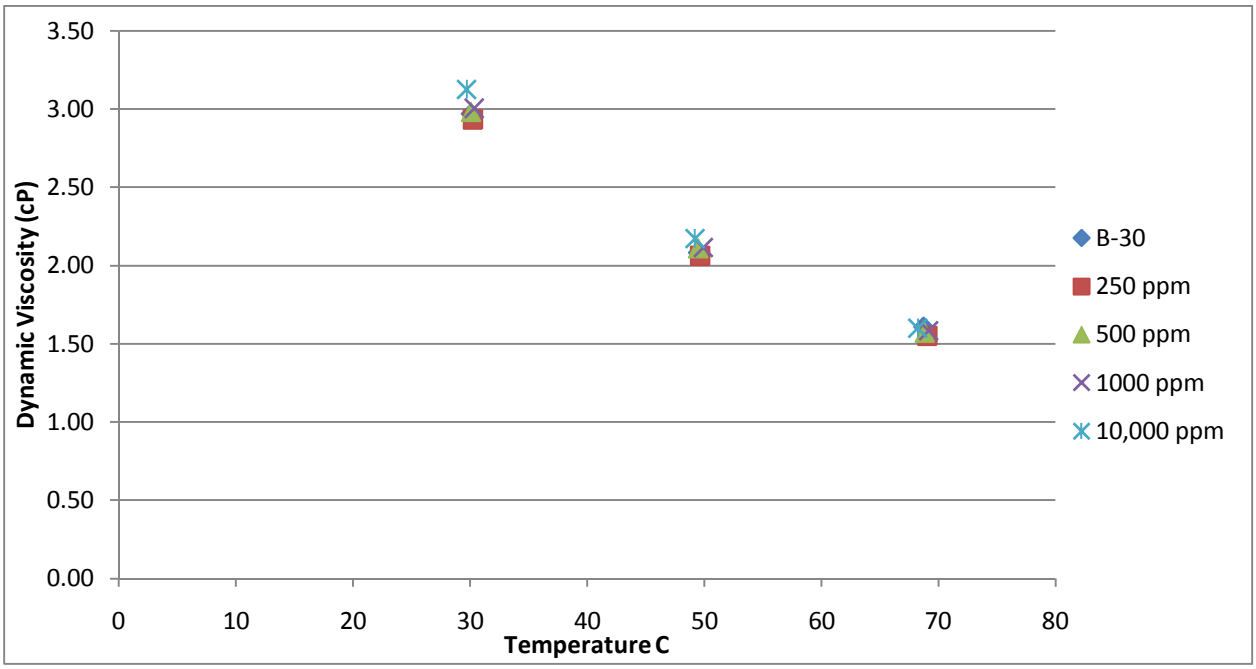

Figure B.1. Dynamic viscosity of B-30 with water contamination

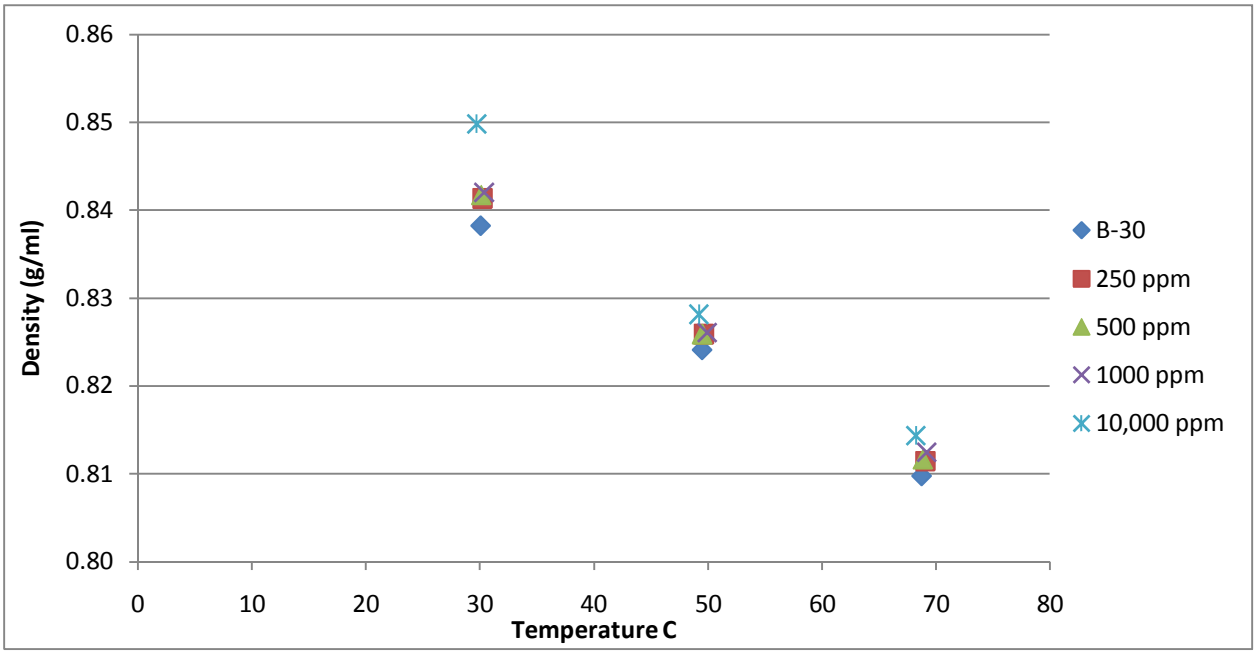

Figure B.2. Density of B-30 with water contamination

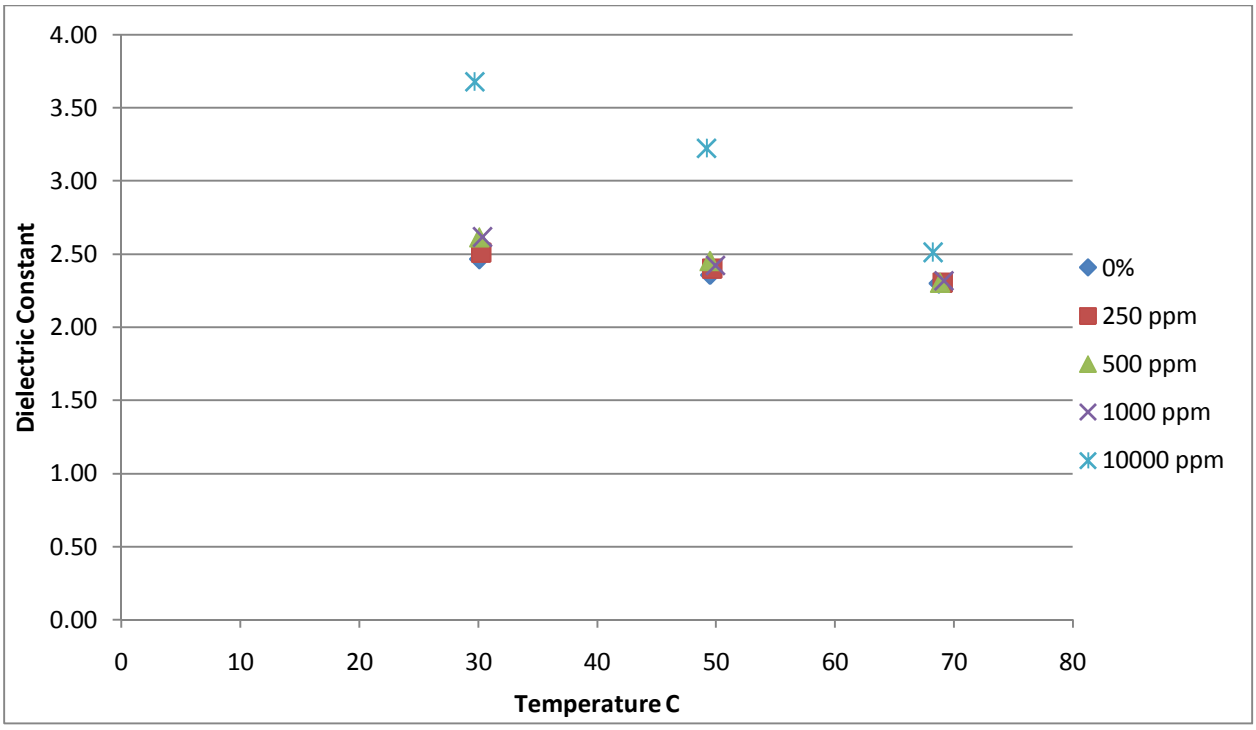

Figure B.3. Dielectric constant of B-30 with water contamination

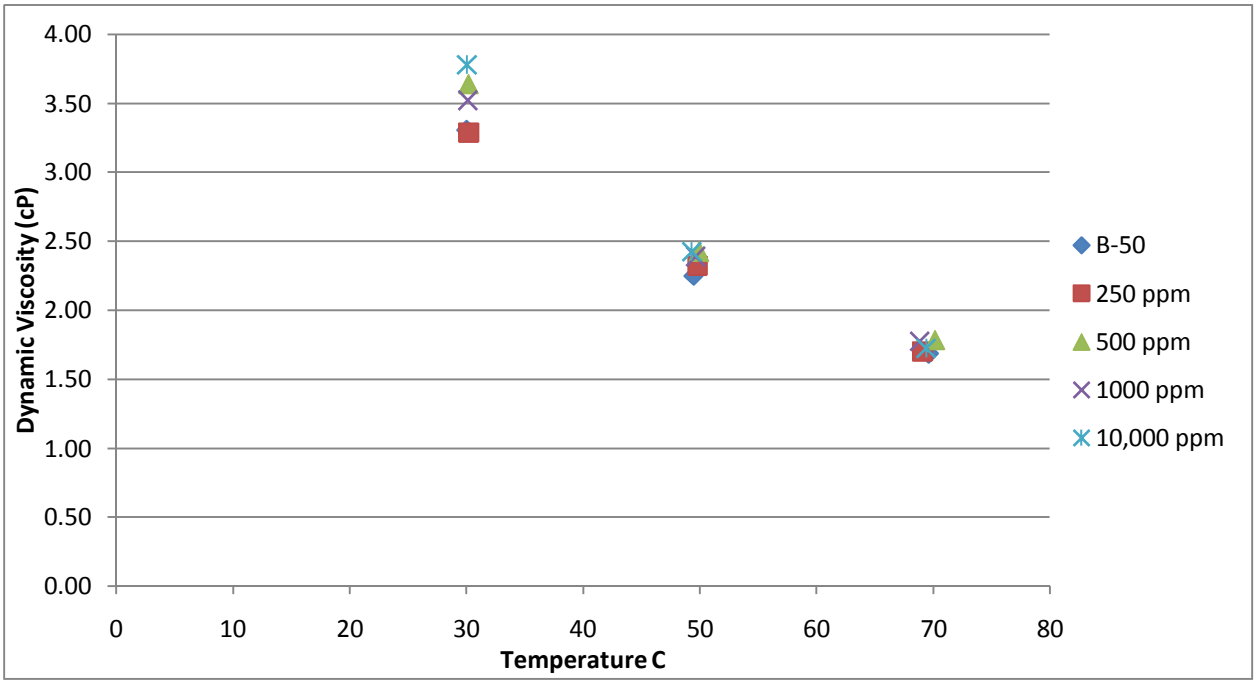

Figure B.4. Dynamic viscosity of B-50 with water contamination

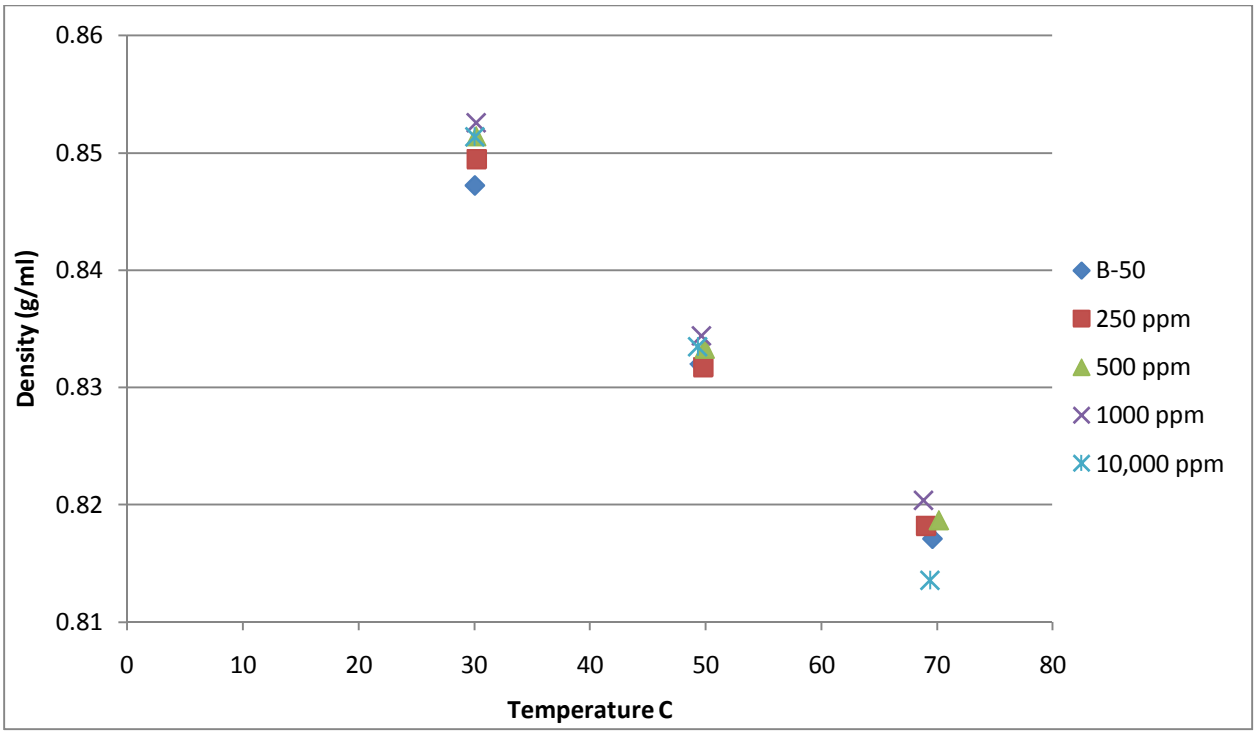

Figure B.5. Density of B-50 with water contamination

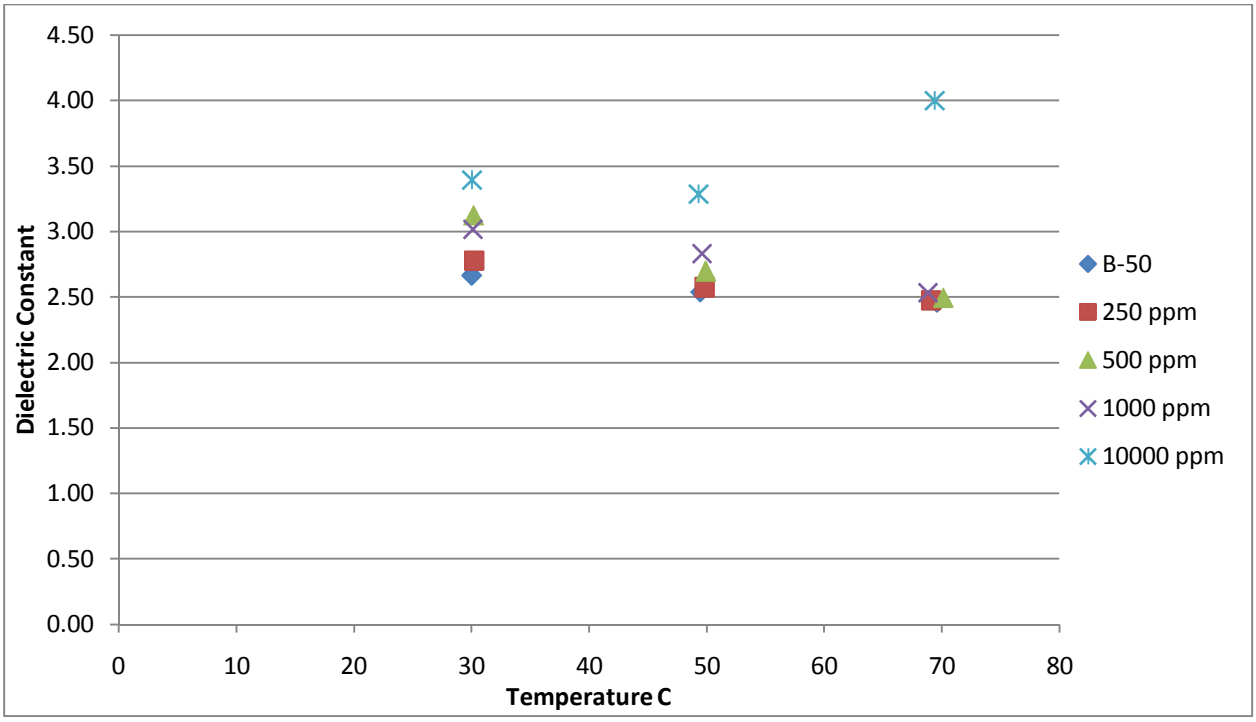

Figure B.6. Dielectric constant of B-50 with water contamination

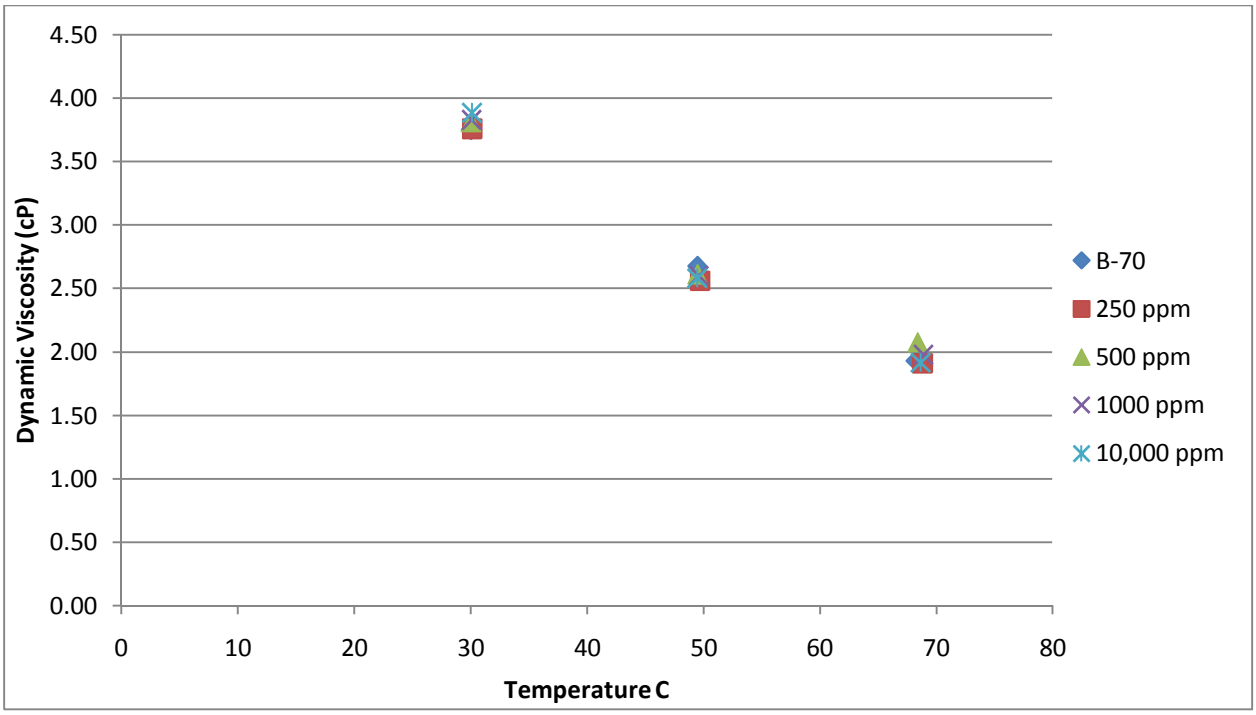

Figure B.7. Dynamic viscosity of B-70 with water contamination

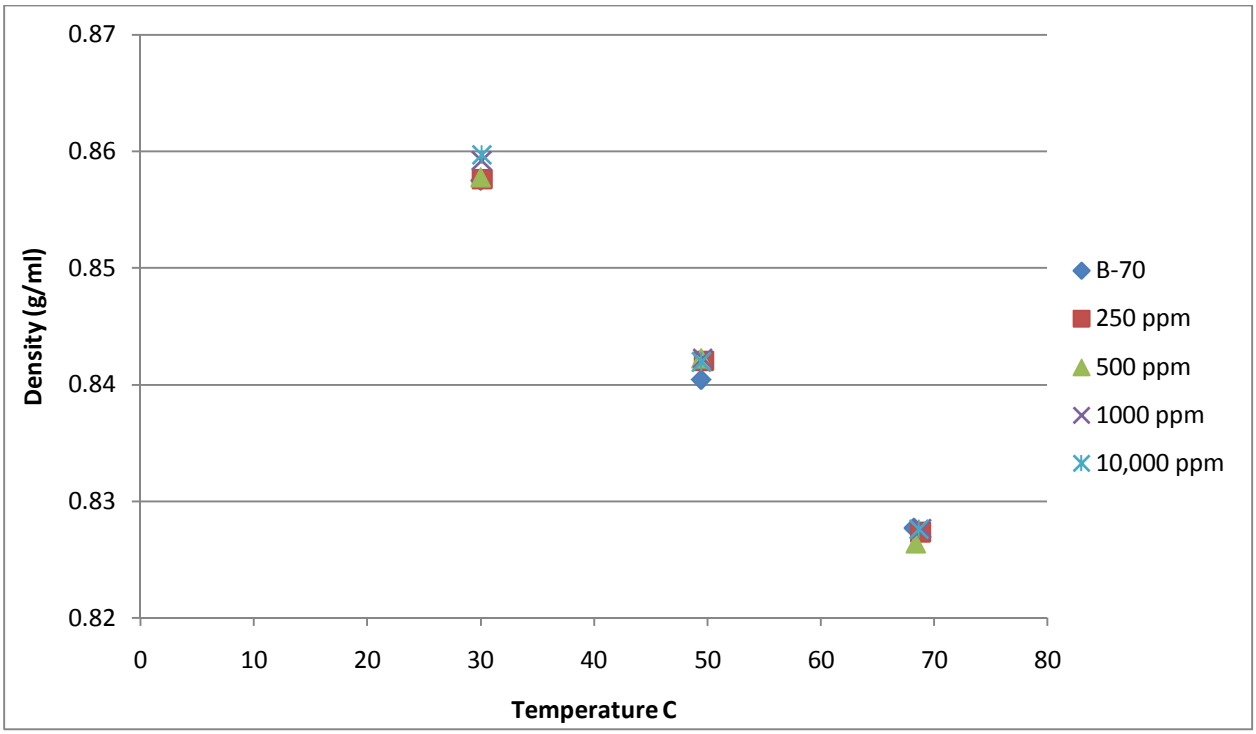

Figure B.8. Density of B-70 with water contamination

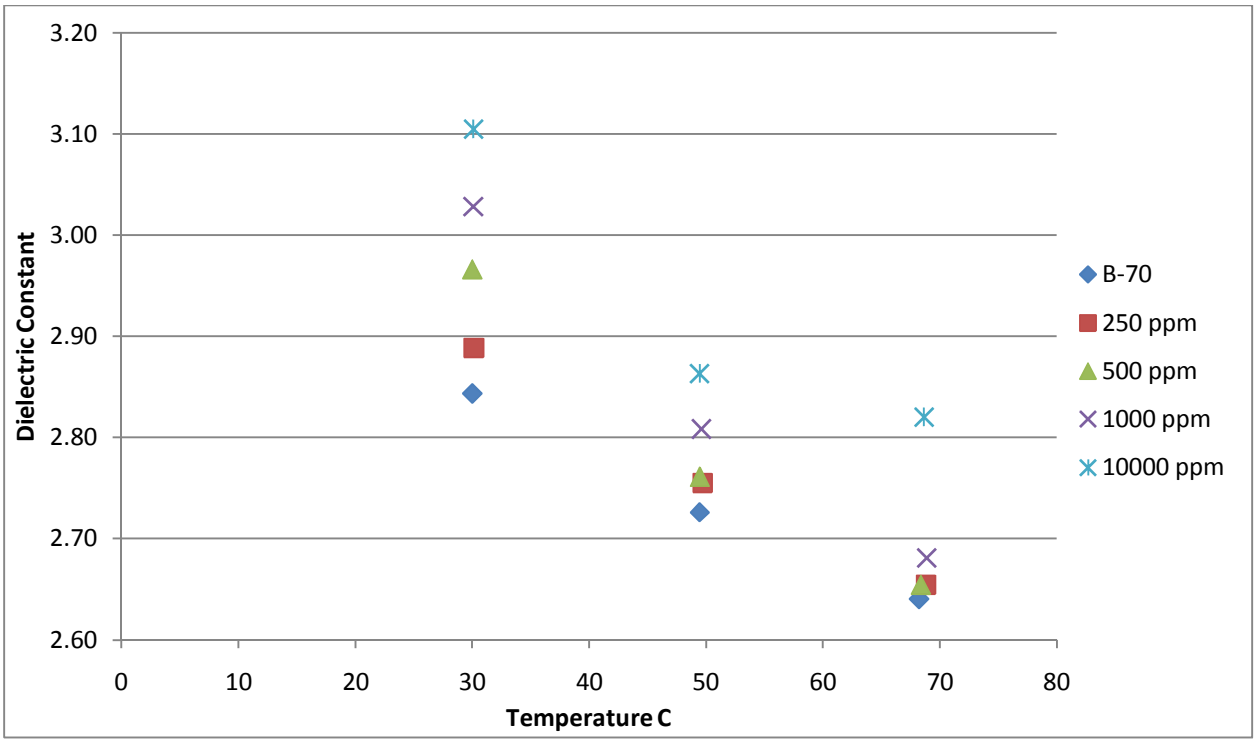

Figure B.9. Dielectric constant of B-70 with water contamination

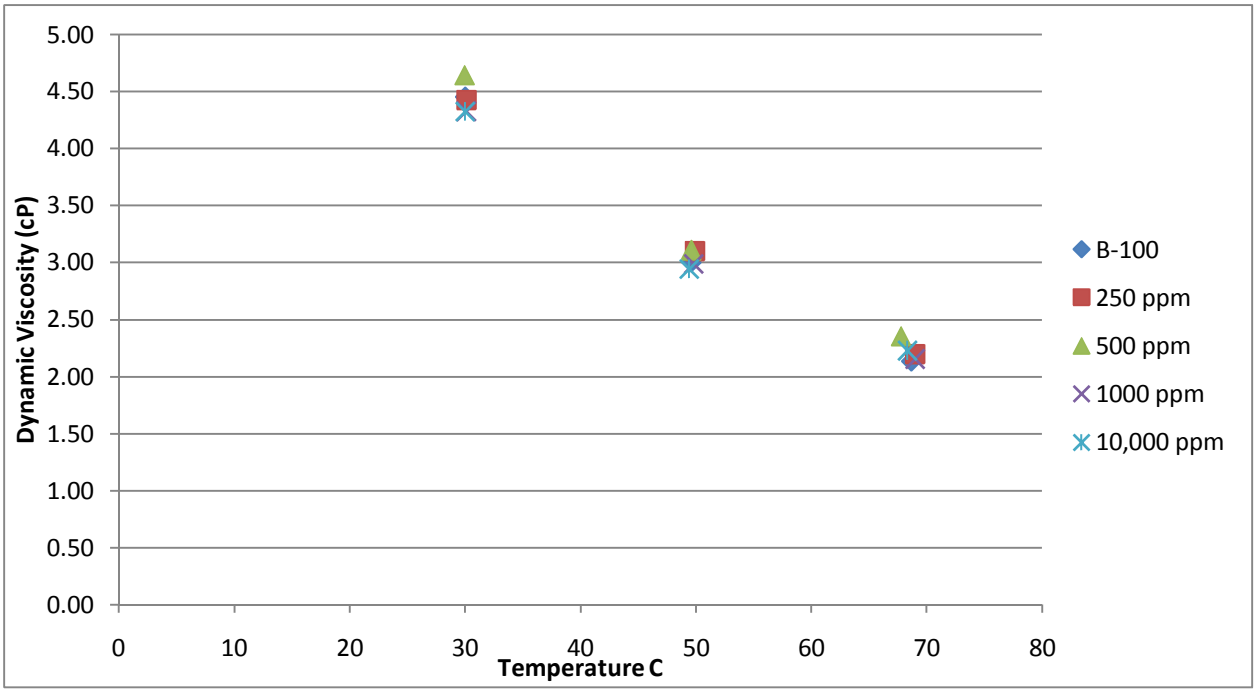

Figure B.10. Dynamic viscosity of B-100 with water contamination

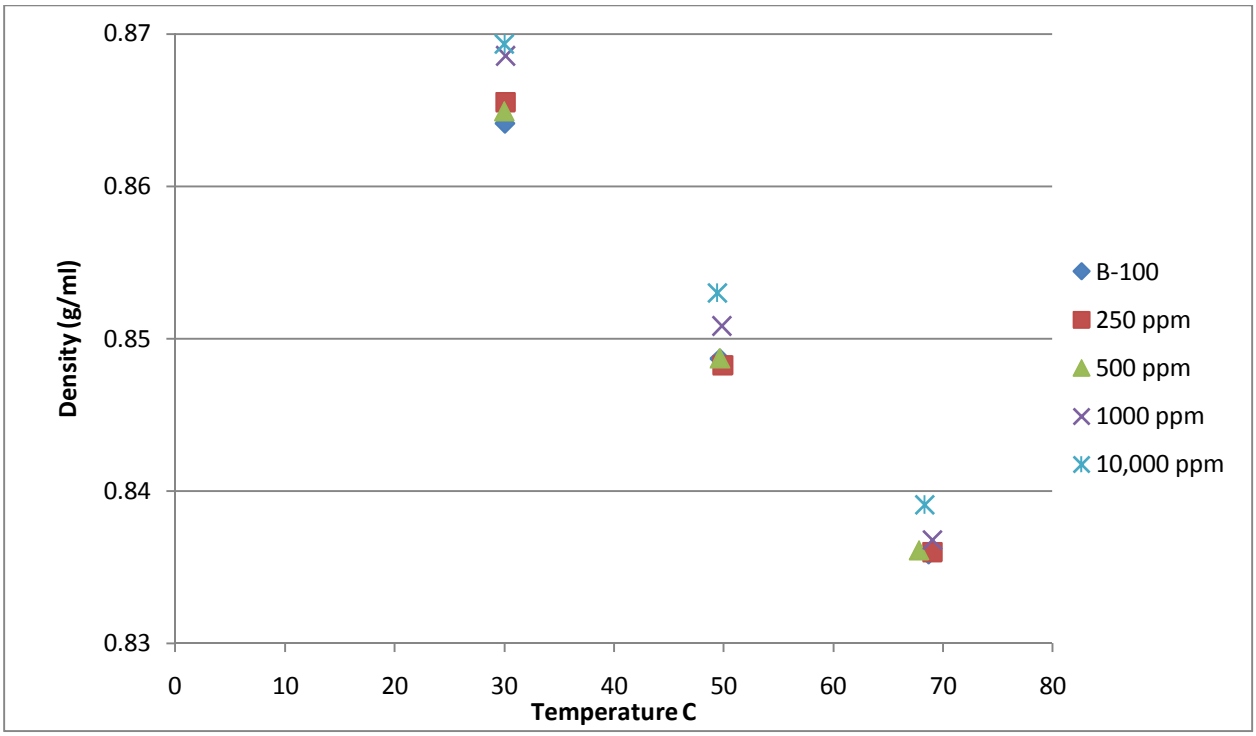

Figure B.11. Density of B-100 with water contamination

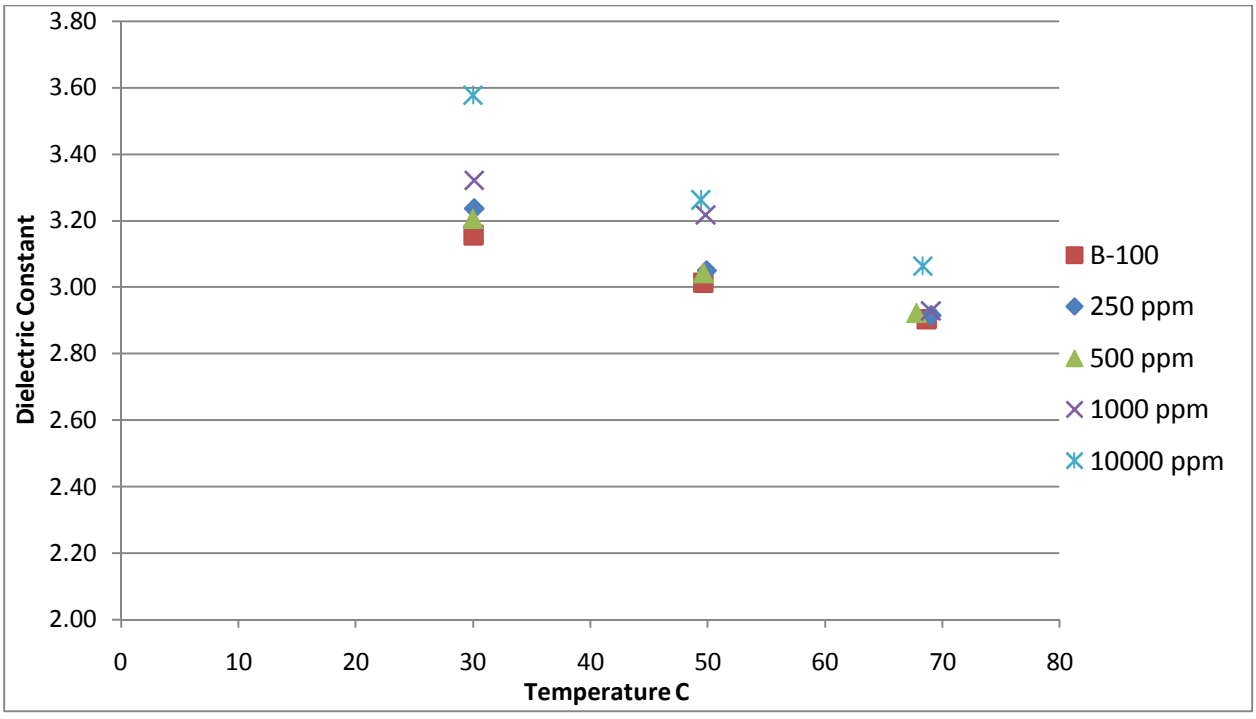

Figure B.12. Dielectric constant of B-100 with water contamination

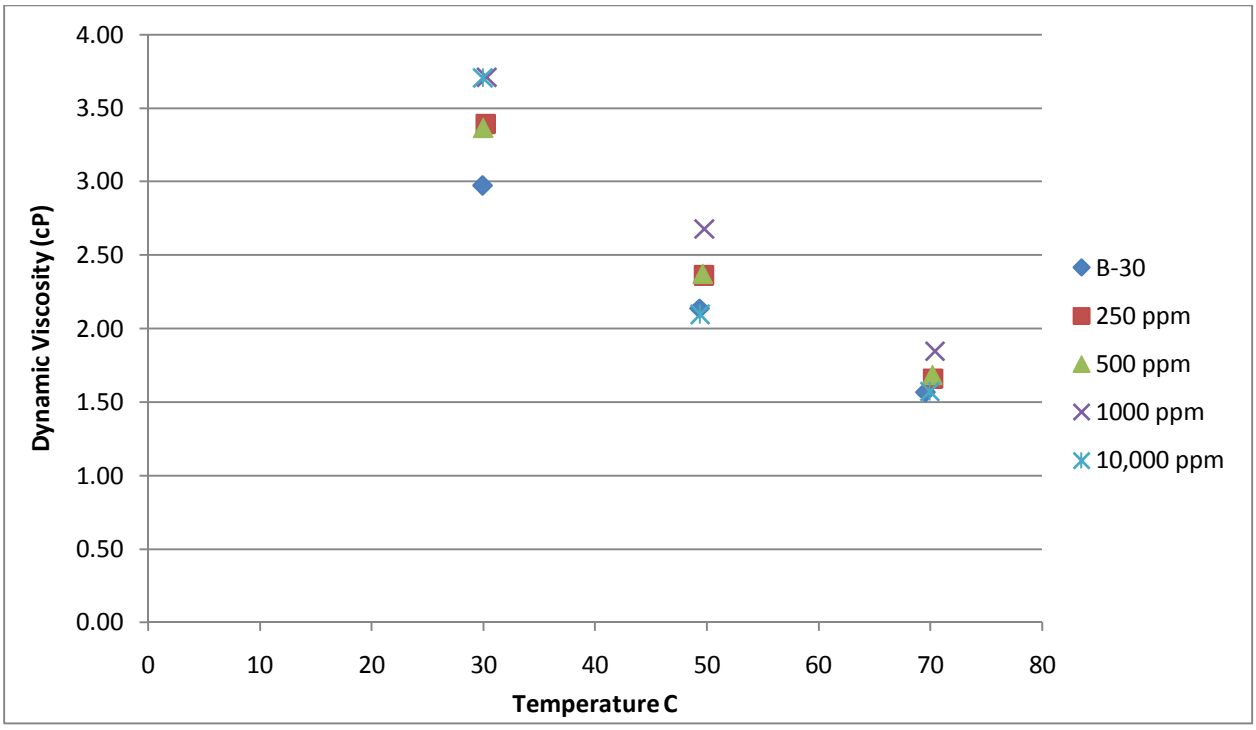

Figure B.13. Dynamic viscosity of B-30 with glycerol contamination

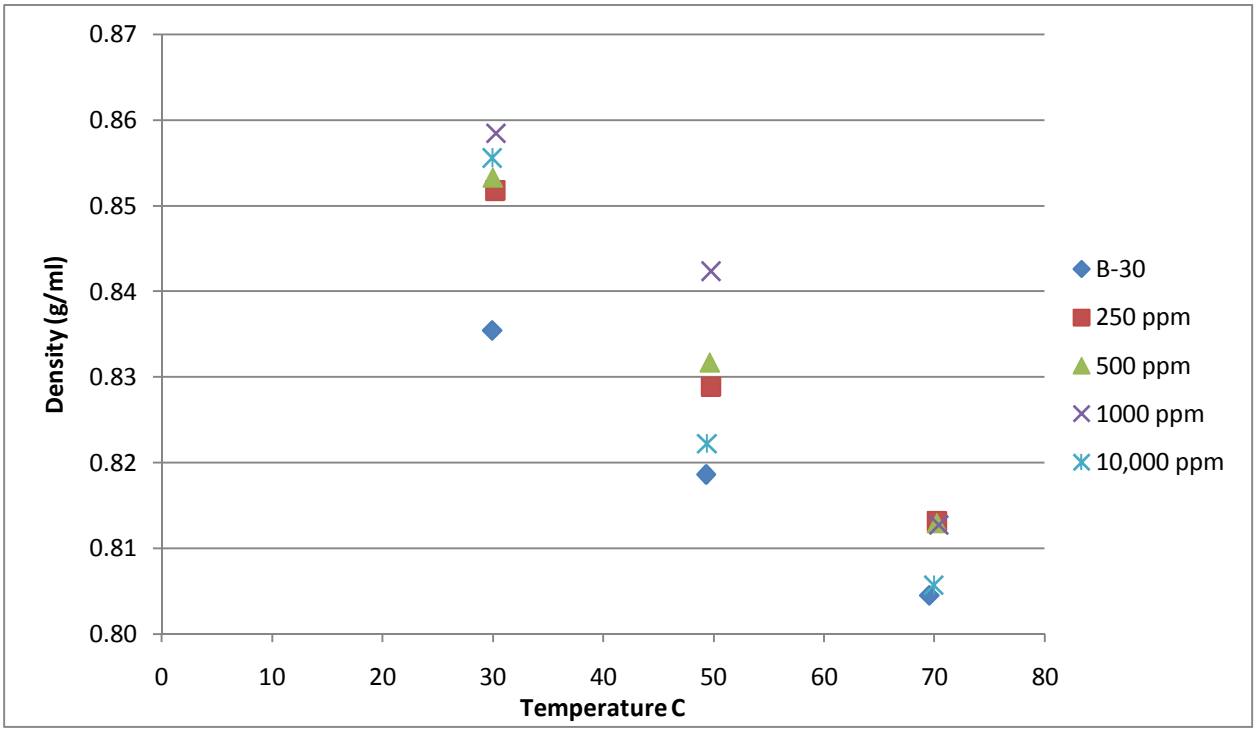

Figure B.14. Density of B-30 with glycerol contamination

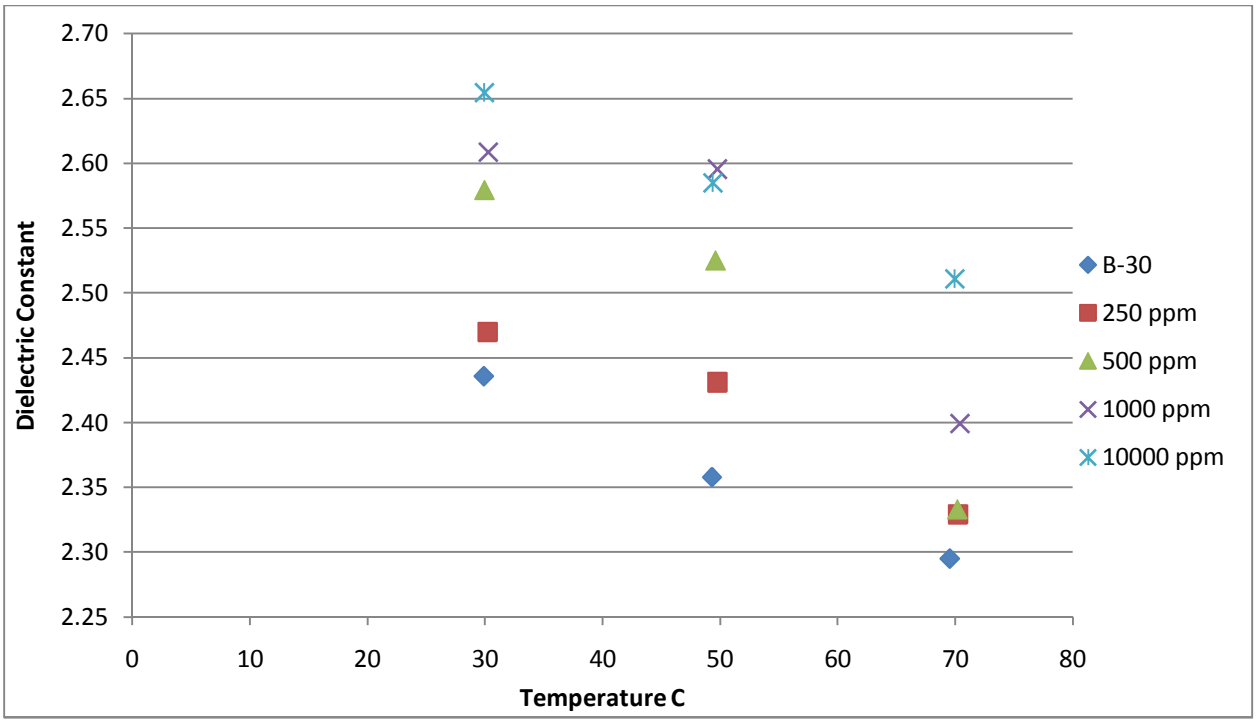

Figure B.15. Dielectric constant of B-30 with glycerol contamination

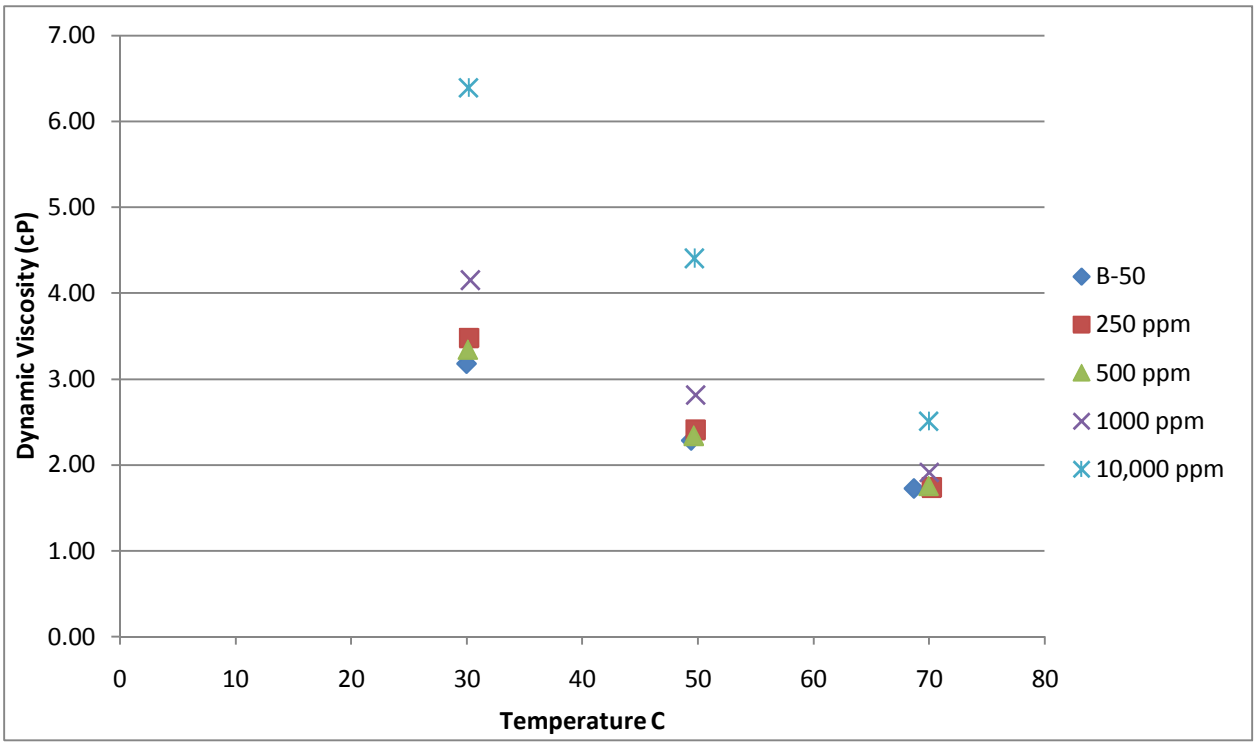

Figure B.16. Dynamic viscosity of B-50 with glycerol contamination

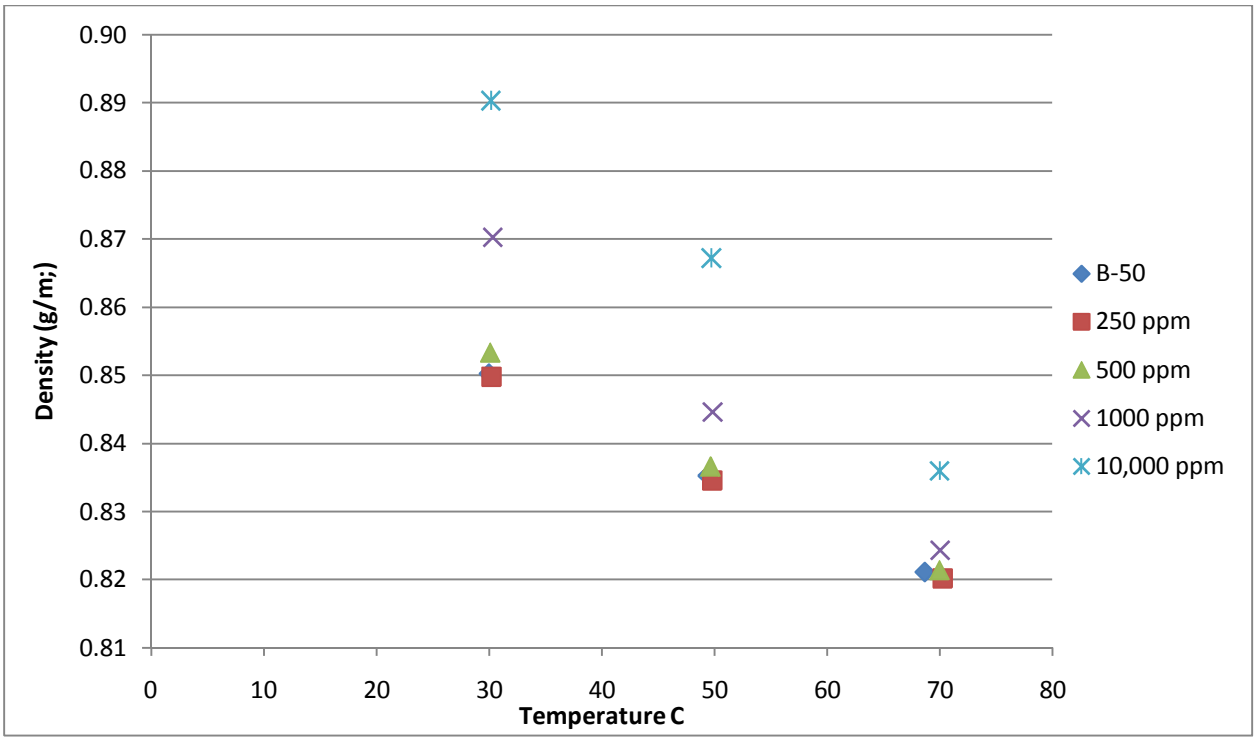

Figure B.17. Density of B-50 with glycerol contamination

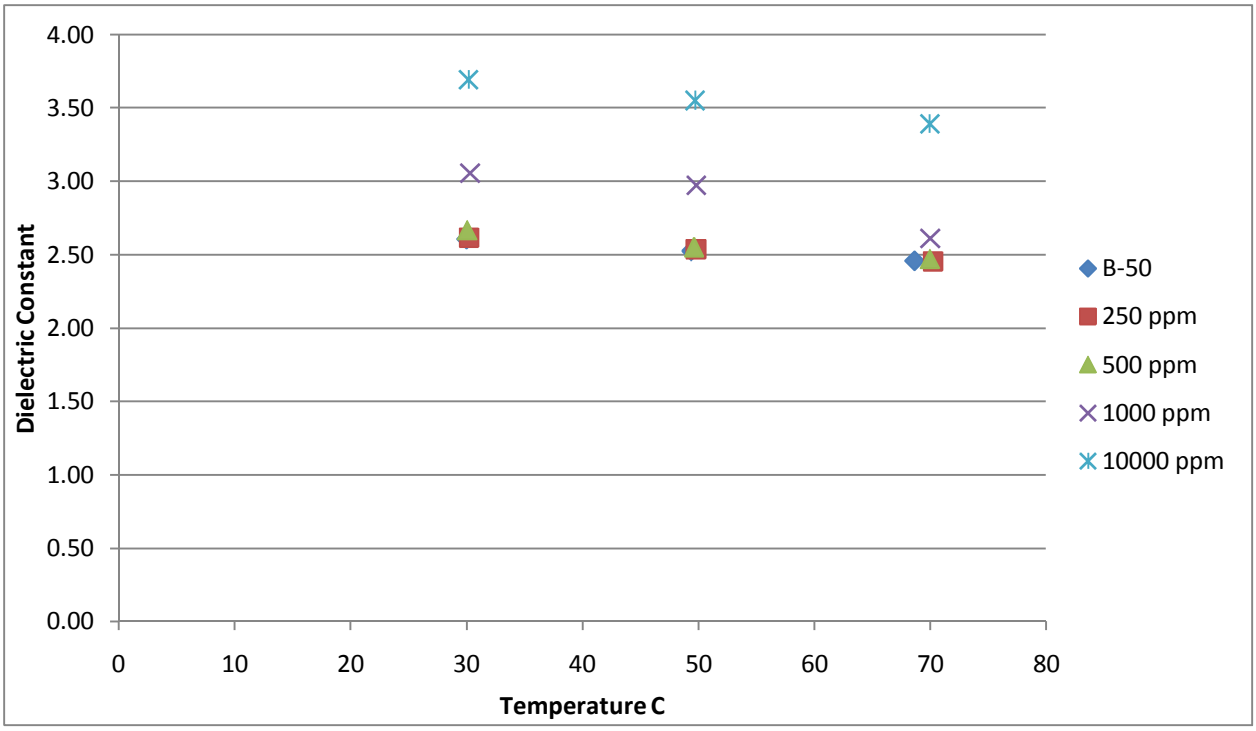

Figure B.18. Dielectric constant of B-50 with glycerol contamination

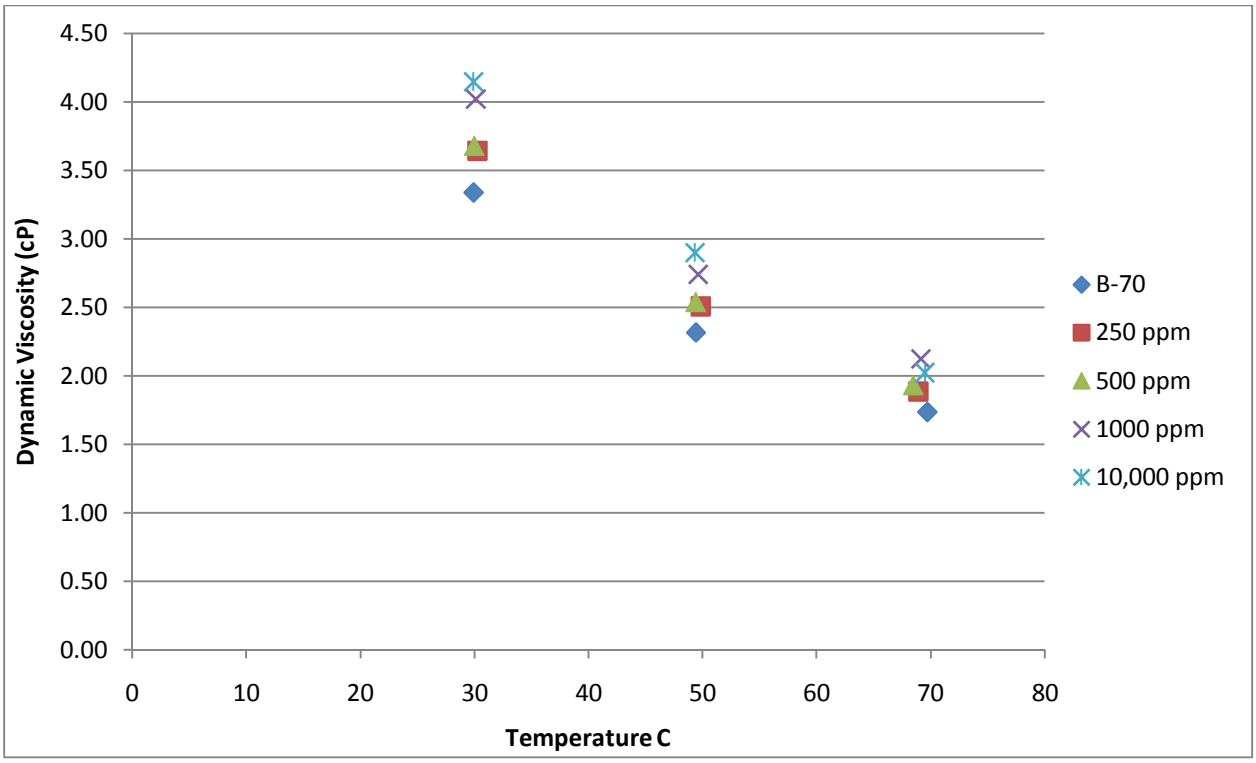

Figure B.19. Dynamic viscosity of B-70 with glycerol contamination

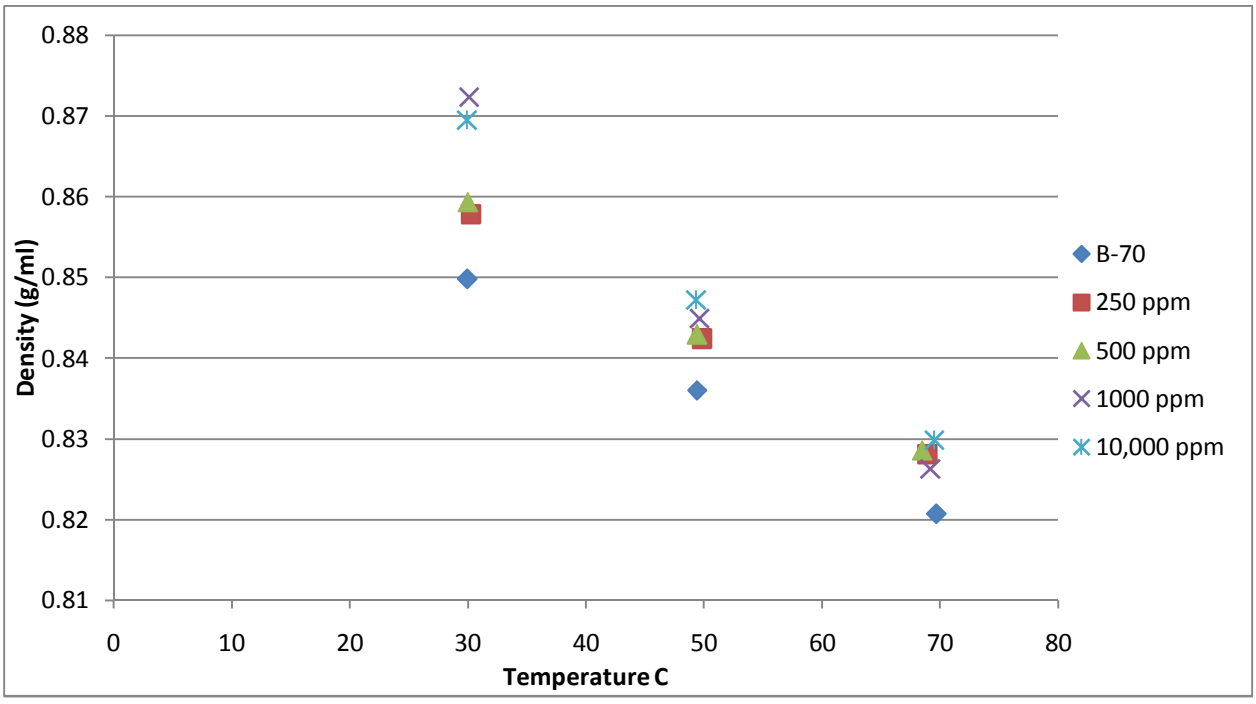

Figure B.20. Density of B-70 with glycerol contamination

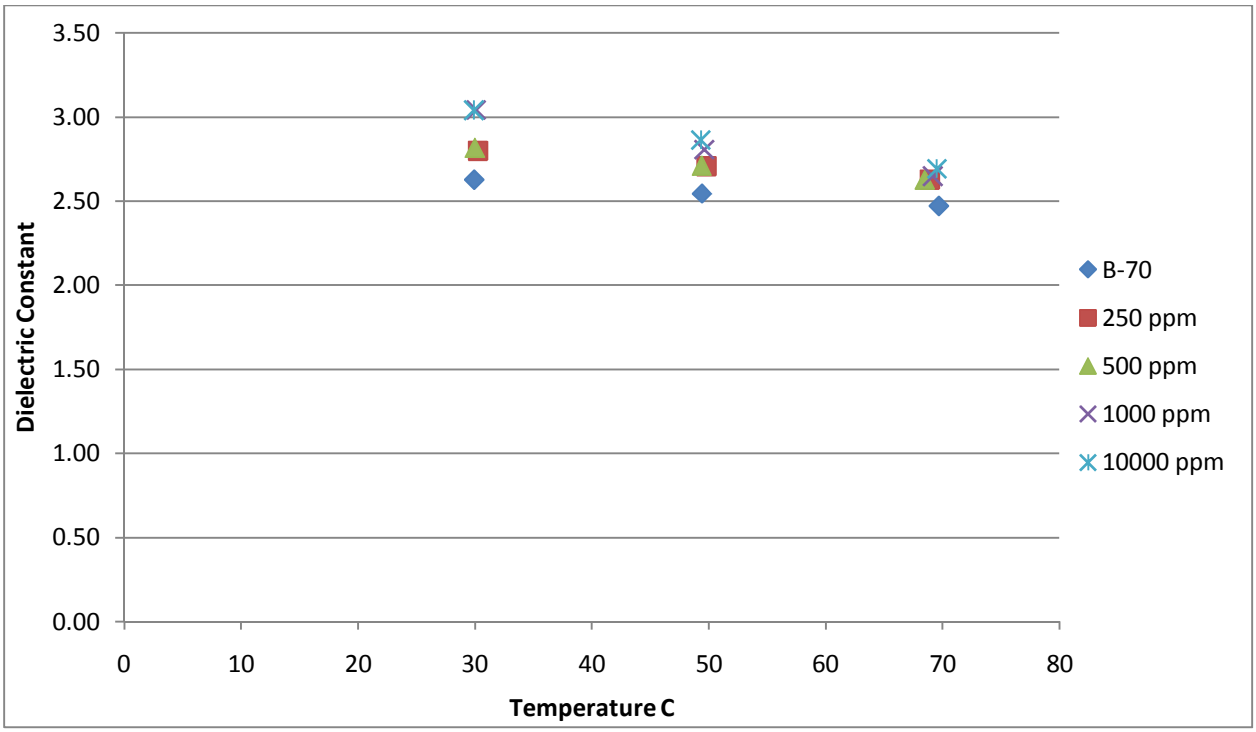

Figure B.21. Dielectric constant of B-70 with glycerol contamination

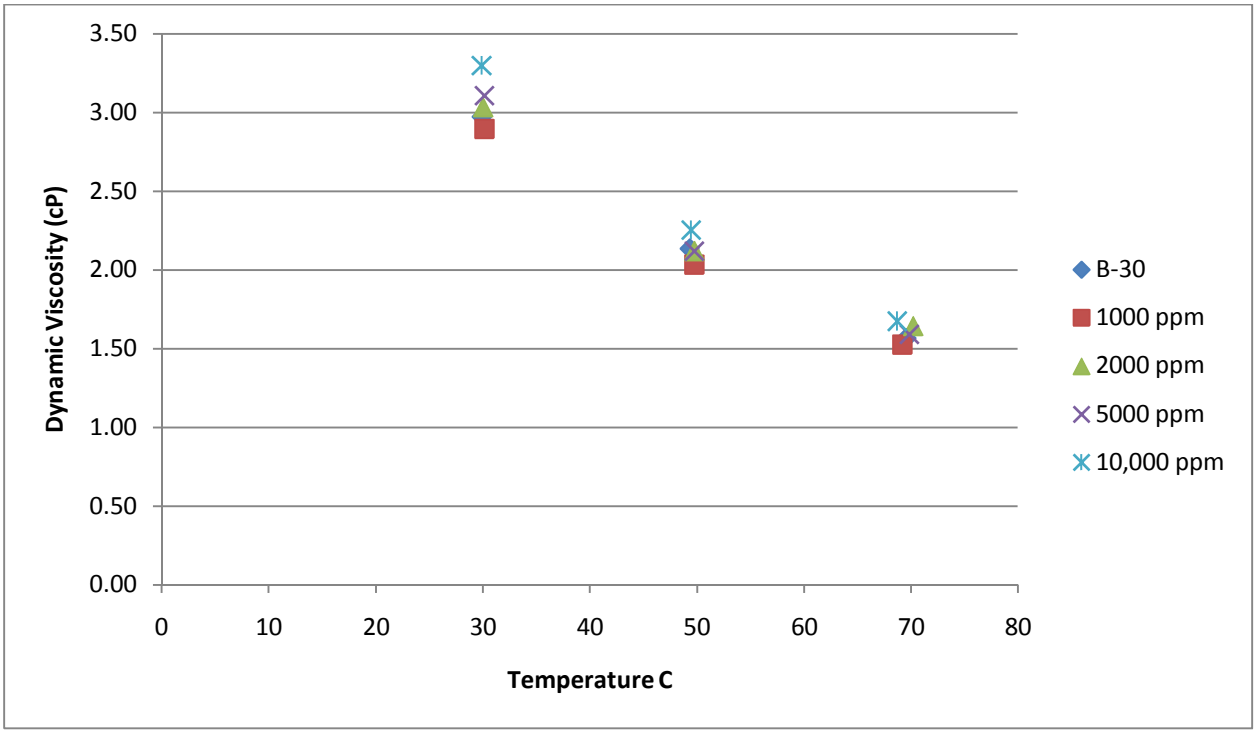

Figure B.22 Dynamic viscosity of B-30 with methanol contamination

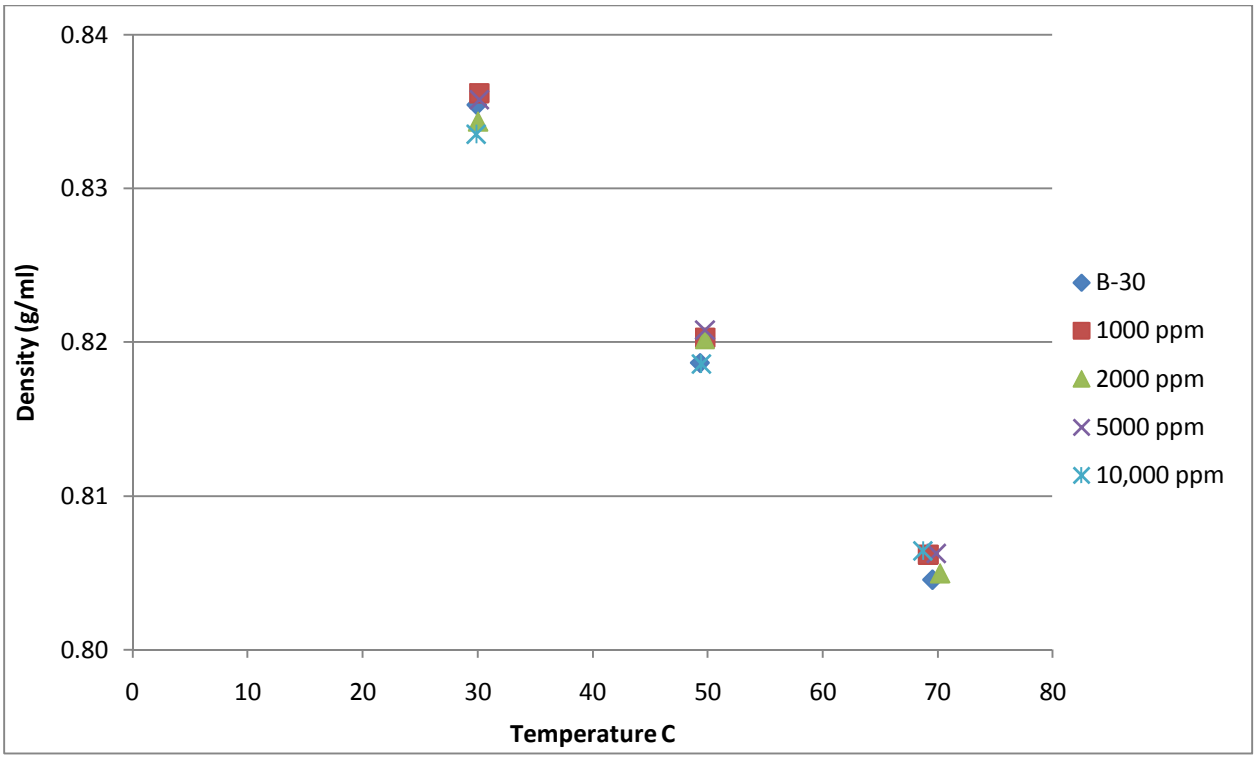

Figure B.23 Density of B-30 with methanol contamination

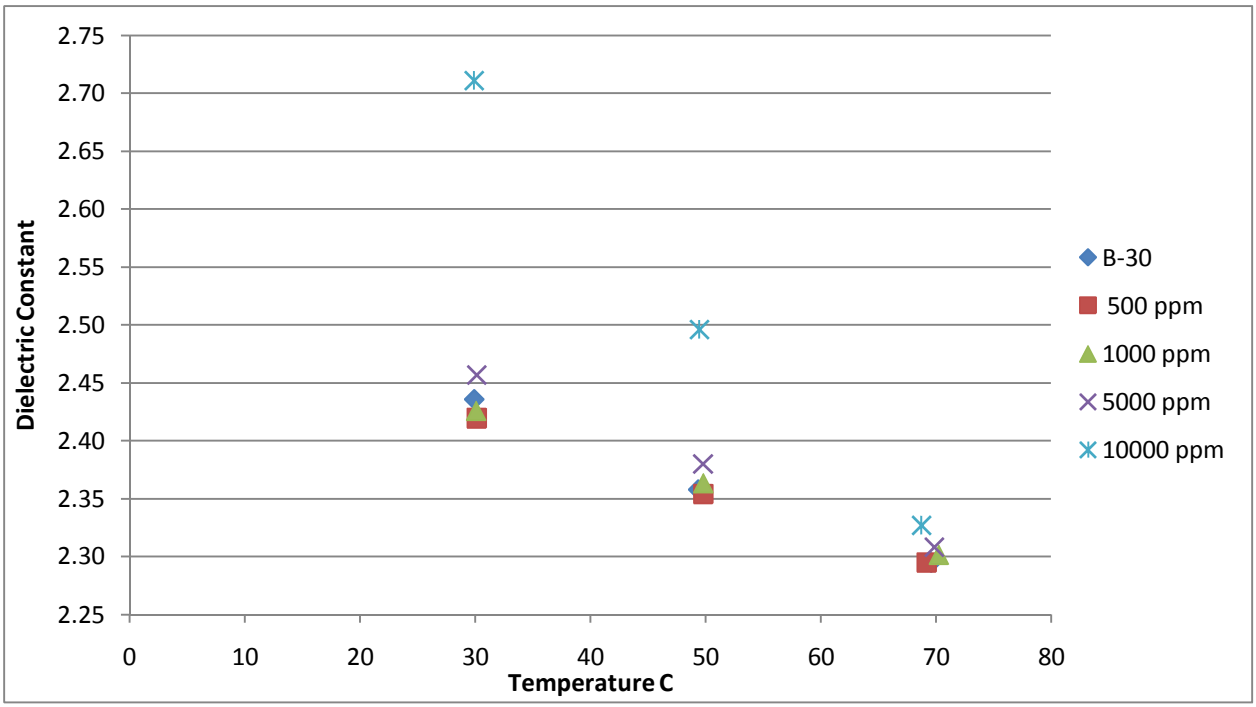

Figure B.24 Dielectric constant of B-30 with methanol contamination

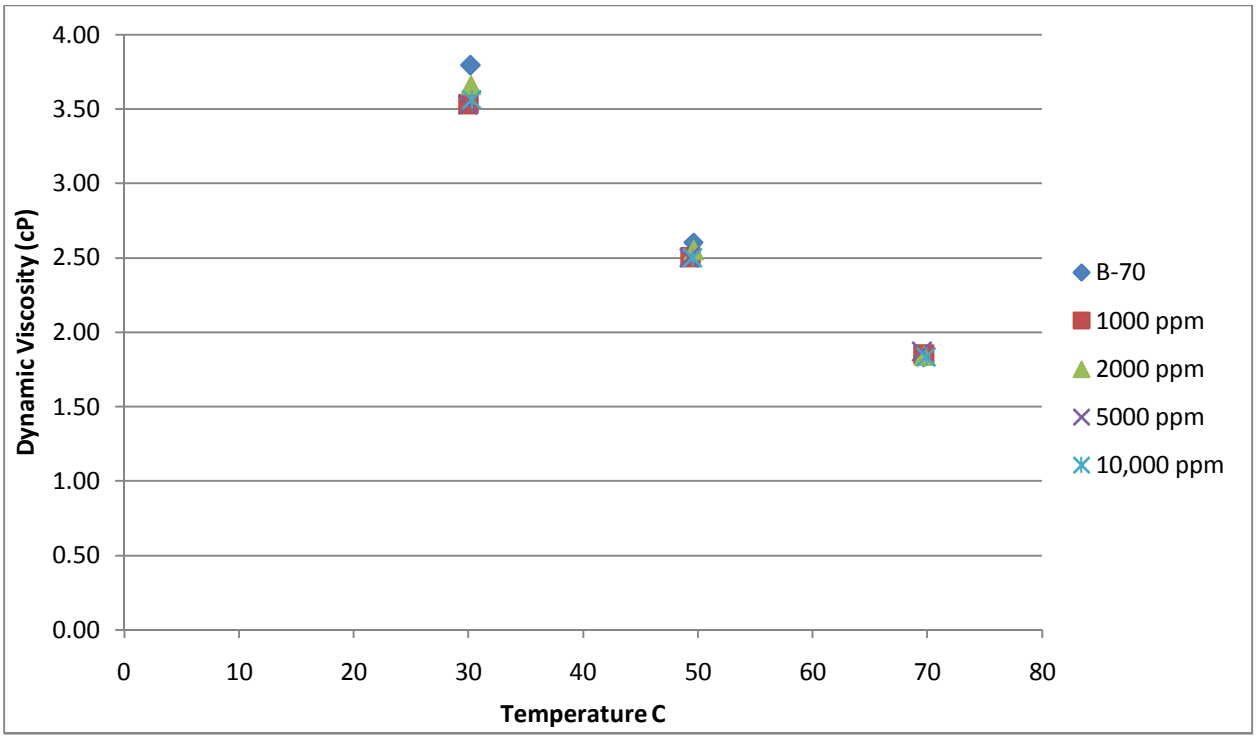

Figure B.25 Dynamic viscosity of B-70 with methanol contamination

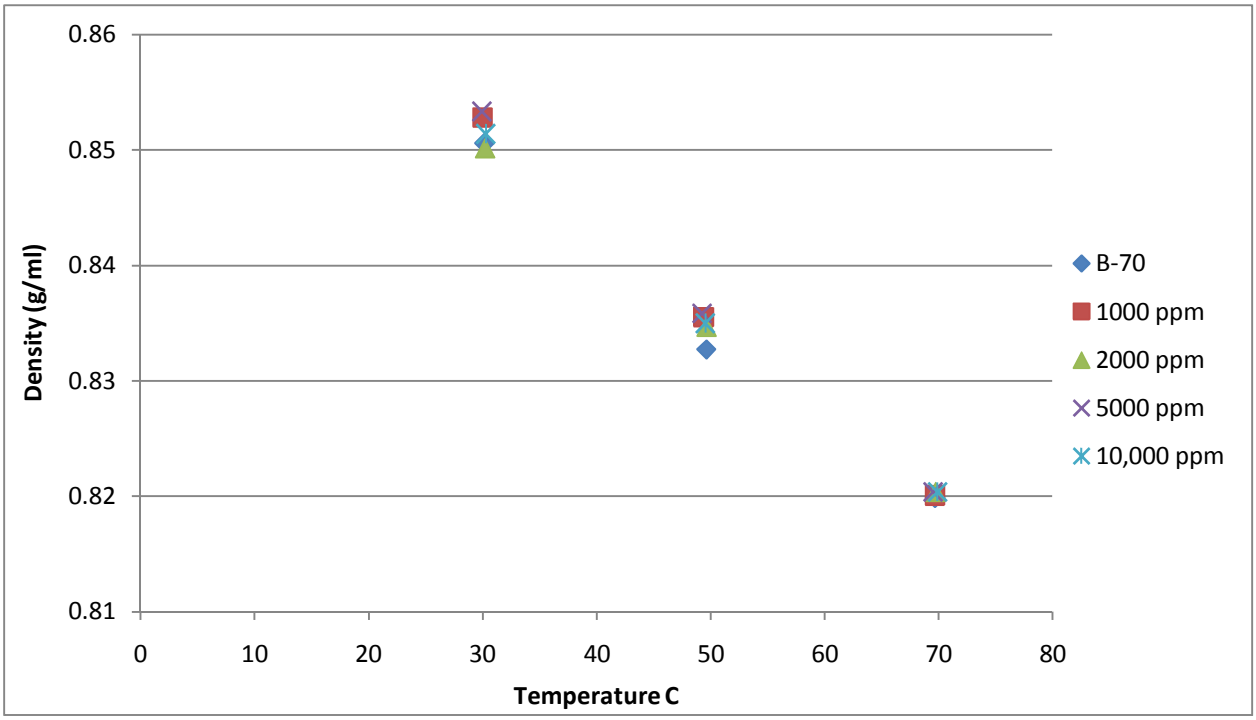

Figure B.26 Density of B-70 with methanol contamination

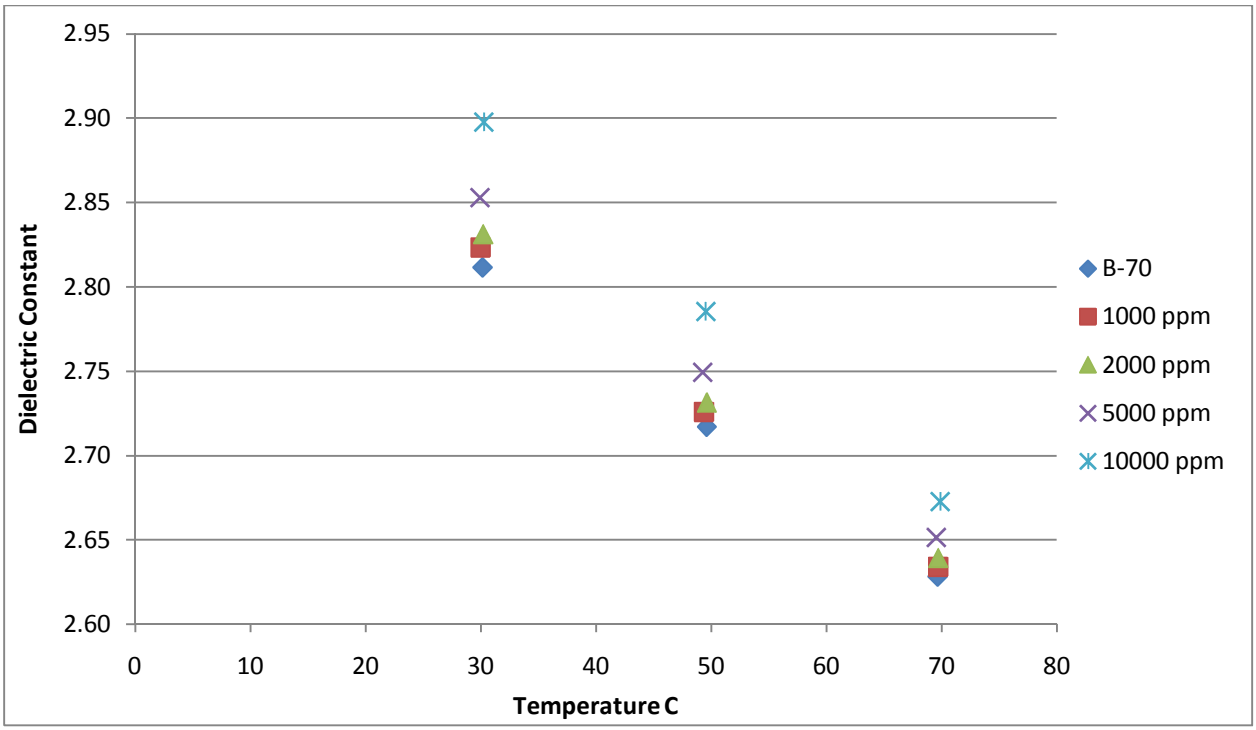

Figure B.27 Dielectric constant of B-70 with methanol contamination

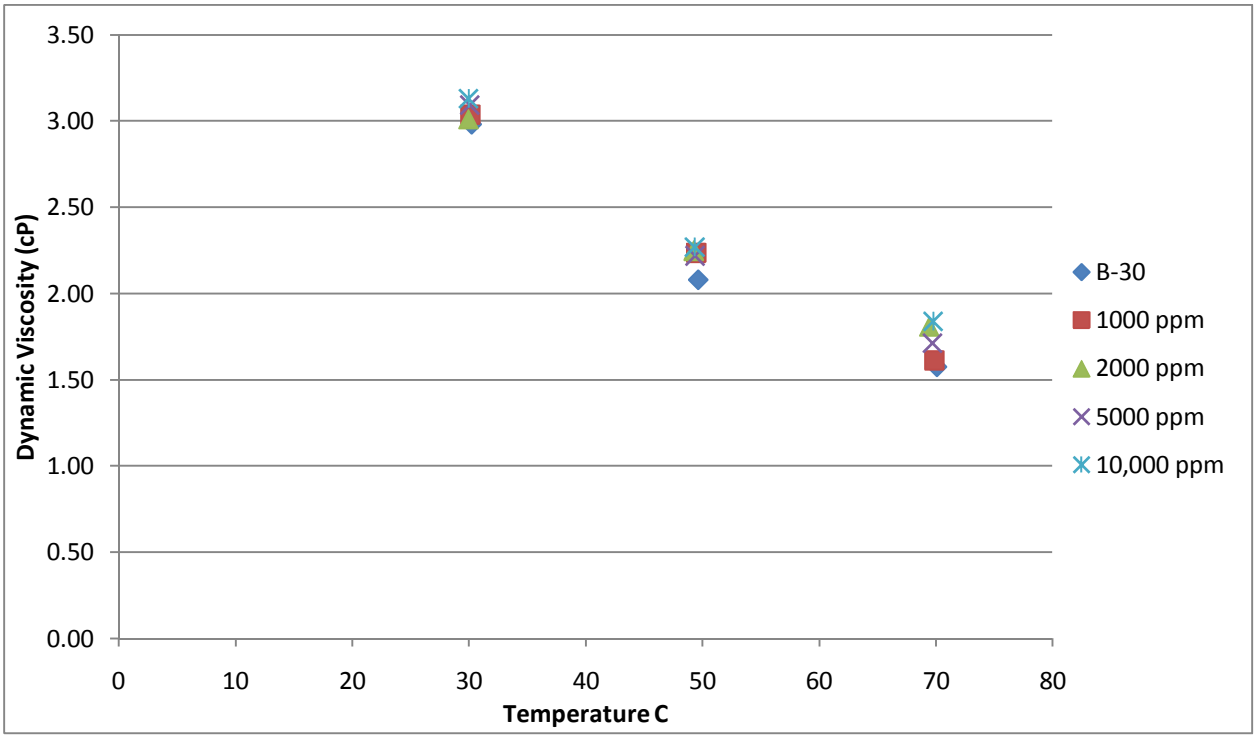

Figure B.28. Dynamic viscosity of B-30 with urea contamination

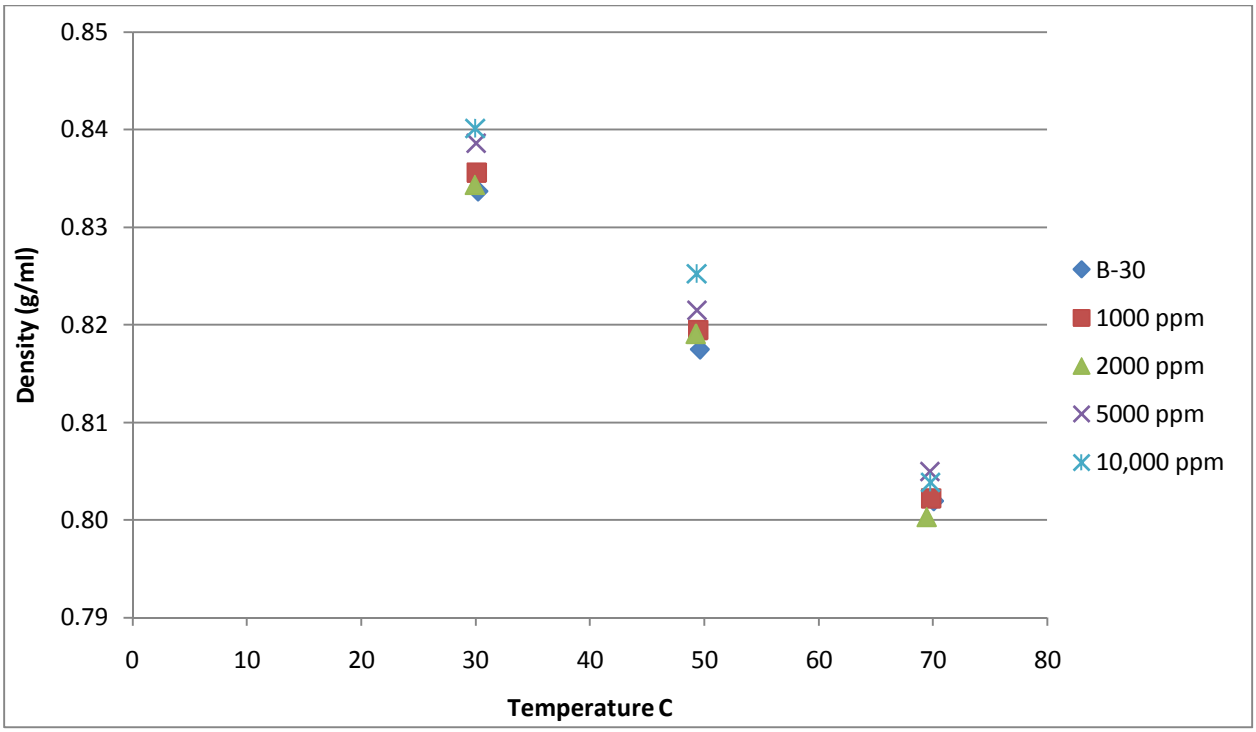

Figure B.29. Density of B-30 with urea contamination

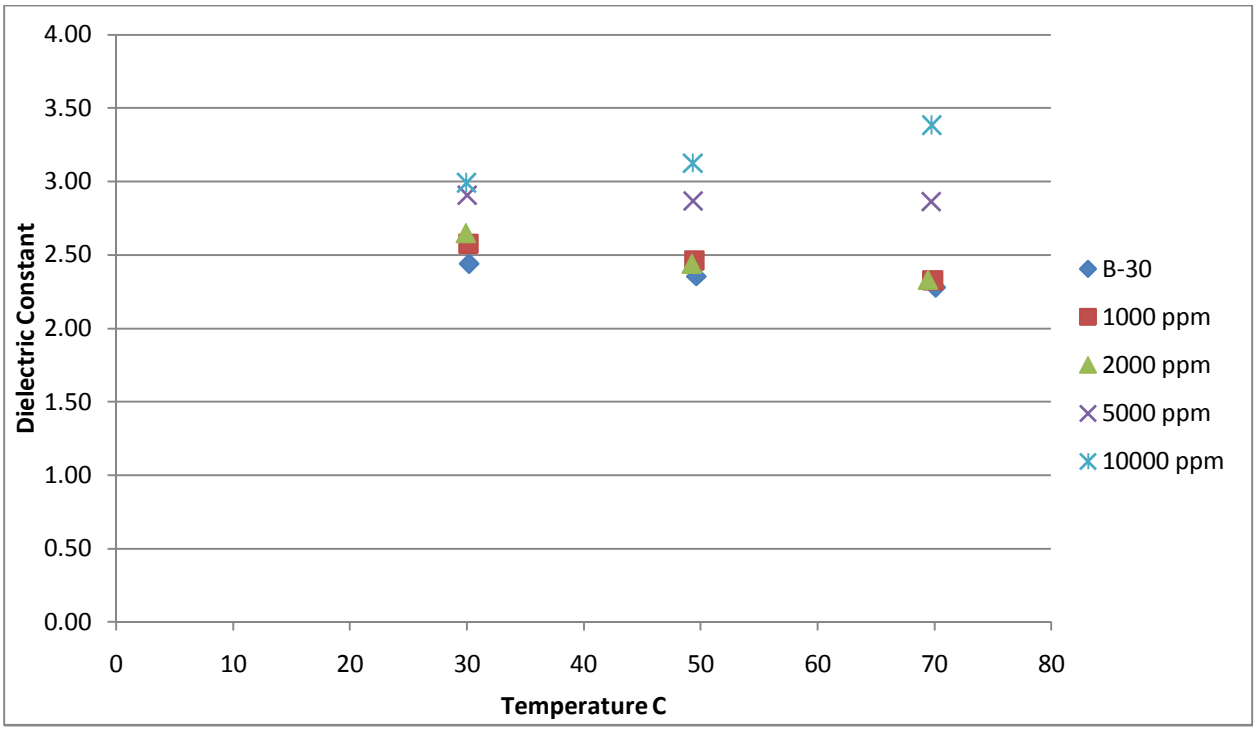

Figure B.30. Dielectric constant of B-30 with urea contamination

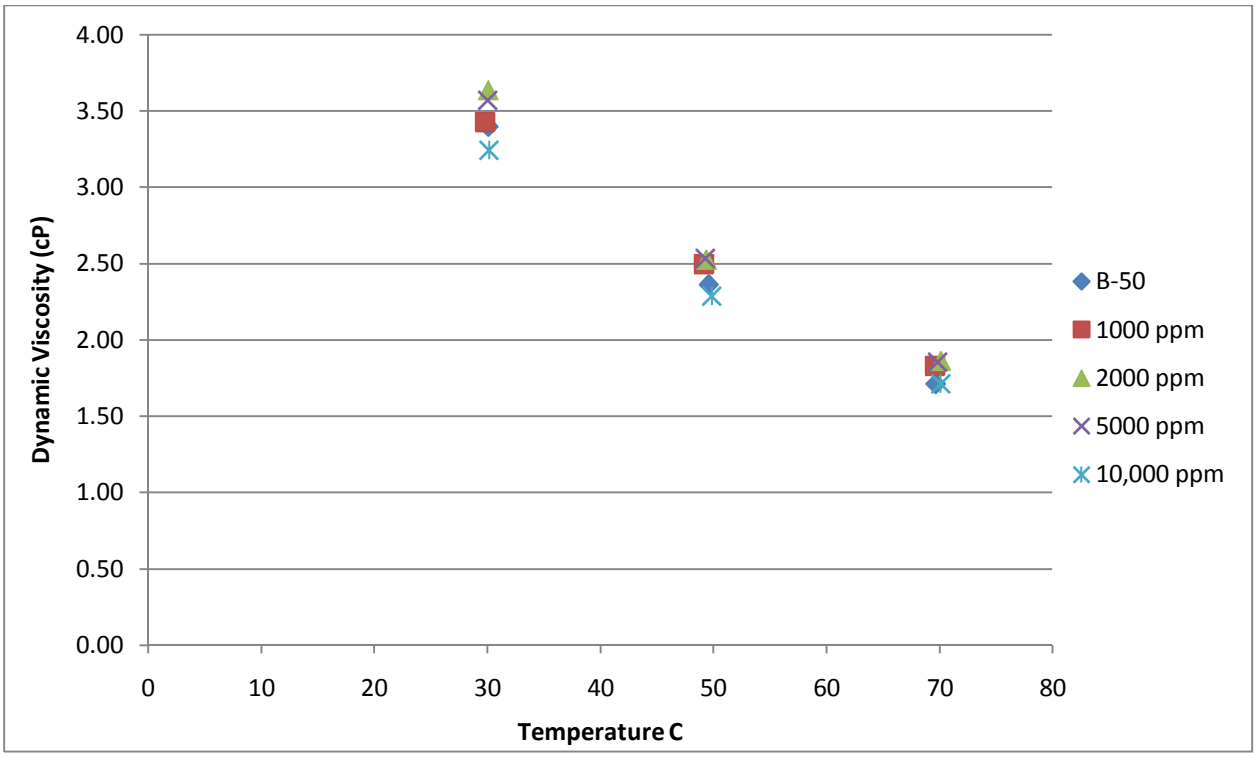

Figure B.31. Dynamic viscosity of B-50 with urea contamination

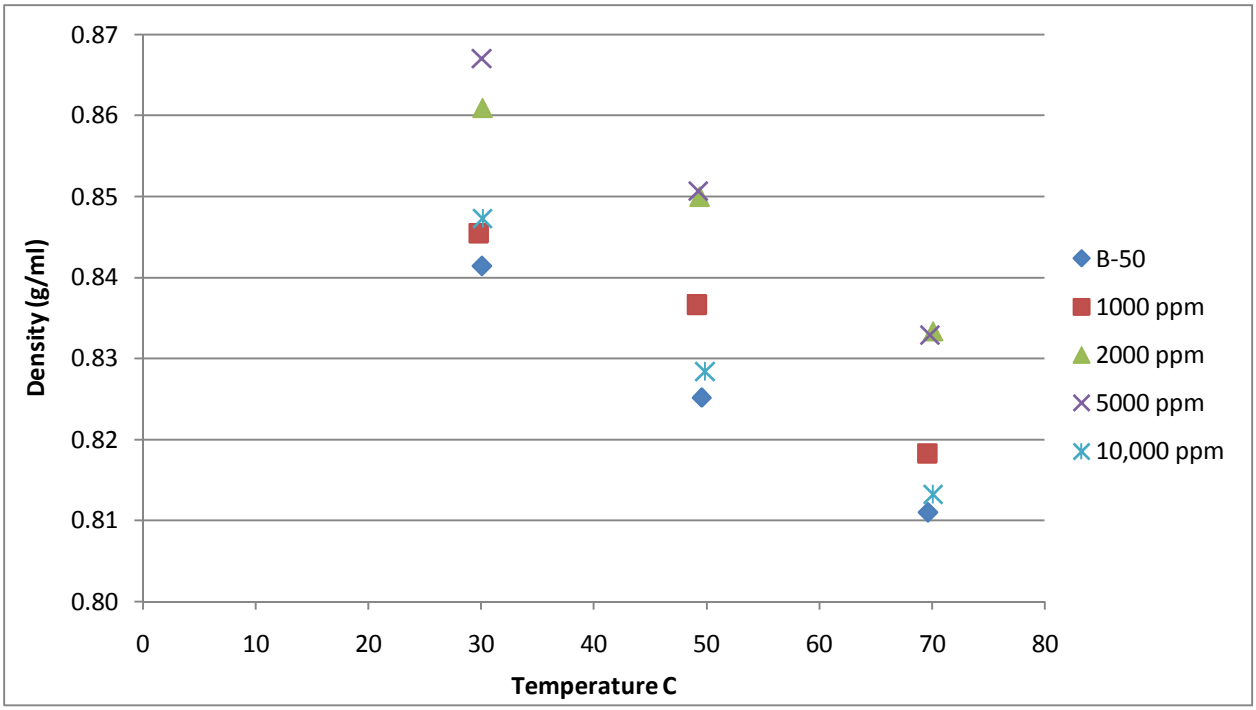

Figure B.32. Density of B-50 with urea contamination

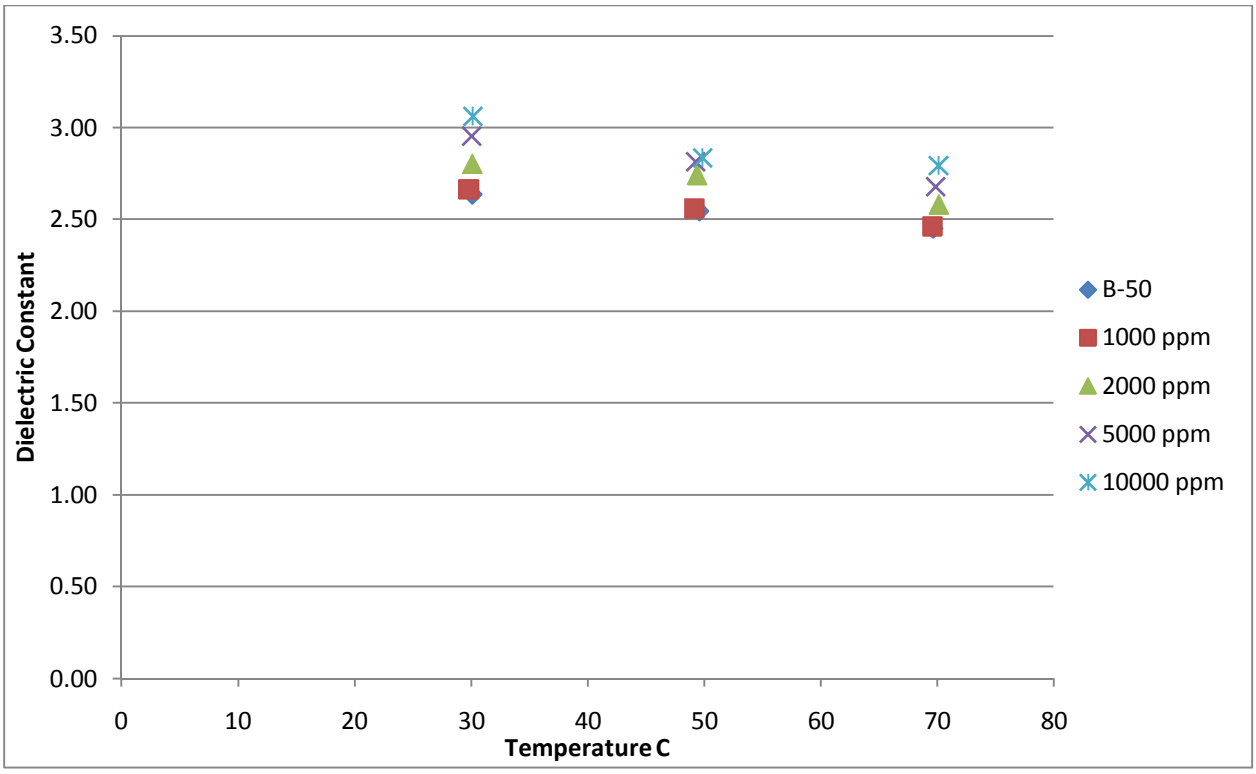

Figure B.33. Dielectric constant of B-50 with urea contamination